Anti-Alzheimer's disease properties and mechanisms of alginate-derived unsaturated mannuronate oligosaccharide

A thesis submitted to Auckland University of Technology in fulfilment of the requirement for the degree of Doctor of Philosophy

Decheng Bi

School of Science

Auckland University of Technology

January 2022

Primary supervisor: Professor Jun Lu

Secondary supervisor: Professor Xu Xu

Abstract

Alginate is a naturally acidic polysaccharide composed alternately of β-D-mannuronic acid and its C-5 epimer α-L-guluronic acid with 1,4-glycosidic linkages and widely exists in the cell walls of various brown seaweeds. Alginate and its derivatives exert a variety of biological and pharmaceutical activities. Alzheimer's disease (AD) is the most common type of dementia in aged people with disorders clinically characterized by cognitive deficits and pathologically characterized by extracellular senile plaques mainly composed of amyloid-β (Aβ) and neurofibrillary tangles composed of hyperphosphorylated tau protein. In ordinary life, the production and clearance of Aβ and hyperphosphorylated tau protein are in a dynamic balance. However, the failure to clear Aβ and hyperphosphorylated tau protein is regarded as an essential mechanism to exacerbate the pathological process of AD. Autophagy is a primary cellular degradation process that is responsible for the degradation and clearance of aggregated proteins and damaged organelles to maintain cellular homeostasis, depending on the fusion of autophagosomes and lysosomes.

In this study, unsaturated mannuronate oligosaccharide (MOS) was obtained from alginate-derived polymannuronate via enzymatic depolymerization. The degree of polymerization of MOS ranged from mannuronate dimer to mannuronate undecamer (M2- M11), and the distribution of the molecular weight of MOS ranged from 352 Da to 1936 Da. MOS significantly inhibited the aggregation of the $A\beta_{1-42}$ oligomer and Tau-K18 oligomer *in vitro.* In N2a-sw cells and 3×Tg-AD primary cortex neurons, MOS

treatment decreased the expression of $A\beta_{1-42}$ and reduced the levels of amyloid precursor protein (APP) and BACE1. Moreover, MOS significantly promoted autophagy in AD cells, which involved inactivation of the mTOR signalling pathway and facilitation of the fusion of autophagosomes and lysosomes induced by MOS. Finally, the MOS-induced decrease in APP and $A\beta_{1-42}$ levels was blocked by the addition of autophagy inhibitors, confirming the involvement of autophagy in the anti-AD activity of MOS.

In HEK293/Tau cells and 3×Tg-AD primary cortex neurons, MOS suppressed the levels of phosphorylated Tau protein. MOS treatment reduced the activity of glycogen synthase kinase-3β (GSK-3β) by decreasing its phosphorylation levels at the Y216 site and increasing its phosphorylation levels at the S9 site. MOS treatment increased the ratio of LC3-II/LC3-I levels and reduced the expression of p62, indicating an increase in autophagy. Finally, the MOS-induced decrease in Tau protein expression was attenuated by the addition of an autophagy inhibitor, confirming the involvement of autophagy.

This is the first comprehensive investigation on the anti-Alzheimer's disease properties of MOS. The results have shed light on a novel application prospect of MOS as a promising functional food or a natural medication for the treatment or assistance of the treatment of AD.

Table of contents

List of figures

Chapter 1

Chapter 2

Chapter 3

Chapter 4

List of tables

Chapter 2

Chapter 3

Attestation of authorship

I hereby declare that this submission is my own work and that, to the best of my knowledge and belief, it contains no material previously published or written by another person, nor material which to a substantial extent has been submitted for the award of any other degree or diploma of a university or other institution of higher learning.

Decheng Bi

January 2022

Candidate contribution to co-authored works

Chapters two, three, and four in this thesis represent papers that have either been published or are under review in peer-reviewed journals. All co-authors in the chapters indicated in the following table have approved the inclusion of these papers in this doctoral thesis.

Chapter publication reference	**Author %**
Chapter 2: Decheng Bi, Xu Yang, Jun Lu, Xu Xu (2022), Preparation and potential applications of alginate and alginate oligosaccharides, *Comprehensive Reviews in Food Science and Food Safety*. (under review).	DB=80%; XY=5%; JL=10%; XX=5%
Chapter 3: Decheng Bi, Lijun Yao, Zhijian Lin, Lianli Chi, Hui Li, Hong Xu, Xiubo Du, Qiong Liu, Zhangli Hu, Jun Lu, Xu Xu (2021), Unsaturated mannuronate oligosaccharide ameliorates β-amyloid pathology through autophagy in Alzheimer's disease cell models, *Carbohydrate Polymers*.	DB=85%; JL=5%; XX=5%; others (5%)
Chapter 4: Decheng Bi, Shifeng Xiao, Zhijian Lin, Lijun Yao, Weishan Fang, Yan Wu, Hong Xu, Jun Lu,and Xu Xu, (2021), Alginate-derived mannuronate oligosaccharide attenuates tauopathy through enhancing autophagy, *Journal of Agricultural and Food Chemistry.*	DB=85%; JL=5%; XX=5%; others (5%)

Supervisors

Prof. Jun Lu Primary	Prof. Xu Xu Secondary

Collaborators (in order of appearance)

Xu Yang Chapter 2	Lijun Yao Chapter 3 and 4	Zhijian Lin Chapter 3 and 4
Lianli Chi Chapter 3	Hui Li Chapter 3	Hong Xu Chapter 3 and 4
Xiubo Du Chapter 3	Qiong Liu Chapter 3	Zhangli Hu Chapter 3
Shifeng Xiao Chapter 4	Weishan Fang Chapter 4	Yan Wu Chapter 4

Acknowledgements

On completion of this thesis, I would like to thank all of the people who have guided and helped me through the last three years. First, I am very grateful to Shenzhen University and Auckland University of Technology for providing me with this opportunity to participate in the joint doctoral supervision program. Second, I am truly indebted and grateful to my primary supervisor Professor Jun Lu. In addition to his expertise in the research area, which has supported me throughout the entire study and ensured its completion, the most important lessons he taught me were to be accurate with every detail, patient, and hard-working, which will enable me to achieve success in the future. Third, I would like to thank my second supervisor Professor Xu Xu, who designed this project, taught me from the beginning, and was very generous in sharing valuable career- and research-related experiences. I would also like to thank Professors Qiong Liu and Xiubo Du, who helped with experiments related to the culture of primary neurons. Here, I would also like to thank all my classmates. Finally, I hope my wife and parents will be pleased with my achievements. They have always encouraged and supported me unreservedly.

Chapter 1. Introduction

1.1 Alzheimer's disease

1.1.1 Overview of AD

Clinically, according to the severity of the disease, AD can be divided into three types: early AD, middle AD, and late AD. AD is an untreatable neurodegenerative disorder characterized by autophagy dysfunction, loss of synapses, nerve inflammation, mitochondrial dysfunction, senile plaques from the aggregation and deposition of amyloid-β (Aβ) and neurofibrillary tangles from the aggregation and deposition of excessive phosphate tau protein, eventually causing brain neuron apoptosis (Jana & Pahan, 2010; Reddy et al., 2010). However, the pathogenesis and specific pathological mechanism of AD have yet to be fully elucidated (Reddy et al., 2017).

1.1.2 Amyloid-β

Soluble Aβ protein aggregates outside nerve cells to form insoluble fibrils and then precipitates to form senile plaques, which is one of the principal pathological features of AD (Mattson, 2004). The Aβ peptide is cut from amyloid precursor protein (APP) by orderly β- and γ-secretases (Figure 1.1). APP is a typical transmembrane glycoprotein that plays a vital role in nerve cell signal transduction, stem cell differentiation, calcium ion metabolism, synaptic growth, neuroprotein transport, cell proliferation, and cell adhesion (Yamin et al., 2008). Under normal conditions, the APP protein is mainly cleaved by α-secretases to generate soluble APP peptide-α (sAPPα) and C-terminal

fragment 83 (CTF83) fragments, which are then cleaved by downstream γ-secretases to produce nontoxic soluble peptides, including CTF and p3 peptides, in cells. However, under pathological conditions, the APP protein is mainly cleaved by β-secretases to generate soluble APP peptide-β (sAPPβ) and C-terminal fragment 99 (C99) peptides. Subsequently, the C99 peptide segment is continuously cleaved by γ-secretases to eventually generate the intracellular structure of APP (AIDC) and Aβ (Lazarov & Demars, 2012). The Aβ peptide is a 36-43 residue peptide, and the primary forms of the Aβ peptide are $A\beta_{1-40}$ and $A\beta_{1-42}$ (Lazarov & Demars, 2012). The amount of $A\beta_{1-40}$ in the brain is higher than that of $A\beta_{1-42}$, but $A\beta_{1-42}$ is much more toxic than $A\beta_{1-40}$. After cleavage from APP, Aβ monomers spontaneously aggregate into oligomers and insoluble fibrils, and in ordinary life, the production of Aβ and clearance are in a dynamic balance (Nixon, 2013).

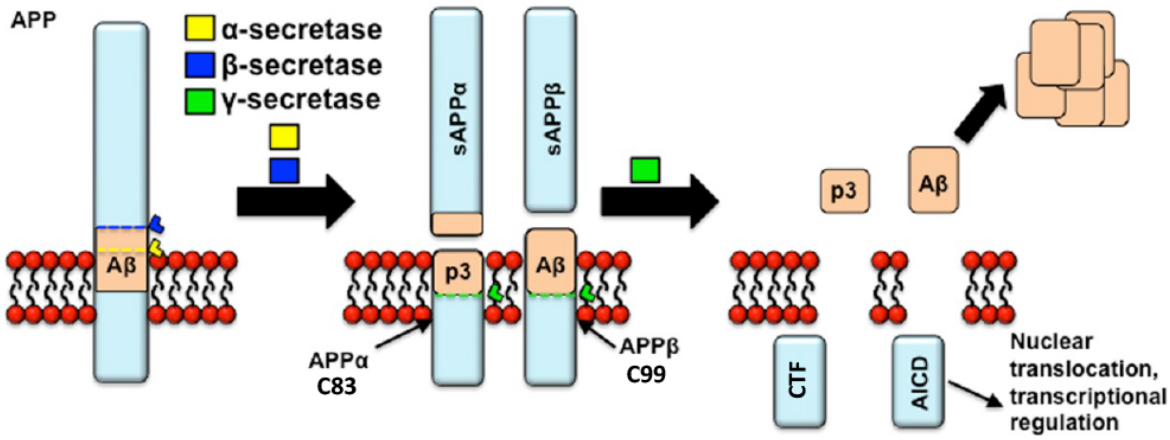

Figure 1.1 The schematic diagram of Aβ production (Lazarov & Demars, 2012)**.**

The amyloid hypothesis put forwards by scientists in 1991 suggests that the imbalance between amyloid production and clearance leads to the massive

accumulation of amyloid in the brain and the degeneration of neurons, which may be the root cause of AD (Hardy & Allsop, 1991). Since Aβ fibrils reside at the core of senile plaques without Aβ oligomers, *in vitro* studies have found that Aβ fibrils can cause damage to cultured neurons (Jana & Pahan, 2010), leading people to believe that Aβ fibrils are the leading cause of AD. However, subsequent studies found that Aβ oligomers possessed more neurotoxicity than Aβ fibrils, and the $A\beta_{1-42}$ oligomer is suggested to be the most neurotoxic form (Pan et al., 2011). In fact, APP, β-secretase, and γ-secretase exert neurotoxic characteristics mainly due to the generation of Aβ (Lazarov & Demars, 2012).

1.1.3 Tau protein

Tau proteins, which are microtubule-associated proteins first discovered in 1975 (Weingarten et al., 1975), are encoded by the MAPT gene located on chromosome 17 and critical for microtubule assembly and stabilization (Baker et al., 2006). Tau proteins are a kind of phosphoprotein, and each tau protein contains 1-3 phosphate groups. However, in the pathological state of AD, the tau protein in the brains of AD patients is hyperphosphorylated, and the phosphorylation level is 3-4 times or even higher than usual. The phosphorylation site of tau proteins is specific and mainly occurs at serine or threonine residues (Wang & Mandelkow, 2016). There are approximately 45 potential phosphorylation sites that have been observed in the longest tau protein form experimentally, such as Ser396, Ser404, Thr231, and Thr235 (Hanger et al., 2009). Furthermore, these sites are the targets of proline-directed protein kinases such as

glycogen synthase kinase 3β (GSK3β), mitogen-activated protein kinases (MAPKs), and cyclin-dependent kinase 5 (CDK5) (Brunden et al., 2009).

The natively unfolded tau protein on microtubules shows little aggregation. However, after excessive phosphorylation by kinases, tau protein detaches from microtubules, showing poor solubility and a tendency toward aggregation (Wang & Mandelkow, 2016). After aggregation into oligomers under diseased conditions, it aggregates into paired helical filaments (PHFs) and neurofibrillary tangles (NFTs) and then deposits in the brain (Orr et al., 2017), which are the major pathological hallmarks of tauopathies, including AD.

1.1.4 Autophagy

Autophagy, literally "self-ingestion," is a degradation pathway in which cytoplasmic proteins and organelles are transferred by the autophagosome to lysosomes for degradation, achieving digestion and nutrient cycling (Tsukada & Ohsumi, 1993). Autophagy plays a crucial role in maintaining homeostasis, which is not only responsible for intracellular nutrient recycling but also a significant pathway for the clearance of damaged intracellular organelles and aggregated proteins depending on the fusion of autophagosomes and lysosomes (Menzies et al., 2015).

The initiation of autophagy is the formation of autophagosomes, which is mediated through a protein complex that comprises ULK1 or ULK2, autophagy proteins (ATG)13, ATG101 and the focal adhesion kinase family interacting protein of 200 kDa (FIP200) (Menzies et al., 2015) and is regulated by NAD-dependent deacetylase SIRT1 (Lee et

al., 2008), myoinositol-1,4,5-trisphosphate (IP3) (Sarkar et al., 2005), adenosine monophosphate-activated protein kinase (AMPK) (Alers et al., 2012; Kim et al., 2011) and mammalian target of rapamycin (mTOR) (Kim et al., 2011; Pantovic et al., 2013). The initial step in the formation of autophagosomes is the fusion of vesicles that have been proposed to arise from a variety of membrane sources, including plasma membrane-derived endosomal intermediates, the endoplasmic reticulum (ER) and the Golgi (Menzies et al., 2015). These vesicles coalesce to form a flattened membrane sac called a phagophore and are regulated by Beclin-1 and vacuolar protein sorting 34 (VPS34) (Russell et al., 2013). Various ATG proteins are essential for the formation of autophagosomes and the fusion of autophagosome-lysosome (Figure 1.2).

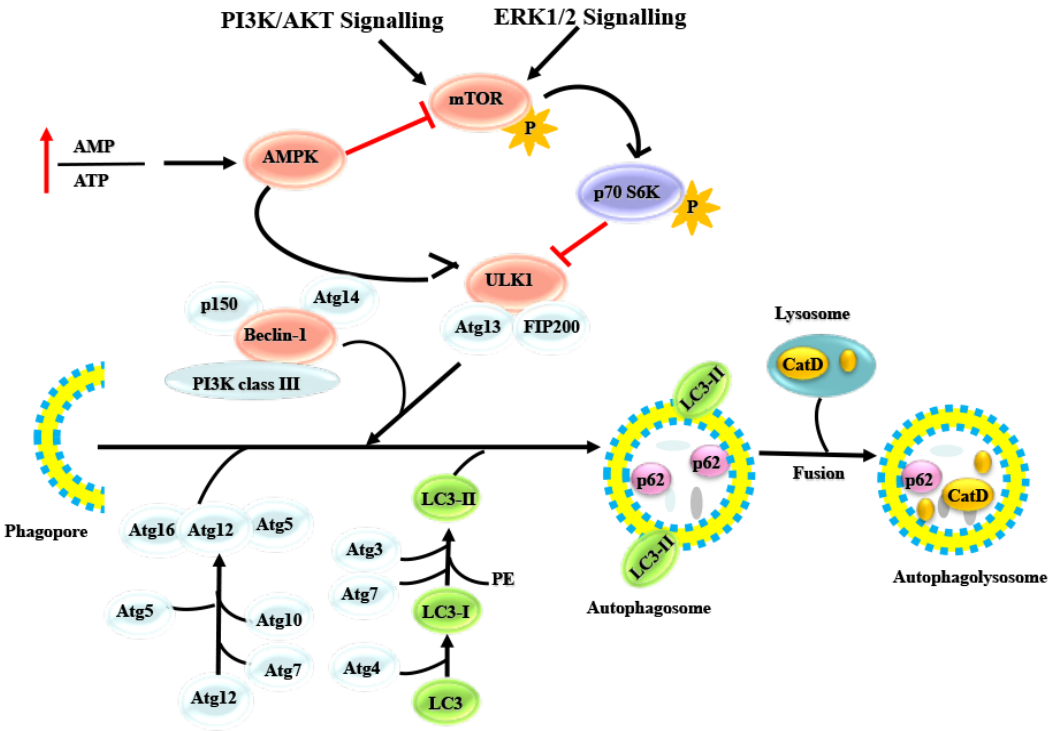

Figure 1.2 The regulation and progress of autophagy.

During the process of autophagosome maturation and fusion with lysosomes, when

the regulatory proteins or genes involved are mutated, autophagosome function is impeded, or fusion with lysosomes is restricted (Menzies et al., 2015); this is particularly evident in neurodegenerative diseases such as AD, Huntington disease (HD), Parkinson's disease (PD), and lysosomal storage disease (LSD) (Menzies et al., 2015).

1.1.5 Alzheimer's treatment strategy

In the pathogenesis of AD, the tau protein pathways and Aβ pathway are dominant, so these two pathways have been the most studied drug targets. However, multiple factors contribute to the pathogenesis of AD, and based on the Aβ hypothesis, inhibiting Aβ production and aggregation are still valuable therapeutic targets (Sikanyika et al., 2019). Aβ is mainly produced by the APP protein through continuous shearing of β-secretase and γ-secretase and then aggregates into oligomer and plaque forms (Lazarov & Demars, 2012). Therefore, inhibiting the activation or expression of β-secretase and γ-secretase and then inhibiting the generation and aggregation of Aβ are effective methods to prevent and treat AD. Some inhibitors of β-secretase and γ-secretase are in phase I or phase II clinical studies, such as AC-91 and E2212 (Bachurin et al., 2017). However, many inhibitors or medicines have been proven to be useless in clinical experiments. For example, semagacestat, an inhibitor of γ-secretase, was dropped in phase III studies by Eli Lilly Company due to its failure to affect the cognitive function of patients with AD (Doody et al., 2013). Solanezumab, an anti-amyloid monoclonal antibody binding soluble Aβ, has also been reported to fail in phase III

trials by Eli Lilly because of nonsignificant differences in improving cognitive impairment compared with vehicle in patients with mild Alzheimer's disease (Sacks et al., 2017).

The tau protein plays an essential role in the process of microtubule assembly and stabilization. Under the pathological state of AD, the tau protein presents a high level of phosphorylation with neurofibrillary tangles (NFTs) (Orr et al., 2017). In recent years, more attention has been given to the development of drugs targeting the tau protein, such as inhibitors of phosphorylation of tau. The inhibition of kinase activity is a direct and effective way to inhibit tau protein hyperphosphorylation. As a GSK-3β inhibitor, leuco-methylthioninium has entered phase III clinical research (Baddeley et al., 2015). Previous studies have proven that soluble tau protein produces toxicity in the process of aggregation into oligomers and fibres, and inhibition of tau protein aggregation into polymer structures can prevent the generation of toxicity (Bulic et al., 2009). As a tau protein aggregation inhibitor, methylene blue can change the structure of paired helical filament tau (PHF-tau), which has shown a significant treatment effect in phase II clinical research. However, it failed in phase III clinical research, and a plausible key to understanding the failure of a clinical trial is that methylene blue cannot inhibit the formation of tau oligomers (Soeda et al., 2019). Therefore, inhibiting tau protein aggregation into oligomers may be important.

It has been reported that failure to clear Aβ and tau is also an important mechanism that promotes Aβ and tau accumulation in neuronal cells and exacerbates the pathological process of AD (Pickford et al., 2008). Additionally, inordinate autophagy

promotes presenilin-1 expression and γ-secretase activity, thus affecting the clearance of Aβ and tau protein (Nixon, 2013; Ohta et al., 2010) and facilitating the pathogenesis of AD. Moreover, the promotion of autophagy initiation and autolysosome formation can reduce aggregate-prone protein aggregation and neurotoxicity in an AD model (Nixon, 2013). Furthermore, autophagy enhancers, such as rapamycin and carbamazepine, or the overexpression of autophagy-related genes, such as *Beclin-1*, can ameliorate the pathological process of AD through Aβ and tau protein clearance in an AD mouse model (Caccamo et al., 2010; Li et al., 2013; Pickford et al., 2008). Therefore, autophagy enhancers may also be an essential treatment strategy for AD.

1.2 Alginate and its oligosaccharides

Alginate was first discovered, extracted, and patented by Stanford (Stanford, 1881) and is a naturally occurring acidic linear exopolysaccharide (Haug et al., 1967). This polysaccharide is recognized as a structural component of various marine brown algae, such as *Macrocystis pyrifera*, *Laminaria hyperborean* and *Ascophyllum nodosum* (Park et al., 2009), and occurs primarily in the cell walls as an insoluble mixture of calcium, magnesium, potassium and sodium salts (Haug et al., 1967).

Alginate consists of β-D-mannuronate (M) and α-L-guluronate (G) with exclusively 1,4-glycosidic linkages; the residues are arranged in a block pattern along the chain with homopolymeric regions of mannuronate (polymannuronate, PM) and guluronate (polyguluronate, PG) interspaced with regions of heteropolymeric regions (a mixed sequence of these residues, PMG), as shown in Figure 1.3 (Xu et al., 2016). PM and PG

can be separated by pH 2.85 fractionation when alginate is hydrolysed using hydrochloric acid (HCl). The soluble fraction at this pH contains 80-90% M residues, whereas the insoluble precipitate contains 80-90% G residues (Haug et al., 1967). The crystalline structures of PM and PG are quite different as a result of epimerization at C-5. The β (1→4) linkages (equatorial-equatorial union) give the M blocks a more linear, flexible and flat conformation, as opposed to the α (1→4) linkages (apical-apical union) of the G blocks that generate steric hindrance around the carboxyl groups and result in folded and rigid structural conformations and stiff molecular chains (Yang et al., 2011). High G content provides a considerably higher strength compared to high M content; alginate with a high content of G blocks produces strong, brittle gels with excellent heat stability, whereas high M content produces weaker, more elastic gels with good freeze–thaw behaviour (Zhang et al., 2006).

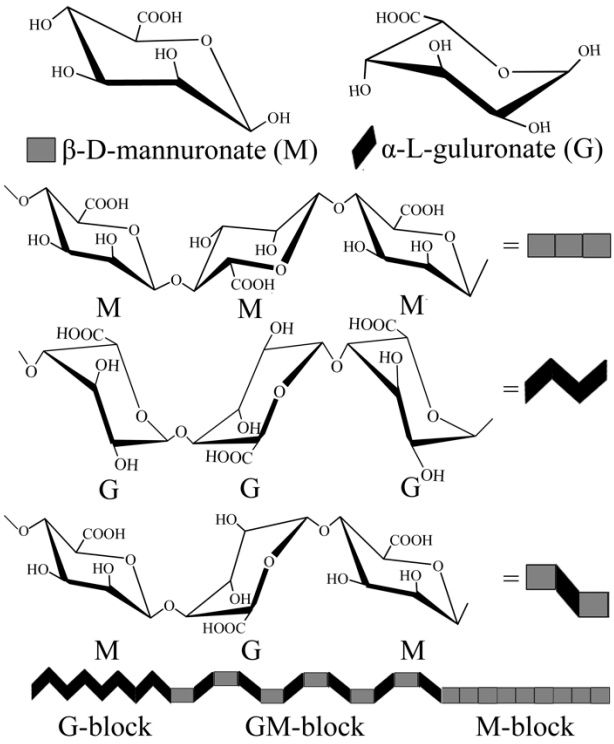

Figure 1.3 Structure of alginate (Xu et al., 2016).

Many methods have been used to prepare alginate oligosaccharides (AOS), including acid hydrolysis, enzymatic digestion using alginate lyase, and oxidative-reductive free-radical depolymerization (Xu, Wu, et al., 2014). These methods are used to decompose polysaccharides, resulting in the formation of AOS with different components or substitutions.

Acid hydrolysis of alginate was performed using HCl in a boiling water bath. Then, the reaction medium was neutralized with NaOH to remove potentially contaminated oligosaccharides with internal 1→4 and 1→5 lactones. By this procedure, the glycosidic bonds are cleaved, and the corresponding saturated oligomers with free carboxyl groups are obtained to maintain the native sugar residues of alginate.

Yang et al. (2004) degraded alginate and derived PM blocks using H_2O_2. In the report,

the PM was incubated with a 30% H_2O_2 solution at a final concentration of 5% at 90 °C for a certain period. Because the reaction system contained H_2O_2, the aldehyde group in the newly generated reducing end was mainly oxidized to carboxyl groups (Yang et al., 2004). This AOS has the famous name GV-971, which has completed a phase 3 clinical trial for AD in China and successfully met its primary endpoint in improving cognitive impairment (Wang et al., 2019). Alginate lyase has been isolated from a wide variety of sources, including decayed brown algae, molluscs, and bacteria (Linker & Evans, 1984). It usually catalyses the degradation of alginate via β-elimination targeting the glycosidic 1→4 O-linkage between monomers to produce oligosaccharides with C4=C5 unsaturated uronic acid at the nonreducing terminal end. This mechanism is similar to that of alkaline degradation to glycuronans (Wong et al., 2000). In a previous study, it was proven that unsaturated AOS exhibit immunostimulatory activity. It could upregulate the expression of macrophage receptor Toll-like receptor 4 and Fcγ receptors, regulate the generation of cellular immune mediators by activating the NF-κB, mTOR and MAPK signalling pathways, promote the phagocytosis of macrophages, and enhance the bacterial clearance ability of mice with acute peritonitis (Fang et al., 2017; Xu, Bi, et al., 2014; Xu, Wu, et al., 2014).

1.3 Research aims and objectives

Chapter two provides a comprehensive review of methods to prepare and analyse alginate and AOS, focusing on the potential use of alginate and AOS in the food and

drug fields. This chapter is under review in the journal ***Comprehensive Reviews in Food Science and Food Safety*****.**

Chapter three describes a study that investigated the potential therapeutic effect of MOS on the Aβ pathway of AD and its molecular mechanism in N2a-sw cells and 3×Tg-AD primary cortex neurons. Additionally, this study confirmed the relationship between the Aβ pathway pathological characteristic improvement and autophagy enhancement triggered by MOS. This chapter has been published in the journal ***Carbohydrate Polymers*** **(Doi: 10.1016/j.carbpol.2020.117124)**.

Chapter four describes a study that investigated the potential therapeutic effect of MOS on the tau pathway of AD and its molecular mechanism in HEK293/tau cells and 3×Tg-AD primary cortex neurons. Additionally, this study confirmed the relationship between the tau pathway pathological characteristic improvement and autophagy enhancement triggered by MOS. This chapter has been published in the journal: ***Journal of Agricultural and Food Chemistry*** **(Doi: org/10.1021/acs.jafc.1c00394)**.

Finally, chapter five discusses the findings from the above data chapters and ties all of the major results obtained and described in each of the preceding chapters. It harmonizes the central findings and describes in detail how these findings achieve the aim of this research. In addition, the idea and expectation of MOS intervention in AD are proposed.

1.4 Originality and significance of the thesis

AD is the most common type of dementia in aged people with disorders clinically characterized by cognitive deficits, including impairment of spatial and episodic memory, language, and behaviours. At present, the number of patients with AD is increasing as the world's population ages. According to the Alzheimer's Association, there are 5 million Americans currently that suffer from Alzheimer's disease, and their loved ones spend nearly 18 billion hours a year caring for and treating these patients. If Alzheimer's disease is not controlled, those numbers are expected to more than quadruple by 2050, with the annual economic burden exceeding $1 trillion. Unfortunately, there are still no significantly effective drugs or other therapeutic drugs that can be used to prevent or delay the progression of AD, and no effective biomarkers can be directly used for the early diagnosis and early detection of AD. Therefore, it is urgent to find effective therapeutic agents.

Alginate is a naturally acidic polysaccharide that can be derived from brown seaweeds, which are abundant in New Zealand. As reported, one kind of alginate oligosaccharide, mannosaccharic acid (GV-971), was approved by the China Food and Drugs Administration for the treatment of mild to moderate patients diagnosed with Alzheimer’s diseases in November 2019. As the structural analogue of GV-971, MOS is worth studying as a promising functional food or medicine for attenuating AD.

1.5 Structure of the thesis

Under Auckland University of Technology's Doctoral Thesis Pathway 2, this thesis is structured and presented in five chapters, three of which are comprised of peer-reviewed journal publication formats.

Chapter two is entitled Preparation and potential applications of alginate and alginate oligosaccharides, which are under review.

The third and fourth chapters comprise original research articles that have been published.

The structure of each chapter includes:

- A short foreword describing the rationale and summary of the research is presented in the article.
- The manuscript following publication. Each article comprises an abstract, introduction, detailed materials and methods, and results and discussion sections.
- Each manuscript has been reformatted according to AUT's guidelines for thesis presentation.

The title of the original research article in chapter three is **Unsaturated mannuronate oligosaccharide ameliorates β-amyloid pathology through autophagy in Alzheimer's disease cell models**, and the original research article in chapter four is titled **Alginate-derived mannuronate oligosaccharide attenuates tauopathy through enhancing autophagy.**

The fifth chapter provides a conclusion.

Chapter 2 Preparation and potential applications of alginate and alginate oligosaccharides

2.1 Abstract

Alginate, a linear polymer consisting of β-D-mannuronic acid (M) and α-L-guluronic acid (G) with 1,4-glycosidic linkages and comprising 40% of the dry weight of algae, possesses various applications in the food and biomedical industries due to its unique physicochemical properties as well as beneficial health effects. However, the potential applications of alginate are restricted in some fields because of its low water solubility and high solution viscosity. Alginate oligosaccharides (AOS) can be obtained by multiple degradation methods from alginate or alginate-derived poly G and poly M. Generally, AOS have low molecular weight, resulting in better water solubility. Alginate and AOS have unique bioactivity and can impart health benefits, including immunomodulatory effects, antioxidative effects, neuroprotective effects, antibacterial effects, antitumor effects, reducing obesity, and gut microbiota regulation. This review comprehensively covers methods of the preparation and analysis of alginate and AOS and also focuses on the potential use of alginate and AOS in the food and drug fields.

2.2 Keywords

alginate, alginate oligosaccharides, health effects, preparation.

2.3 Introduction

Seaweeds, which have been part of the diet of Asian countries for hundreds of years, are a sustainable source of bioactive compounds that are largely absent from the terrestrial biomass (Flórez-Fernández et al., 2019). Some attractive and edible alternatives could be *Laminaria ochroleuca*, *Undaria pinnatifida* and *Laminaria japonica*, which belong to the brown algae and are wildly distributed in oceans around the world (Assis et al., 2018; Shen et al., 2021). Most of them are perennial and relatively long-lived species, mainly influenced by temperature and nutrient availability (Franco et al., 2018). Different biological activities have been reported for brown algae extracts, including the neuroprotective effect (Bi, Yao, et al., 2021; Wang et al., 2019), hypoglycemic activity (Lamela et al., 1989), anti-inflammatory effect (Zhou, Shi, Gao, et al., 2015), antitumor activity (Mak et al., 2014) and antioxidant activity (Falkeborg et al., 2014; Tusi et al., 2011).

Alginate comprises 40% of dry weight of algae, which provides algae flexibility and stability against the marine currents (Flórez-Fernández et al., 2019). It is an acidic linear polysaccharide consisting of β-D-mannuronic acid (M) and α-L-guluronic acid (G) with 1,4-glycosidic linkages (Figure 2.1) (Brownlee et al., 2005). The physicochemical and mechanical properties of alginate are critically affected by the ratio of mannuronic acid residues to guluronic acid residues (M/G ratio) and the length of each block (Flórez-Fernández et al., 2019). Also, alginate is able to form a gel matrix in the presence of divalent cations, primarily Ca^{2+} ions. These features of this polysaccharide have been used in encapsulation and controlled-release systems for food ingredients,

bioactive compounds, and pharmaceutical materials (Ching et al., 2017). However, due to their large molecular weight and viscosity and low water solubility, alginate did not show many good biological activities.

Alginate oligosaccharides (AOS) are a degradation product of alginate, or alginate-derived poly M (PM) and poly G (PG). AOS have many physical and chemical properties similar to their parent polymers, such as high negative charges that make them have affinities to monovalent and divalent ions (Rye et al., 2018). The significant water solubility and low viscosity, mean it can be better used as drugs. As reported, AOS have shown significant bioactivities and therapeutic potential including immunoregulation (Xu, Bi, et al., 2014), plant growth-promoting (Xu et al., 2003), antioxidants (Falkeborg et al., 2014), and neurogenerative (Tusi et al., 2011) and anti-allergic activities (Uno et al., 2006). Keeping in view the potential of alginate and AOS, we aim to update the new progress in this specific area in light of current literature data, focusing on the preparation and analysis of alginate and AOS and their application in food gels and pharmacology.

2.4 Structure and preparation

2.4.1 Alginate

Alginate, first discovered, extracted and patented by Stanford (Stanford, 1881), is a naturally acidic linear extracellular polysaccharide produced by brown algae and bacteria (Linker & Jones, 1964, 1966). Alginate is a general name for water-soluble alkali metal salts such as sodium alginate and potassium alginate, and water-insoluble

alginate and alginate combined with more than divalent metal ions, but the most commonly used the alginate sodium salt (Onsøyen, 1997). Alginate exists in the cell wall of brown algae, mainly from sargassum algae and kelp. Due to the high solubility of alginate in alkaline solution, and that this form of alginate is insoluble in water, the alginate can be extracted with sodium carbonate solution, and then the pH value of the extract can be adjusted by acid to precipitate alginate (Haug, 1964). *Laminaria hyperborean*, *Macrocystis pyrifera*, *Laminaria digitata*, and *Ascophyllum nodosum* are species commonly used for commercial alginate production. Sometimes, *Sargassum spp*., *Laminaria japonica*, *Ecklonia maxima*, and *Lessonia nigrescens* are also used for alginate production (Liu et al., 2019). Because there is no modification group such as sulfate in brown alginate, there is no need to consider the problem of modification groups dropping in the process of acid precipitation (Haug, 1964; Onsøyen, 1997).

The residues of alginate are arranged in block patterns along the chain with homopolymeric regions of mannuronic acid (polymannuronic acid, PM) and guluronic acid (polyguluronic acid, PG) interspaced with hetero-polymeric regions (a mixed sequence of these residues, PMG) (Figure 2.1). The proportion and sequence of M and G residues in alginate derived from different brown algae are different, which determines the molecular weight and physical properties of alginate (Ching et al., 2017). These structures in alginate are the result of a unique biosynthetic pathway in which G residues are generated from preformed polymers of mannuronic acid by a family of isoenzymes with C-5 epimerase activity (Haug & Larsen, 1971; Larsen & Haug, 1971a, 1971b). PM and PG can be separated by hydrolyzing alginate with hydrochloric

acid (HCl) at pH 2.85. At this pH, the soluble portion contains 80-90% M residue and the insoluble precipitate contains 80-90% G residue (Haug et al., 1967). The content of G in Sargassum is higher, while the content of M in kelp is higher. The M/G ratio in alginate is not fixed. Even for the same seaweed, the proportion will change with different growth years, picking seasons and locations (Llanes et al., 2000).

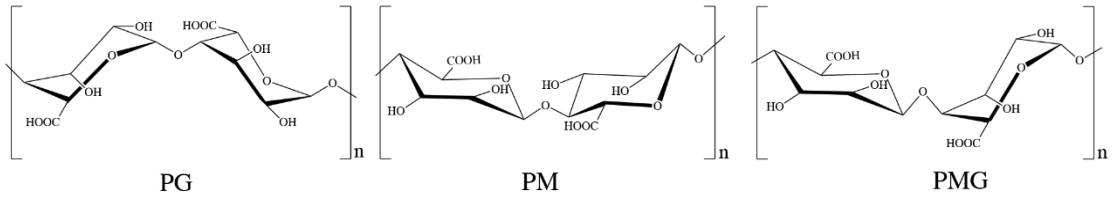

Figure 2.1 Structure of alginate.

For the primary structure, M and G differ only in the position of the carboxyl group on the C5 site, but just because of this small difference, they have significant differences in spatial structure and physical properties. The spatial structure of PG shows that monosaccharide units are in the 1C chair conformation and are stabilized by hydrogen bonds between intramolecular O2 and O6, while PM is a boat conformation and stabilized by hydrogen bonds between intramolecular O2 and O5, resulting in folded and rigid conformations of PG and a linear, flexible and flat conformation of PM (Atkins et al., 1973). Therefore, the high G content provides higher strength for alginate than the high M content (Xu et al., 2016). Also, these structural differences lead to great differences in the acid hydrolysis resistance of PM, PG and PMG fragments. PMG is easily hydrolyzed, while PM and PG are not easily hydrolyzed, and the acid hydrolysis resistance of PG is obviously stronger than that of PM (Haug et al., 1967).

Alginate is widely used in industry because of its ability to gel with calcium ions, however this property is also strongly influenced by its uronic acid composition, i.e., M/G ratio (Penman & Sanderson, 1972). The M/G ratio was originally determined using two-step hydrolysis of sulfuric acid at different concentrations and paper chromatography to separate M and G. Haug et al. improved this method, which was to separate each fragment by heterogeneous partial acid hydrolysis and fractional precipitation, and then determine the uronic acid composition of each fragment by complete acid hydrolysis (Haug et al., 1967). However, identifying blocks in this way is laborious and time-consuming, requiring a large amount of material (Morris et al., 1980). Based on the carbazole reaction, which can give very different colour intensities for mannuronic and guluronic acids (Dische, 1947), Knutson et al. established a method to determine the M/G ratio under two different reaction conditions and this method worked well on mixtures of mannuronic and guluronic acids (Knutson & Jeanes, 1968a, 1968b). However, in the specific application of M/G ratio detection of alginate, the content of G is consistently overestimated, which may be because carbazole reagents react differently from acids in polymer and monomer form (Penman & Sanderson, 1972). The determination of the M/G ratio by nuclear magnetic resonance (NMR) spectroscopy after alginate hydrolysis has improved substantially in terms of time and material requirements (Grasdalen et al., 1979; Grasdalen et al., 1981; Penman & Sanderson, 1972), but it is still not fully suitable for routine screening of the large numbers of samples and spectra often needed to be acquired at high temperature to decrease the viscosity of the alginate solution (Lu et al., 2015;

Rahelivao et al., 2013). Morris et al. found that the circular dichroism (CD) spectra of alginates showed a peak at 200 nm, and a trough at 215 nm, whose relative magnitudes vary systematically with composition (Morris et al., 1980). Based on this, they established a simple equation to determine the relative amounts of M and G from the observed ratio of peak height to trough depth. This method can obtain a reliable compositive estimate from 1 mg alginate and the results obtained are consistent with those obtained by the hydrolysis and NMR analysis of the same sample (Morris et al., 1980). For high sensitivity analysis of the M/G ratio of alginate and its derivatives, which were deeply hydrolyzed and then performed on high-performance liquid chromatography (HPLC) (Voragen et al., 1982), anion-exchange liquid chromatography (AELC) (Gacesa et al., 1983), capillary electrophoresis (CE) (Guttman, 1997), gas chromatography (GC) (Rumpel & Dignac, 2006) and high-performance anion-exchange chromatography (HPAEC) combined with using pulsed amperometric detection for separation-based analysis (Lu et al., 2015). These methods, however, need to hydrolyze the polysaccharide samples and cannot take into account the recovery, or require derivatization after hydrolysis of polysaccharides to monosaccharides, which needs additional validation analysis and may introduce impurities.

2.4.2 Alginate oligosaccharides

When a significant quantity of alginate is required, the high viscosity and gelation properties restrict its application in foods, thereby affecting its beneficial health effects. AOS is a functional oligosaccharide produced by alginate degradation, which has the characteristics of strong solubility and high stability, as well as a wide range of good

biological activities (Chunhua Zhang et al., 2021). Generally, oligosaccharides are a group of natural carbohydrates that consist of 3 to 10 monosaccharides (Weijers et al., 2008). Due to the similar functions and physicochemical properties of sugar compounds with polymerization degree of 10 to 20 and oligosaccharides, some researchers also refer to those with DP 10 to 20 as oligosaccharides when studying the functions of sugar substances (Xu et al., 2016). Due to its low viscosity and high solvency at neutral pH, as well as its biodegradable, biocompatible, non-toxic and non-sensitive properties, oligosaccharides have attracted extensive attention in the biomedicine, food and other fields (Pillai et al., 2009). The main preparation methods of AOS include acid hydrolysis, irradiation, enzymatic digestion, oxidative-reductive degradation, thermal degradation (Chunhua Zhang et al., 2021);(Xu et al., 2016). Different methods can be used to form different components or substituted AOS. In the following content, we will classify and introduce the degradation methods of alginate according to the structure of the AOS prepared.

2.4.2.1 Acid hydrolysis and irradiation degradation

Some alginate oligosaccharides are prepared by directly breaking the glycosidic bonds between the C1 and C4 in alginate to obtain a low molecular weight product, which does not generate new structures, such as acid hydrolysis and irradiation degradation. Acid hydrolysis of sodium alginate or its derived PM and PG is performed using oxalic acid, HCl, H_2SO_4 or formic acid in a boiling water bath (Xu et al., 2016). This approach is one of the most rapid methods to depolymerize alginate, but it is high cost and not eco-friendly (Lee et al., 2003; Chunhua Zhang et al., 2021). The irradiation

depolymerization technique and photolysis also are an alternative means to degrade alginate for the mass production of AOS. Similar to acid hydrolysis of alginate, these degradations of alginate also directly break glycosidic bonds, thus reducing the degree of polymerization and molecular weight of alginate (Xu et al., 2016). Among these, γ-irradiation is known to be the most energy saving and effective procedure for alginate degradation procedure, which does not require additional reagents to depolymerize the alginate (Abd El-Mohdy, 2017). In addition to γ-irradiation, UV- irradiation is also applied to degrade alginate. However, alginate should dissolve in an aqueous solution with titanium dioxide (TiO2) particles, which was used as catalyzer (Burana-osot et al., 2009). Microwave-irradiation degradation has been applied to hydrolysis of polysaccharides as a clean, efficient, and economical technology, and the alginate oligosaccharides prepared by this method were saturated (Hu et al., 2013). Table 2.1 shows the preparation of AOS by these methods.

Table 2.1 Experimental conditions for the preparation by some acid hydrolysis and irradiation methods.

Preparation conditions	Product details	References
1% alginate solution heated with 0.3 M HCl (pH 4.0) at 121°C for 80 min	Primary oligomers were a monomer (176Da), a dimer (352Da), and a trimer (528 Da)	(Yamasaki et al., 2012)
Alginate solution heated with 1 M oxalic acid at 100 °C for 10 h	The average DP was 20 to 30	(Haug & Larsen, 1966)
0.25% alginate solution heated with 0.1 M HCl (pH 5.6) at 95°C for 3.5 h and then pH adjusted to 3.5 with 0.1 M HCl for another heat at 95 °C for 4 h.	A polymer of 2-16 uronic acid residues	(Holtan et al., 2006)
1% alginate solution heated with 0.1 M HCl at 100°C for 20 min and then heated with 0.3 M HCl at 100 °C for another 2 h.	The depolymerization was 28.1%	(Zimoch-Korzycka et al., 2021)
1% alginate solution heated with 0.3 M HCl at 100°C for 6 h	The average DP was 2 to 10	(Ariyo et al., 1998; Ariyo et al., 1997)

2.5 mg/mL and 5.0 mg/mL PM or PG solution heated with 2 M trifluoroacetic acid at 100 °C or 120 °C for 24 h in	Not mentioned in detail	(Lu et al., 2015)
1% PG solution heated 0.3N HCl at 121°C for 80 min	The DP was 1 to 9	(Shimokawa et al., 1996)
0.05% Alginate solution mixed 1N H_2SO_4 or 1 N oxalic acid on water bath	Not mentioned in detail	(Larsen, 1962)
1 or 4% aqueous solution of alginate irradiated by γ-rays from Co-60 sources (0-500 kGy)	Mw of alginate was reduced significantly	(Nagasawa et al., 2000)
Alginate powder irradiated by γ-rays from Co-60 sources (20-100 kGy)	Low Mw alginate	(Abd El-Mohdy, 2017)
1 g/L alginate solution mixed with TiO_2 particles and exposed to UV-light for 6 h	Depolymerized to 40% of its average molecular weight	(Burana-osot et al., 2009)
4% Alginate solution irradiated by γ-rays from Co-60 sources (0-500 kGy)	The molecular weight was reduced by two orders of magnitude	(Hien et al., 2000)
2% Alginate solution irradiated by γ-rays from Co-60 sources (100 kGy)	The Mw of alginate was reduced from 300 kDa to 25 kDa	(Lee et al., 2003)
1% PG solution hydrolyzed under microwave irradiation (1600 W) at 130 °C for 15 min	The DP was 1 to 10	(Hu et al., 2013)
1% PG solution hydrolyzed hydrolyzed at 121 °C with 0.1 mol/L HCl for 6 h	Mw of PG decreased from the initial 6.1 kDa to 4.9 kDa	(Hu et al., 2013)

2.4.2.2 Oxidative-reductive degradation

Oxidative-reductive degradation is kind of chemical hydrolysis of alginate, which is a simple, cheap method, and easy to operate compared with acid hydrolysis. In this degradation process, the most common reagent used was hydrogen peroxide (H_2O_2) (Zimoch-Korzycka et al., 2021), and periodate was sometimes used (Balakrishnan et al., 2005). Oxidative-reductive degradation of alginate has been resolved to be achieved by cleavage of glycosidic bonds (Li et al., 2010) (Yang et al., 2004), in which the C-1 position was mostly oxidized to a carboxyl group, but the exact mechanism of

the depolymerization of alginate H_2O_2 is unclear (Liu et al., 2019). Due to the presence of H_2O_2 in the reaction system, not only is the alginate degraded to sugar compounds with smaller molecular weight, but also most of the newly generated reducing aldehyde groups are oxidized to carboxyl groups (Yang et al., 2004) (Figure 2.2). Meanwhile, some researchers combine radiation with H_2O_2 to synergically degrade alginate, thereby reducing the dose of radiation used and better controlling product quality (Luan et al., 2012; Şen & Atik, 2012). Table 2.2 shows the preparation of AOS by oxidative-reductive degradation.

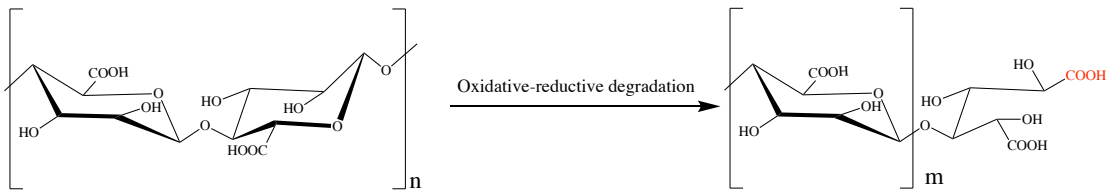

Figure 2.2 Oxidative-reductive degradation of alginate.

Table 2.2 Experimental conditions for the preparation of AOS by some oxidative-reductive degradation methods.

Preparation conditions	Product details	References
150 mL of 2% alginate solution mixed with 150 mL of 10% H_2O_2 and stirred for 210 min at 25°C.	Depolymerization was 87%	(Zimoch-Korzycka et al., 2021)
400 mL of 5% alginate solution mixed with 100 mL 65% periodate equivalents and stirred magnetically in the dark at 25 °C for 6 h.	Low Mw saccharides	(Balakrishnan et al., 2005)
8% PM solution mixed with 30% H_2O_2 (final concentration was 5%) and heated at 90 °C for 4 h.	The DP was 2 to 7 and C-1 position was mostly oxidized to a carboxyl group	(Yang et al., 2004)
1.5% alginate solution mixed with 30% H_2O_2 (final concentration was 1.5%) and heated at 50 °C for 5 h.	Low Mw alginate with 12.2 kDa	(Li et al., 2010)
4% alginate solution containing 5% H_2O_2 was permitted to proceed for a maximum reaction time of 96 h at room temperature.	Degraded alginate compounds with Mw of 40−77 kDa	(Luan et al., 2012)

4% alginate solution containing 0.5% H_2O_2 exposed to a γ Co-60 source for irradiation at doses of 4−16 kGy.	Degraded alginate compounds with Mw of 11−26 kDa	(Luan et al., 2012)
2% alginate solution containing equal mass of H_2O_2 heated at 70°C for 10 h	Degraded alginate compounds with Mw ≤ 5.5 kDa and the degree of polymerization was 2 to 24. C-1 position was mostly oxidized to a carboxyl group	(Soukaina et al., 2020)
2% alginate solution containing 2% H_2O_2 exposed to a γ Co-60 source for irradiation at doses of 5 kGy.	Degraded alginate compounds with molecular weights 1−3.75 kDa	(Şen & Atik, 2012)
1% alginate solution containing 3% H_2O_2 for a reaction time of 4 h at 2°C	Small Mw alginates	(Mao et al., 2012)

2.4.2.3 Enzymatic digestion and thermal degradation

Enzymatic digestion of alginate using alginate lyase has been proposed as a mild, environmentally friendly and reproducible method. Alginate lyase, also known as alginase or alginate depolymerase, has been isolated from a variety of sources, such as decaying brown algae, mollusks, and bacteria (Liu et al., 2019; Ming et al., 2021; Xu et al., 2016). Alginate lyase usually cleaves glycosidic bonds (1→4 O- linkage between monomers) through the β-elimination reaction and produces oligosaccharides with C4=C5 unsaturated uronic acid as a non-reducing terminal, i.e., 4-deoxy-α-L-erythro-hex-4-enopyranosyluronate, to achieve the purpose of degrading alginate (Zhu & Yin, 2015) (Figure 2.3). The detailed reactions of alginate lyase through β-elimination proceed as follows: (I) neutralization of alginate carboxyl negative charge and pKa reduction of the H-5 proton; (II) general base-catalyzed proton abstraction on C-5 and formation of carboxylate dianion intermediate; (III) proton donation for double bond formation between C-4 and C-5 (Liu et al., 2019). Alginate lyase is classified based on

its substrate specificities, including PM lyase [(1→4)-β-D-mannuronan lyase] that is specific for PM to produce mannuronic acid oligosaccharide (EC 4.2.2.3), PG lyase [(1→4)-α-L-guluronan lyase] that is specific for PG to produce guluronic acid oligosaccharide ((EC 4.2.2.11), and bifunctional lyases (EC 4.2.2.-). Compared to other processes to degradation of alginate, AOS formed from enzymatic digestion is more bioactive with a lower degree of polymerization, including disaccharide, trisaccharide, tetrasaccharide, and pentasaccharide (Xu, Wu, et al., 2014; Chunhua Zhang et al., 2021). Since there are so many reports about enzymatic oligosaccharides, only the preparation methods of enzymatic oligosaccharides from brown algae in recent years, that is, since 2017, are summarized here (Table 2.3)

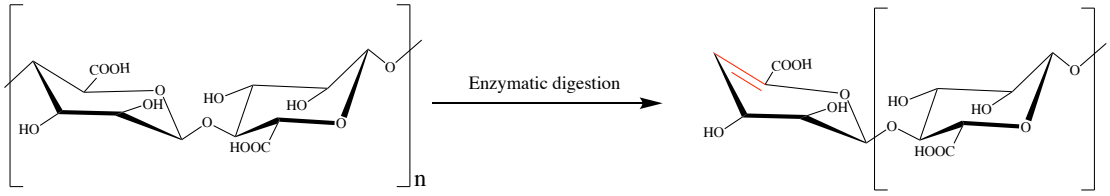

Figure 2.3 Enzymatic digestion of alginate.

Table 2.3 Experimental conditions for the preparation by some enzymatic digestion methods.

Preparation conditions	Enzyme sources	Product details	References
Alginate solution incubated with alginate lyase for 5 h.	*Isoptericola halotolerans CGMCC 5336*	The DP was 2 to 5.	(Chen et al., 2018)
1% alginate solution incubated with 0.01 mg/ml alginate lyase at 37 °C for 12 h.	*Paenibacillus* sp. str. FPU-7	The DP was 3 to 7.	(Itoh et al., 2019)
1 % PG solution incubated with 0.5 units of enzyme at 30 °C.	*Flavobacterium multivorum*	The Mw was 3.742 kDa	(Boucelkha et al., 2017)
Alginate solution incubated with Alg7A at 30°C for 72 h.	Marine bacterium *Vibrio* sp. W13	The DP was 2 to 8.	(B. Zhu, K. Li, et al., 2019)
10% alginate solution incubated with 13,900 U of Alg2A at 30 °C for 24 h.	*Flavobacterium* sp. S20	The DP was 2 to 8.	(Liu et al., 2020)

5.0 mg/ml alginate solution incubated 6 U of AlgL17 at 35 °C for 8 h, and then additional 3 U of alginate lyase was added to for another 9 h.	*Microbulbifer* sp. ALW1	The DP was 1 to 5.	(Jiang et al., 2019)
0.1 g of alginate incubated with 10 units of enzyme in 9 mL buffer at 50 °C for 8 h.	*Flavobacterium* sp. H63	The DP was 2 to 7.	(Li et al., 2018)
2% alginate solution incubated with AlyM at 45°C for 6h.	Marine bacterium *Microbulbifer* sp. Q7	The DP was 2 to 5.	(Yang et al., 2018)
2 mg of alginate incubated with 1 μg Aly7A in 800 μL reaction buffer at 30°C for 48 h.	*Vibrio* sp. W13	The DP was 1 to 5.	(Hu et al., 2021; Hu et al., 2020)
2 mg of alginate, PG, or PM incubated with 1 μg FsAlgB in 800 μL reaction buffer at 40°C for 72 h.	*Flammeovirga* sp. NJ-04	The DP was 2 to 6.	(B. Zhu, F. Ni, et al., 2019)
0.5% alginate solution incubated with 80 U Alyw201 at 35°C for 40 min.	*Vibrio sp.* W2	The DP was 2 to 6.	(Z. Wang et al., 2020)
2% alginate, PG, or PM incubated with 2 mg/mL Alg17B at 30 °C for 6 h.	Marine strain BP-2 screened and identified from rotted Sargassum	The DP was 1 to 6.	(Huang et al., 2019)
2 mg of alginate, PG, or PM incubated with 1 μg FsAlyPL6 or FsAlgA in 800 μL reaction buffer at 50°C for 24 h.	*Flammeovirga* sp. NJ-04	The DP was 2 to 5.	(Q. Li et al., 2019; Zhu et al., 2017)
Alginate solution incubated with alginate lyase at 45 °C for 10 h.	*Streptomyces violaceoruber*	The DP was 2 to 6	(Wan et al., 2020)
2 mL of alginate lyase was mixed with 100 mL of 1% alginate and incubated at 30 °C for 48 h.	*Flavobacterium* sp. S20	The DP was 2 to 8	(Wan et al., 2021)
25 mg/mL PM solution incubated with 0.3 mg/mL alginate lyase at 37°C for 2 h, and then equal enzyme solution was added for another 18 h.	*Pseudoalteromonas* sp. strain 272	The DP was 2 to 11	(Bi, Xiao, et al., 2021; Bi, Yao, et al., 2021)

4 mg/ml alginate or PM and 100 nM BcelPL6 alginate lyase were incubated at 37°C for120 min	Human gut microbe *Bacteroides cellulosilyticus*	The DP was 2 to 7	(Stender et al., 2019)

Thermal depolymerization is another environmentally friendly method for alginate degradation, which is performed at high temperatures in the solid state. Similar to enzymatic digestion, it was catalyzed simultaneously by protons and hydroxide ions (Holme et al., 2003). Sometimes, thermal depolymerization can also be achieved by general acid-base catalysis using water as a base or acid. However, M-rich alginate is more easily degraded than the G-rich alginate (Xu et al., 2016), which may be related to the structure of alginate mentioned earlier. The thermally degraded alginate was evaluated by NMR spectroscopy and the results suggested that unsaturated uronic acid as a non-reducing terminal, i.e., 4-deoxy-α-L-erythro-hex-4-enopyranosyluronate, was also involved in the thermal depolymerization (Holme et al., 2003). Table 2.4 shows the preparation of AOS by thermal degradation. However, compared with enzymatic digestion, thermal degradation is not widely used in AOS production, which may be due to some disadvantages such as weak depolymerization strength.

Table 2.4 Experimental conditions for preparation by some thermal degradation methods.

Preparation conditions	Product details	References
Raw alginate (in solid state) was heated at 140 °C for 7.5 h.	Mw decreased from about 200 kDa to 80 kDa	(Kelishomi et al., 2016)
Alginate powder was performed in a drying oven held at a constant temperature of 22.5, 36, 60 and 80 °C	Mixture of oligosaccharides	(Holme et al., 2008)
Alginate powder was performed in a drying oven held at a constant temperature of 120, 105, 80 or 60 °C	Mixture of oligosaccharides	(Holme et al., 2003)

2.4.2.4 Separation and structure analysis

In general, AOS are mixtures with different or identical DP and its biological activity is strongly correlated with its purity, Mw and DP. Therefore, a quantitative separation and analysis method is necessary for AOS to obtain the information about the structural determination, which will help in molecular understanding of its structure-function relationship (Chunhua Zhang et al., 2021); (Xie & Cheong, 2021). Thin-layer chromatography (TLC) and high-performance liquid chromatography (HPLC) are the main methods.

TLC is a preliminary separation and detection method to analyze the DP of oligosaccharides, with the advantages of simple sample preparation, simple operation, simple colour rendering, and a relatively low cost. Xu et al. prepared six kinds of AOS and all 2-7 saccharide units were detected by TLC (Xu, Wu, et al., 2014). Huang et al. prepared AOS by from alginate enzymatic digestion and analyzed by TLC. The results showed that the main reaction products of AOS were monosaccharide and trisaccharide (H. Huang et al., 2021). However, the limitation of TLC is its low resolution, which is only suitable for preliminary analysis of oligosaccharides (Xie & Cheong, 2021).

Ion exchange chromatography is a traditional biochemical separation technology belonging to HPLC, which has been widely used in the separation and purification of proteins. Ion exchange generally refers to a reversible example exchange reaction between the stationary and mobile phases used to separate various molecules that can be dissociated (Ebere et al., 2019). Because of containing polar groups, carboxyl

group, this provides a premise for the separation of AOS by ion exchange chromatography. High-performance anion exchange chromatography in tandem with a pulsed amperometric detector (HPAEC-PAD) is a method that has high resolution for AOS separation. Soukaina et al. prepared AOS by controlled radical hydrolysis and obtained a single low molecular weight fraction (Mw ≤ 5.5 kDa), which was analyzed by HPAEC-PAD and the results showed that the DP was 2 to 24.

In the separation and purification of AOS, gel filtration chromatography/size exclusion chromatography, belonging to HPLC, is more widely used than ion exchange chromatography. The principle of gel filtration separation is to use eluent to clean the oligosaccharide samples through a column with a specific separation medium and separate it according to different molecular sizes (Kumar & Nayak, 2019). The main separation media are glucan gel (Sephadex), agarose gel, and polyacrylamide gel (Bio-gel). This method is also suitable for desalination and other impurities. In addition, this method can be used to estimate the DP. Yang et al. have prepared the oligomannuronates from PM via oxidative-reductive degradation using H_2O_2 on a Bio-gel P-4 column, and the results showed that the DP was 2 to 7 (Yang et al., 2004). Xu et al. have isolated and purified the oligosaccharide prepared from PG via enzymatic digestion by a P-6 Bio-gel chromatography, showing that the DP of oligosaccharide was 2 to 9, and removed the phosphate in each fraction a P-2 Bio-gel (Xu, Wu, et al., 2014). Chen et al. have prepared an enzyme hydrolyzed AOS and then used Sephadex G-15 column to remove salt and Bio-Gel P2 column to measure the DP, which was 2 to 9 (Chen et al., 2018).

The detailed structure information of AOS was mainly obtained by electrospray ionization mass spectrometry (ESI-MS) and matrix-assisted laser desorption ionization time of flight mass spectrometry (MALDI-TOF-MS) (Ushasree et al., 2021). MALDI has higher sensitivity, lower sample consumption and resistance to contaminants than ESI. However, combining MALDI with the separation technologies currently in use is a challenge. In contrast, ESI-MS can be easily coupled with HPLC online to enable pre-concentration, analytical separation and precise quantification, providing higher analytical sensitivity and selectivity (Kuklenyik et al., 2011). MALDI-TOF MS was used to determine the DP of oligosaccharide prepared from PM unsaturated AOS by alginate lyase, and the result showed that the DP of oligosaccharide ranged from 2 to 7, which was also quantified by LC-ESI-MS (Stender et al., 2019). In our previous studies, the DP of oligosaccharide prepared from PG (GOS) and PM (MOS) via enzymatic digestion was determined by ESI-MS, which was 2-8 (Xu et al., 2015) and 2-11 (Bi, Yao, et al., 2021), respectively. Zhang et al. attempted ESI-MS and collision induced dissociation for sequence determination of AOS derived from alginate, PG, and PM by partial depolymerization using either alginate lyase or mild acid hydrolysis and found this method was effective in determining the sequence and linkages of homo and hetero AOS (Zhang et al., 2006). Nuclear magnetic resonance (NMR) spectroscopy also is a method to analyse the detailed structure information of AOS (Iwamoto et al., 2002). The existence of the double bond at the C-4 and C-5 positions in AOS was confirmed by the chemical shift in the downfield region of signals at C-4 and C-5 positions of the deoxy residue (Zhang et al., 2004). Yang et al. used 1D-NMR

to analyze the structure of oligomannuronates obtained from H_2O_2 degradation and found that the H signal of the obtained oligosaccharides disappeared at 4.8 ppm to 5.2 ppm, and the C signal also disappeared at about 94 ppm. Combining with 2D-NMR, the structure of the oligosaccharides was further confirmed, and it was found that that the oxidation occurred on the reducing-end C1, which is oxidized to a carboxyl group (Yang et al., 2004). However, the proton signals on the AOS are mostly stacked in a narrow range, and when the composition of AOS is complex, its NMR spectrum is difficult to elucidate (Liu et al., 2019). In addition, for NMR analysis, a highly enriched AOS isomer is usually required and a relatively large number of pure analytes are required in order to obtain a defined spectrum (Ushasree et al., 2021).

2.5 Traditional Application in food

2.5.1 Hydrocolloidal gel

Hydrocolloidal gel particles have potential application value in the food, chemical and pharmaceutical industries. Alginate gel particles with the advantages of good biocompatibility, non-toxic, biodegradable, low price and simple production, are one of the most widely used gel particles at present (Ching et al., 2017). Also, they are particularly valuable for encapsulating applications, protecting cells, DNA, nutrients and microorganisms, and also enabling the slow release of flavors, minerals and drugs by encapsulating in gel particles (Özbilenler et al., 2020).

Alginate has the ability to form ionic gel in the presence of multivalent cations, which is widely utilized in the encapsulation of active substance in the food industry.

The binding of alginate with divalent cations has high selectivity and the affinity of alginate to cations is Mn < Zn, Ni, Co < Fe < Ca < Sr < Ba < Cd < Cu < Pb, which depends directly on G content in the alginate (Mørch et al., 2006). This is because in the formation of gels, it is mainly G that binds to divalent cations, and the mechanism is the dimerization of G, resulting in a tightly bound polymer whose structure forms an "egg-box" shaped junction region (Ching et al., 2017). Alginate with high G content can format gels which are strong and brittle, with good thermal stability, while alginate gels with high M content are weak and more elastic, with good freeze-thaw properties (Draget et al., 1994); (Ching et al., 2017; Xu et al., 2016). In practical applications, considering toxicity and other reasons, the calcium ion is the most widely used to prepare the alginate gel. At present, researchers have not only used alginate to prepare gels, but also introduced some new substances to enhance colloidal properties. A new core-shell structure (sporopollenin exine capsules as the core and Ca-alginate (Alg)/carboxymethylpachymaran (CMP) gel as the shell) was developed to protect probiotics, both to improve the storage and lyophilization stability of probiotics and to achieve sustained release in the gastrointestinal tract (Deng et al., 2021). A double cross-linked emulsion gel with a dense mesh structure and high viscoelasticity was prepared by cross-linking zein with transglutaminase and alginate with the calcium ion. By comparing the effects of gels on the photostability and bio-accessibility of co-loaded polyphenols (curcumin and resveratrol), it was found that double crosslinked emulsion gels had higher photostability and bio-accessibility than single crosslinked emulsion gels (Yan et al., 2021). However, a major limitation of

calcium-alginate gels is that they become unstable in the presence of calcium chelators such as citrate, phosphate, carbonate and lactate (Ching et al., 2017).

In general, AOS formed during the depolymerization process do not have the ability to form gels (Zimoch-Korzycka et al., 2021). But new research has also reported that AOS can be used as a stabilizer for zein to prepare complex nanoparticle gel for the delivery of curcumin, which can protect Zein during gastrointestinal digestion, resulting in a good sustained-release effect of curcumin in the intestinal tract (Jiang et al., 2021). Also, our new study showed that AOS prepared from PG via enzymatic digestion has a good prospect as a stabilizer to fabricate the nano-emulsion gel to encapsulate hydrophobic nutrients, which could be applied as a food-grade component in the beverage and other food fields (unpublished data).

2.5.2 Film packaging

Environmentally safe and biodegradable natural polysaccharide materials are a new type of film packaging, mostly made from extracts of by-products of fruit and vegetable processing, which not only maximizes the value of fruit and vegetables, but also reduces waste and improves the environment (Li et al., 2021). Alginate has unique colloidal properties, including thickening, stabilization, suspension, film formation, gel formation and emulsion stabilization. This allows films made from alginate to be strong and resistant to oil and grease (Umaraw & Verma, 2017), but to have poor water resistance due to their hydrophilicity (Maizura et al., 2007). Therefore, alginate is generally mixed with other biopolymers, to improve the mechanical properties of the

films. Ismillayli et al. reported that the carboxyl group of alginates and the ammonium group of chitosans can have electrostatic interaction. Under the same thickness, the tensile strength and resistance to pH changes of alginate-chitosan film was higher than that of natural alginate film and chitosan film. In addition, the alginate-chitosan membrane has good antibacterial potential against *Staphylococcus aureus* and *Escherichia coli*(Ismillayli et al., 2020). Reyes-Avalos et al. reported that alginate-chitosan coating is an excellent post-harvest technology for preserving not only the organoleptic and sensory properties of figs during cryopreservation, but also their bioactive constituents by modifying the internal atmosphere of figs (Reyes-Avalos et al., 2016; Reyes-Avalos et al., 2019).

The complex film prepared by alginate only or with other polymers combined with some substances with antibacterial and antioxidant activities not only has good mechanical properties, but also has some special bio-activities. For example, Gelatin–alginate film containing 1.5% oregano essential oil could effectively delay bacterial growth on rainbow trout (*Oncorhynchus mykiss*) slices, including lactic acid bacteria, *Pseudomonas spp.* and Enterobacteriaceae (Kazemi & Rezaei, 2015). While the gelatin-alginate film was prepared by incorporating tea polyphenols, not only were the mechanical properties of the films improved, but also their antioxidant activity (Dou et al., 2018).

The vitamin C addition to the alginate based edible film decreased the tensile strength of the film, but it made the film more stable and it could store at refrigeration in the dark for up to five months (da Silva Bastos et al., 2009). A new polysaccharide

composite film packaging with good tensile strength and elongation at break was prepared from citrus pectin and alginate. After being crosslinked with calcium chloride, the water solubility of the film decreased, and the thermal stability increased. The addition of pterostilbene as an antioxidant reduced the values of tensile strength and elongation at break, but gave better water resistance and oxidation resistance, showing that this film could be utilized as an excellent antioxidant packaging material in fruit and vegetable preservation (Li et al., 2021). The addition of epigallocatechin gallate into alginate and carboxymethyl cellulose prepared edible films could improve the tensile strength of the edible films and reduce their elongation at break, and also showed strong antioxidant activity in fatty foods (Ruan et al., 2019).

Alginate films incorporated with lemon-grass oil and glycerol, which acted as a natural antimicrobial agent and plasticizer, respectively, are also effective in inhibiting the growth of *Escherichia coli* (Maizura et al., 2007). Adding AgNPs to alginate-based edible film improved the tensile strength and elongation at break, and the growth inhibition rate of alginate-based edible film was higher than 79% in all strains (Martínez-Molina et al., 2021). Adding hawthorn berry (*Crataegus pinnatifida*) extract (Lim et al., 2021), mulberry (*Morus australis*) leaf extract (Kuan et al., 2020) or essential oils (D. Zhu et al., 2019) to alginate-based edible film made not only similar mechanical property improvements and antibacterial effects, but also can improve the sensory sensation of foods (Mahcene et al., 2021). In films prepared from alginate/pullulan and capsaicin, with the increase of capsaicin content, the light transmittance, elongation at break, and moisture content of the films decreased, while

the tensile strength, permeability and surface contact angle increased. In addition, the film has good antibacterial performance against *Escherichia coli* and *Staphylococcus aureus* and has achieved good results in apple protection (Zhang et al., 2018).

Alginate is widely found in seaweed, so the alginate-based film has the advantage of low cost. Although the alginate-based film has poor water resistance, its compatibility with other polysaccharides can ameliorate this shortcoming. Also, the addition of some active substances into the film endows the film with good antibacterial and antioxidant activities, thus extending the shelf life of food. Up to now, there have been few studies on the application of AOS in the preparation of edible films, possibly due to poor colloidal properties. However, AOS have good biological activity and may play certain functions in other polysaccharide-based films.

2.6 Beneficial health effects and potential applications of alginate and AOS

2.6.1 Immunomodulatory activities

The innate immune system uses a variety of receptors on the cell surface to recognize pathogens and initiate immune responses. These receptors play roles in regulation, complement activation, phagocytosis, initiation of pro-inflammatory signalling pathways, and induction of apoptosis (Gordon, 2002). *In vitro* and *in vivo* studies have shown that both alginate and its oligosaccharides have immunomodulatory activities, but the specific structure-activity relationship of oligosaccharides is better than that of polysaccharides (Xu, Bi, et al., 2014; Xu, Wu, et al., 2014).

Kurachi et al. compared the abilities of alginate polymers with different Mw and M/G rations on the tumour necrosis factor (TNF)-α production in RAW264.7 cells, confirming that alginate treatment could induce TNF-α release in RAW264.7 cells (Kurachi et al., 2005). Yang et al. found that alginate caused innate immune responses in macrophage-like cells (RAW264.7 cells), inducing the production of cytokines, such as interleukin (IL)-1β, IL-6, IL-12, and TNF-α with time and dose-dependence, was through a nuclear factor kappa-light-chain-enhancer of activated B cells (NF-κB) signalling pathway activation (Yang & Jones, 2009). Further study showed that alginate can not only activate the NF-κB signalling pathway, but also the p38 mitogen-activated protein kinase (MAPK) signalling pathway by Toll-like receptor 4 (TLR4) activation in RAW264.7 cells, and then enhance the intracellular phagocytosis of gold nanoparticles, fluorescent microspheres and immunoglobulin G (IgG)-opsonized *Staphylococcus aureus* (Bi et al., 2017). Alginate also can attenuate the systemic anaphylaxis response in compound 48/80-induced Wistar rats via the suppression of NF-κB activation (Jeong et al., 2006). In addition, the alginate aqueous solution (Mw = 108 kDa) also exhibited non-Newtonian characteristics, including viscoelasticity and shear-thinning behaviour, which may be a significant factor affecting the ability of the gastrointestinal tract to contact and take in ovalbumin, the main allergen that causes egg allergy. In ovalbumin-induced mouse models of egg allergy, oral alginate aqueous solution can effectively attenuate the occurrence of allergic reactions, decrease the histamine IgE and IL-4 levels in serum, increase the level of IFN-γ in serum, increase the number of Treg cells in spleen tissues, and inhibit differentiation of T-helper type 0 (Th0) cells into Th2 cells

(Yu et al., 2020). Further research showed that oral alginate can restore the ovalbumin-induced gut microbiota disorder, recovering the richness and diversity of *Alloprevotella, Bacteroides*, *Parabacteroides* and *Rikenellaceae_RC9_gut_group* (Yao et al., 2021).

Interestingly, AOS produced by depolymerization with alginate lyase from alginate or alginate-derived PG and PM increased cytokine secretion from RAW264.7 cells more than unprocessed polysaccharide (Ueno et al., 2015). Iwamoto et al. confirmed that unsaturated AOS prepared by enzymatic digestion induced cytokine secretion, including TNF-α, granulocyte colony-stimulating factor (GCSF), monocyte chemoattractant protein-1 (MCP-1), regulated upon activation normal T cell expressed and secreted (RANTES), granulocyte macrophage (GM)-CSF, IL-1α, IL-1β, IL-6, IL-9, and IL-13, from RAW264.7 cells in a structure-depending manner, while the activities of saturated AOS prepared by acid hydrolysis, as well as PG and PM, were fairly low or only trace levels (Iwamoto et al., 2005). Among that, the most potent activities were G8 and M7, and in TLR2 and TLR4 antibodies treated RAW267.4 cells, the G8 and M7 induced cytokine secretion was significantly reduced. These results suggested that G8 and M7 may have the most suitable molecular size or entire structural conformation as stimulants for cytokine secretion and they may stimulate innate immunity through the pattern recognition receptors on macrophages (Iwamoto et al., 2005). Intraperitoneal administration of 700 mg/kg AOS prepared by enzymatic hydrolysis stimulated the production of more than 20 cytokines and modulated the activation of normal T cells (Yamamoto et al., 2007b). Further study on the results of the structure-

activity relationship from the Bio-Plex assay system showed that unsaturated G oligosaccharides (G3–G6) and unsaturated M oligosaccharides (M3–M6) prepared by alginate lyase-digestion of PG and PM could significant induce cytokine secretion on RAW264.7 cells, and unsaturated M oligosaccharides tended to be more potent than unsaturated G oligosaccharides (Yamamoto et al., 2007a). A similar structure-activity relationship study was reported by Xu et al, and the results showed that the immunomodulatory effects of unsaturated AOS obtained by enzymatic digestion were greater than those of AOS obtained by oxidative-reductive degradation and acid hydrolysis, as well as PM and PG (Xu, Wu, et al., 2014). However, compared with the report from Yamamoto et al, there is a contrary conclusion that the immunomodulatory activity of unsaturated G oligosaccharides prepared by alginate lyase-digestion of PG was better than that of unsaturated M oligosaccharides prepared by alginate lyase-digestion of PM, including inducing the production of nitric oxide (NO), reactive oxygen species (ROS), and TNF-α in RAW264.7 cells (Xu, Wu, et al., 2014). Further mechanistic studies suggest that unsaturated G oligosaccharides regulate the production of these immune mediators in RAW264.7 cells by activating the NF-κB and MAPK signalling pathways (Xu, Wu, et al., 2014). The more detailed molecular mechanisms of unsaturated G oligosaccharides activating macrophages was reported by Fang et al. (Fang et al., 2017). The improvement of innate immunity by unsaturated G oligosaccharides was dependent on the TLR4 recognition and activation of differentiation protein 2 (MD2), resulting in the activation of the myeloid differentiation factor 88 (MyD88) and pro-inflammatory signalling cascades, including

the activation of phosphatidylinositol-3-kinase (PI3K) and protein kinase B (Akt or PKB). Subsequently, the NF-κB, MAPK and mechanistic target of rapamycin (mTOR) signalling pathways was activated. All these events contribute to the production of improvement of innate immunity in macrophages triggered by unsaturated G oligosaccharides (Fang et al., 2017). Morphological analyses revealed that unsaturated G oligosaccharides stimulated RAW264.7 cells with cytoskeleton remodelling and changes in the morphologies (Xu et al., 2015). Proteomic analyses with two-dimensional electrophoresis and MALDI-TOF/TOF-MS confirmed that unsaturated G oligosaccharide treated RAW264,7 cells activated not only a NF-κB signalling pathway, but also inflammation, antioxidant, glycolysis, cytoskeletal processes and translational elongation signalling pathways (Xu et al., 2015).

Excessive macrophage activation is an important cause of inflammation, which is a double-edged sword that must be carefully regulated. Chronic or excessive inflammation is involved in the pathogenesis of almost all human degenerative diseases，including Alzheimer's disease, diabetes, cancer, cardiovascular diseases and so on (Mouton et al., 2020). G oligosaccharides prepared by oxidative-reductive degradation of alginate-derived PG significantly attenuated the production of NO, prostaglandin E2 (PGE2), and ROS, the expression of inducible nitric oxide synthase (iNOS) and cyclooxygenase (COX)-2, and the secretion of pro-inflammatory cytokines including TNF-α, IL-1β and IL-6 in lipopolysaccharide (LPS)-activated RAW 264.7 cells by blocking the LPS-induced TLR4 signalling pathway and its downstream NF-κB and MAPK signalling pathway, and other forms of AOS showed no anti-inflammatory

activities (Zhou, Shi, Gao, et al., 2015). Also, AOS prepared by oxidative-reductive degradation of alginate showed similar anti-neuroinflammatory activities, inhibiting pro-inflammatory mediator overproduction in LPS or β-Amyloid (Aβ)-triggered BV2 microglia (Zhou, Shi, Bi, et al., 2015). Although PM has no such activity, Se-PM derived from the selenation of PM exhibits similar anti-inflammatory and neuroprotective effects (Bi, Lai, Cai, et al., 2018; Bi, Lai, Han, et al., 2018; Bi et al., 2019). Inflammation is also involved in food allergies. Oral administration of AOS prepared by enzymatic hydrolysis of alginate, with an average DP of 4.4, could significantly inhibit Th2 activation and suppress serum IgE production by increasing IL-12 secretion, enhancing Th1 cells' response in bovine β-lactoglobulin-induced BALB/c mice (Yoshida et al., 2004); (Uno et al., 2006).

2.6.2 Antioxidative effects

Oxidative stress, caused by a lack of cellular balance between pro-oxidants and antioxidants, is characterized by an excessive increase in ROS and a weak protective mechanism that leads to damage to key biomolecules. Oxidative stress is closely related to initiation and progression of many diseases, including cancer, arterial diseases, neurodegeneration, diabetes and so on (Pisoschi et al., 2021). Unsaturated AOS prepared by enzymatic digestion or thermal depolymerization were identified as effective free radical scavengers *in vitro*.

In vitro, the 2,2'-Azino-di-(3-ethylbenzothiazo line)-6-sulfonic acid (ABTS) and superoxide radical scavenging assays confirmed that the antioxidant properties of AOS

prepared from alginate by thermal depolymerization changed depending on concentration and treatment time, which was possibly based on hydrogen or electron donation properties (Kelishomi et al., 2016). Similarly, AOS prepared from alginate by enzymatic digestion using an extracellular alginate lyase from the marine bacterium *Microbulbifer sp.* ALW1 displayed scavenging of radicals (DPPH, ABTS+, and hydroxyl) and reducing power (Zhu et al., 2016), and AOS prepared from alginate by alginate lyase (from *Sphingobacterium*-mediated depolymerization) were able to completely inhibit lipid oxidation in emulsions and radical scavenging activity against $ABTS^{+}$, hydroxyl, and superoxide radicals (Falkeborg et al., 2014). In addition, AOS prepared from alginate by enzymatic digestion also showed stronger antioxidant activity *in vitro* than fucoidan oligosaccharides and chitosan oligosaccharides on hydroxyl radical scavenging activity (P. Wang et al., 2007).

In H_2O_2/$FeSO_4$-induced NT2 neural cells, treatment with AOS prepared from alginate by enzymatic digestion can inhibit the oxidative damage of cells by upregulating the expression of hemeoxigenase-1 (HO-1), glutamylcysteine synthetase (γ-GCS), heat shock protein (Hsp)-70, nuclear respiratory factor (Nrf)2 and inhibiting caspase-3 and NF-κB (Eftekharzadeh et al., 2010). In another neural cells, treated neuron-like PC12 cells with the same AOS can effectively alleviate the H_2O_2-induced endoplasmic reticulum (ER) and mitochondrial- dependent apoptotic cell death by promoting Bcl-2 expression, while blocking Bax expression, and inhibiting H_2O_2-induced caspase-3 activation (Tusi et al., 2011). The effects of AOS on H_2O_2-induced oxidative stress and apoptosis in human umbilical vein endothelial cells (HUVECs) and the associated

mechanisms was investigated by Zhao et al., and the results showed that AOS protected HUVEC cells against oxidative stress-induced apoptosis by decreasing the expression levels of caspase 3 and Bax, and increasing Bcl-2 expression via regulating the integrin-a/FAK/PI3K pathway (Zhao et al., 2020). Unfortunately, the author does not mention how AOS are prepared, so the structural information is not particularly clear.

At the animal level, the use of AOS to intervene in a variety of diseases has also been reported. Studies showed that AOS (with an average molecular weight < 2000 Da) supplementation in diets could maintain the intestinal integrity of weaned pigs associated with the elevated antioxidant capacity via increasing the activity of catalase, SOD, and GSH both in the jejunal and ileal (Wan et al., 2017; Wan et al., 2018). Administering C57BL/6J mice with AOS via gastrogavage significantly delayed the progress of cataracts induced by D-galactose via inhibiting oxidative stress and up-regulating antioxidant system, including inhibited p53 protein expression and increased SOD, Nrf2 and HO-1 expression (Feng, Yang, et al., 2021). Treating rats with monocrotaline-induced AOS can effectively prevent MCT-induced pulmonary vascular remodelling via inhibition of the TGF-β1/p-Smad2 signalling pathway, as well as the expression of malondialdehyde and nicotinamide adenine dinucleotide phosphate oxidase, suggesting that the anti-oxidative effects of AOS in pulmonary arteries may contribute to the alleviation of pulmonary hypertension and pulmonary vascular remodelling (Feng et al., 2020). A study of the potential effects of AOS on kidney aging and its possible mechanisms showed that treatment with AOS can effectively

ameliorate D-galactose-induced kidney aging in C57BL/6J through increasing the expression of antioxidant enzymes and activation of the Nrf2 signalling pathway (Pan et al., 2021). A similar study on D-galactose-induced cardiac ageing in C57BL/6J mice showed that AOS treatment could decrease the ROS production and oxidative stress status in the heart tissue, which, in turn, inhibited cardiac mitochondria from being destroyed, resulting in alleviation of cardiac ageing alleviation (Feng, Liu, et al., 2021). However, these above studies did not mention the detailed preparation method of AOS, so the structural information of AOS was not clear. Unsaturated AOS prepared from enzymatic digestion has been shown to be effective in heart protection by its significant antioxidative activity. Pretreatment with unsaturated AOS could protect against myocardial ischemia/reperfusion (I/R) injury in mice by inhibiting nitrative/oxidative stress-mediated apoptosis via decreasing 3-nitrotyrosine content and superoxide generation (Guo et al., 2017). Also, pretreatment with unsaturated AOS increased the survival rate of doxorubicin (DOX) insulted mice, improved DOX-induced cardiac dysfunction and attenuated DOX-induced myocardial apoptosis by attenuating the expressions of gp91 (phox) and 4-hydroxynonenal (4-HNE) (Guo et al., 2016).

The *in vitro* antioxidant mechanism of unsaturated AOS have been studied. Şen et al. claimed that the radical scavenging activity of alginate was found to be dependent on its molecular weight (Şen & Atik, 2012). Falkeborg et al. reported that the radical scavenging activity of AOS is suggested to originate mainly from the presence of the conjugated alkene acid structure formed during enzymatic depolymerization and the

proposed mechanism may be hydrogen abstraction, presumably from the hydrogen-bonded hydrogens, combined with radical addition to the conjugated alkene acid structure yielding an addition product stabilized by resonance (Falkeborg et al., 2014). *In vivo*, the unsaturated AOS can reduce oxidative stress by increasing the activity of antioxidant enzymes, leading to antagonized oxidative damage caused by the change of the external environment. The antioxidant activity of AOS would contribute to its application in the food system.

2.6.3 Neuroprotective effects

Alzheimer's disease (AD) is the most common type of dementia in aged people with the disorder clinically characterized by the cognitive deficit and pathologically characterized by the extracellular senile plaques mainly composed by Aβ and neurofibrillary tangles composed by hyper-phosphorylated tau protein (Lane et al., 2018). In ordinary life, the production and clearance of Aβ and hyper-phosphorylated tau protein are in a dynamic balance. However, the failure of clearing Aβ and hyper-phosphorylated tau protein is regarded as an essential mechanism to exacerbate the pathological process of AD (Bhatia & Sharma, 2021). Aβ oligomer and tau protein oligomer-induced neuro-inflammation and oxidative stress also play an important role in the progression of AD (Uddin et al., 2020). As we mentioned above, AOS prepared by oxidative-reductive degradation of alginate could attenuate neuroinflammation in Aβ-induced BV2 microglia. Also, this AOS exerted a positive effect Aβ-induced cytotoxicity and augmented microglial phagocytosis of Aβ by TLR4 activation (Zhou, Shi, Bi, et al., 2015). Treated with AOS prepared from alginate by enzymatic digestion

as mentioned above can not only alleviate the oxidative stress induced by H_2O_2 in neuron-like PC12 cells, but also can inhibit the Aβ-induced neural damage in adult male Wistar rats (Tusi et al., 2011), and in NT2 neural cells, treated with the same AOS can suppress the Aβ formation, which was induced by oxidative stress (Eftekharzadeh et al., 2010). These results raised the possibility of developing AOS prepared from alginate by enzymatic digestion as a potential neuroprotective agent.

The acidic oligosaccharide sugar chain (AOSC) is an alginate-derived oligosaccharide depolymerized by alginate lyase and rich in mannuronic acid blocks, with an average molecular weight of 1300 Da (J. Hu et al., 2004). AOSC treatment could significantly inhibit the apoptosis induced by Aβ and H_2O_2 in SH-SY5Y cells by reducing the elevated level of intracellular calcium concentration and suppressing the generation of ROS (Fan et al., 2005; J. Hu et al., 2004). Similar to the low-molecular-weight Glycosaminoglycans, surface plasmon resonance analysis has demonstrated that AOSC could interact with Aβ and block the fibril formation of Aβ via binding to the HHQK epitopes, which may be responsible for its anti-cytotoxic effects in Aβ-induced cells (J. Hu et al., 2004; Liu et al., 2008). In an *in vitro* neuroinflammatory cell model, Aβ-induced rat primary cortical astrocytes, a similar neuroprotective effect of AOSC was found. Results showed that AOSC treatment inhibited the reactive phenotype of astrocytes, blocked cellular oxidative stress, reduced the production of TNF-α and IL-6 and prevented the influx of calcium (S. Wang et al., 2007). In scopolamine-induced male Wistar rats, AOSC treatment can alleviate the memory damage caused by scopolamine in mice, which is manifested by shortened escape latency and swimming

distance, and increased swimming time in the Morris water maze (Fan et al., 2005). Biochemical index analysis in the cerebral cortex and hippocampus showed that AOSC ameliorated oxidative injuries in the brain caused by scopolamine by increasing the activities of uperoxide dismutase (SOD), glutathione peroxidase (GSH-Px) and ATPase (Fan et al., 2005). The Gial derived neurotrophic factor (GDNF) associated signalling pathway, a regulator on neuronal cell differentiation during development and protection against neurodegeneration, was increased in AOSC treated PC12 cells, suggesting a clinical benefit of AOSC by enhancing the neuroprotective function of GDNF (X. Wang et al., 2007). However, structure-activity relationship studies showed that sulfated AOSC inhibited GDNF associated signalling events, illustrating the importance of the structure and charge of oligosaccharide in playing their neuroprotective role (X. Wang et al., 2007). These results indicated that AOSC has a good potential in the intervention of AD, and surface plasmon resonance (SPR) assay showed that AOSC is able to cross the blood-brain barrier (BBB), which provided a basis for further understanding the therapeutic value of AOSC (Guo et al., 2006). Liu et al. mentioned that a Phase I clinical trial of AOSC in China as an anti-AD drug candidate was completed before 2008, and they confirmed that 349 proteins including clathrin, adaptor protein-2 (AP-2) and amyloid precursor protein (APP) in rat neuro bound to AOSC using affinity chromatography and LC-MS/MS analysis (Liu et al., 2008). However, since then, there has been only one report about AOSC in the treatment of AD, which reported that AOSC could attenuate the rapid disruption of hippocampal long-term potentiation (LTP) *in vitro* induced by Aβ-oligomers due to the prevention on the Aβ

aggregation by AOSC (Chang et al., 2014), and no relevant reports have involved clinical studies on AOSC.

Unsaturated mannuronate oligosaccharide (MOS) also is an alginate-derived oligosaccharide depolymerized by alginate lyase and rich in mannuronic acid blocks, with the DP of 2-11(Bi, Yao, et al., 2021). Similarly, MOS also can significantly inhibit the aggregation of Aβ oligomer *in vitro*. Furthermore, in two Alzheimer's disease cell models, N2a-sw cells and Triple-transgenic AD mice primary cortex neurons, MOS treatment resulted in decreasing the expression of Aβ by inhibiting the expression of APP and BACE1/β-secretase. Further studies of molecular mechanisms showed that MOS treatment also can enhance the autophagy to promote clearance of APP and Aβ in AD cell models (Bi, Yao, et al., 2021). In another AD cell model with tau protein as a pathological feature (HEK293/Tau cells), MOS treatment decreased the phosphorylation levels of Tau protein on the sites of Ser404, Ser396, Ser262, and Ser202 as well as the total Tau protein level, which was involved in reducing the activity of glycogen synthase kinase-3β (GSK-3β) by decreasing its phosphorylation levels on the sites of Y216 and increasing phosphorylation levels on the sites of S9. In addition, MOS-induced decrease in Tau protein expression in HEK293/Tau cells was attenuated by the addition of an autophagy inhibitor, confirming the involvement of autophagy (Bi, Xiao, et al., 2021). These studies suggest that MOS have a multi-target effect in the intervention of AD, in which autophagy may play an important role.

The abnormal pattern of gut bacteria is correlated with increased differentiation and proliferation of peripheral T cells, elevated infiltration of a pro-inflammatory

subtype of T cells into the brain and activation of a resident pro-inflammatory subtype of microglia, as well as the appearance of AD pathological markers such as Aβ plaques (Poo, 2020). GV-971, a M oligosaccharide with a DP of 2-10, has demonstrated solid and consistent cognition improvement in a phase 3 clinical trial in China. Similar to oxidation-degraded AOS, the reducing ends of GV-971 are opened and C-1 position was a carboxyl group (Wang et al., 2019). As mentioned by Wang et al., GV-971 can pass BBB in its original form which was regulated by the type 1 glucose transporter (GLUT1). GV-971 can bind to several subregions of Aβ, inhibiting the formation of Aβ fibrin. It also can promote microglia-mediated Aβ phagocytes *in vitro* and reverse the cognitive impairment of a variety of AD models (Wang et al., 2019). Wang et al. also reported that treatment with GV-971 restored the normal gut microbiota, reduced the level of inflammatory cells and Aβ plaques in the brain, and ameliorated cognitive impairment of the AD model mice (Wang et al., 2019). In November 2019, GV-971 was approved by the China Food and Drugs Administration for the treatment of mild to moderate patients diagnosed with Alzheimer's diseases, to improve cognitive function (Cheng et al., 2020). However, Cheng et al. also reported that the use of GV-971 induced liver injury in an Alzheimer's disease patient (Cheng et al., 2020).

In 2013, Jiang et al. synthesized a series of truncated derivatives of the oligomannurarate 971 which was derived from a marine plant and has shown neuroprotective effects. They also investigated the effect of these derivatives against Aβ peptide toxicity *in vitro*. They found that synthetic homogeneous short chain β-(1,4)-D-mannans significantly attenuated Aβ-induced toxicity in SH-SY5Y cells and they,

like oligomannurarate 97, also have the potential to intervene in AD (Jiang et al., 2013). This was confirmed by Liu et al. who found that supplementation of mannan oligosaccharide significantly attenuated the cognitive and mental deficits in 5×FAD mice and this could be partly explained by the reshaped microbiome and enhanced SCFAs formation in the gut (Q. Liu et al., 2021).

2.6.4 Antimicrobial activity

In the case of infection, bacterial biofilms provide resistance and tolerance to host immune defenses and antibiotics, enabling their populations to survive in conditions that would destroy their planktonic counterparts. Thus, the destruction of biofilms is a key step in eradicating persistent bacterial infections, which have been seen in many types of chronic diseases (Wang et al., 2016). AOS have shown strong bacteriostatic effects on some pathogenic bacteria of plants and animals. AOS prepared from alginate by enzymatic digestion using alginase from newly isolated *Flavobacterium sp.* LXA, with an average DP of 6.8, could directly inhibit the growth of *Pseudomonas aeruginosa* (An et al., 2009). Dietary AOS prepared from alginate by enzymatic digestion can also decrease *Salmonella* colonization and improve the intestinal barrier function and performance of chickens (Yan et al., 2011).

OligoG, also named OligoG CF-5/20, was generated from alginate extracted from brown seaweed *Laminaria hyperborean* with 10-15 G monomer residues and an average molecular weight of 3200 Da, which has been in phase IIb/III clinical trials in cystic fibrosis (CF) patients (Oakley et al., 2021). Based on conventional and robotic

MIC screening and microscopic analyses of biofilm structure, OligoG was able to perturb multi-drug-resistant (MDR) bacteria by modulating biofilm formation and persistence and reducing resistance to antibiotic treatment. OligoG increased (up to 512-fold) the efficacy of conventional antibiotics against important MDR pathogens, including *Pseudomonas*, *Acinetobacter*, and *Burkholderia spp*., appearing to be effective with several classes of antibiotic. Increasing concentrations of OligoG were shown to have a direct effect on the quality of the biofilms produced and on the health of the cells within that biofilm, including decreased biomass and increased intercellular spaces, with the bacterial cells themselves becoming distorted and uneven due to apparently damaged cell membranes (Khan et al., 2012). On oral biofilms, OligoG was biocidal to *Porphyromonas gingivalis*, but not *Streptococcus mutans* (Roberts et al., 2013). The effects of OligoG on the biofilm-disrupting was assessed by minimum biofilm eradication concentration (MBEC) assays *in vitro* and the results showed that 5% OligoG significantly reduced the MBEC for colistin from 512 μg/ml to 4 μg/ml after 8 h. And in an *in vivo* mice model of chronic biofilm infection by tracheal instillation of a mucoid clinical isolate of *Pseudomonas aeruginosa*, OligoG disrupted the biofilm in a dose-dependent manner over 24 h, with up to a 2.5-log reduction in CFU in the infected mouse lungs (Wang et al., 2016).

Powell et al. found that binding to a bacterial surface modulated surface charge, induced microbial aggregation, and inhibited motility by OligoG represented important direct mechanisms by which antibiotic potentiation and biofilm disruption is affected (Powell et al., 2014). However, in Gram-negative bacteria, OligoG had

virtually no membrane-perturbing effects. Also, with lipopolysaccharide (LPS) surface charge, aggregation and structure were unaltered in the presence of OligoG, suggesting that the antimicrobial effects of OligoG are not related to the induction of structural alterations in the LPS or cell permeability (Pritchard, Powell, Khan, et al., 2017). Although there was no interaction with LPS, OligoG was shown to disrupt the biofilm exopolysaccharide network. This disruption of the exopolysaccharide structure was not simply related to interaction between OligoG and the high-molecular-weight pseudomonal M-block alginate, but rather may reflect modification of the quinolone signal within the biofilm, as well as interactions with Ca^{2+} and DNA (Pritchard, Powell, Jack, et al., 2017). Powell et al. confirmed the mechanistic importance of direct interaction of OligoG with Ca^{2+} in impairing the formation and facilitating disruption of the extracellular polymeric network of *Pseudomonas aeruginosa* biofilms (Powell et al., 2018). Further mechanism studies have found that OligoG induced modification of the *lasI-lasR* and *rhlI-rhlR* quorum-sensing systems in *Pseudomonas aeruginosa*, which may influence critical down-stream functions such as virulence factor production and biofilm formation (Jack et al., 2018).

OligoG also potentiated the antimicrobial effect of antibiotics against oral pathogen-related biofilms. For overcoming the resistance to colistin, an oligoG–polymyxin conjugate was generated and antimicrobial susceptibility tests demonstrated that oligoG–polymyxin conjugates had similar antimicrobial efficacy of ester and amide-linked conjugates to that of the parent antibiotic but with more sustained inhibition of bacterial growth. OligoG–polymyxin conjugates exhibited improved selectivity for

Gram-negative bacteria, including significant disruption of *Pseudomonas aeruginosa* biofilm formation and induced bacterial death (Stokniene et al., 2020). Surface-coating incorporated with cellulose nanofibrils and OligoG was proven to be effective against both single and mixed-species bacterial biofilms (*Pseudomonas aeruginosa* and *Staphylococcus aureus*), with the treated dressings exhibiting impaired bacterial growth, disrupted biofilm architecture, and reduced bacterial virulence factor production *in vitro* (Jack et al., 2019). Another AOS, low molecular weight alginate-derived oligosaccharide by enzymatic digestion, in conjunction with azithromycin, could more effectively inhibit the growth of wild-type and resistant *Pseudomonas aeruginosa* by modulating the bacteria's quorum sensing system, thus regulating biofilm formation and reducing resistance to antibiotic treatment (He et al., 2014). Furthermore, in gastric fluid, this kind of AOS controlled system can maintain the lysozyme activity similar to that of pure lysozyme, maintaining the *E. coli* antimicrobial activity (Park et al., 2016).

In addition, OligoG was shown to modulate the polyanionic components of this host- and bacteria-derived extracellular polysaccharide coating by binding respiratory mucins, resulting in alterations in the mucin surface charge and the porosity of the three-dimensional mucin networks in the CF sputum, improving the viscoelasticity of CF-sputum (Pritchard et al., 2016). Ermund et al. found that OligoG could also detach CF mucus by calcium chelation, promoting the normal mucin unfolding in bacteria induced mucus stagnation (Ermund et al., 2017). Furthermore, OligoG interacted with mucin glycans and terminal moieties, resulting in β-sheet conformational changes in

the mucin peptide, which confirmed the previous observations wherein OligoG modifies the viscoelastic properties of CF sputum (Pritchard et al., 2019). In combined respiratory therapies, inhaled treatment of OligoG may facilitate increased access of therapeutic agents to bacteria and/or the lung cell surface, leading to the drug delivery efficiency improving (Pritchard, Powell, Jack, et al., 2017).

OligoG can not only perturb fungal growth, but can also potentiate conventional antifungal agents, including nystatin, amphotericin B, fluconazole, miconazole, voriconazole and terbinafine, on *Aspergillus* and *Candida* (Tøndervik et al., 2014). OligoG induced marked alterations of *Candida albicans* in hyphal formation and reduced its invasion in the epithelial model, as well as a significant dose-dependent inhibition of phospholipase activity, including phospholipase B and secreted aspartyl proteinases. These results suggested that OligoG could reduce virulence factor expression and invasion by *Candida albicans in vitro*, indicating a potential therapeutic opportunity in the treatment of invasive candidal infections (Pritchard, Jack, et al., 2017). Fortunately, there are no apparent adverse effects from long-term exposure to OligoG, instead resulting in fewer colonies with multidrug resistance (MDR)-associated phenotypes and improved antibiotic susceptibility of *P. aeruginosa* (Oakley et al., 2021).

AOS can not only inhibit the growth and biofilms of microbes, but also promote phagocytosis and killing of bacteria by macrophages through activating cellular immunity. Unsaturated G oligosaccharides prepared by alginate lyase-digestion of PG also can enhance the antibacterial activities of macrophages (Xu, Bi, et al., 2014). In

contrast to PG, unsaturated G oligosaccharides markedly increased the phagocytosis of IgG-opsonized *Escherichia coli* and *Staphylococcus aureus* in THP-1 cells and RAW264.7 cells and reduced the survival of intracellular bacteria in these macrophages. Also, *in vivo* results showed that unsaturated G oligosaccharides, but not PG, significantly improved bacterial clearance in murine acute peritonitis. Inhibitor experiments and mechanism studies indicated that unsaturated G oligosaccharides enhanced the antibacterial activities of macrophages by inducing the expression of Fcγ receptors on macrophages and the activation of NF-κB signalling pathways, which resulted in the production of NO, ROS, and TNF-α (Xu, Bi, et al., 2014).

Although the antibacterial activity of AOS has been well studied, most of the antibacterial literatures reported on AOS are G oligosaccharides, so the roles of the unsaturated terminal structure, molecular size, M/G ratio and other factors in antibacterial are still not understood. In addition, the antibacterial activity of AOS against food microorganisms needs to be further studied to expand its application in food preservation.

2.6.5 Antitumour activity

Cancer is the leading cause of death in economically developed countries and the second most common cause of death in developing countries. Chemotherapy has been an important cancer treatment for a long time, but is often accompanied by a serious side effect. In order to solve the toxicity problem of existing chemotherapeutic drugs, more and more scientists are looking for non-toxic antitumour natural products

in the ocean (Xing et al., 2020).

More than 30 years ago, Fujihara et al. reported the alginate showed antitumour activity against various murine tumours, such as Sarcoma-180 and Ehrlich ascites carcinoma tumours (Fujihara et al., 1984) and found that the higher content of M block in alginate may correlate with the higher antitumour activity (Fujihara & Nagumo, 1992) and that the antitumour activity of alginate could be improved by adding Ca^{2+} (Fujihara & Nagumo, 1993). Now, there are a few reports that alginate is convenient for antitumour directly. Scientists focus on the preparation of a nano-carrier using alginate to deliver more effective antitumour drugs. Details can be found in the **Section 3** of this paper.

Both unsaturated AOS prepared from guluronate and mannuronate oligomers by enzymatically depolymerized significantly inhibited the growth of human leukemic U937 cells with cytotoxic cytokines production (Iwamoto et al., 2003). Unsaturated AOS, prepared from alginate by enzymatically depolymerized using alginate lyase isolated from a marine culture of *Vibrio sp. 510,* and its sulphated substitution derivatives both exhibited no direct cytotoxic effects on tsFT210 cells, but showed tumour inhibition against solid Sarcoma 180. Also, sulphated substitution derivatives were better than the original AOS (X. Hu et al., 2004). Another study showed that AOS prepared from alginate by enzymatically depolymerized represses the growth of residual aneurysms and reduces aneurysm recurrence by indirectly reducing TLR signalling via miR-29b, as well as the inactivation of NF-κB and MAPK signalling pathways and the reducing production of IL-1 and IL-6 (Yang et al., 2017). AOS with DP

5, prepared using alginate lyase from *Agarivorans sp. L11*, showed antitumour functions on osteosarcoma cells. After a 2-year therapy with this AOS for osteosarcoma patients after surgery, the oxidant and inflammatory level was obviously decreased with increased serum levels of SOD, GSH, and high-density lipoprotein cholesterol (HDL-c) but reduced IL-1β and IL-6, and the mean tumour volume was decreased with reduced rates of local recurrence compared with control groups (Chen et al., 2017). AOS of DP 2 to 10 obtained by enzymatic hydrolysis (but the oligosaccharide structure given in the paper is from acid hydrolysis) inhibited human prostate cancer cell growth. The mechanism studies show that AOS treatment attenuated the α2,6-sialylation modification and ST6Gal-1 promoter activity by activating the Hippo/YAP pathway and blocking the recruitment of both the coactivator YAP and c-Jun. *In vivo* data also showed that AOS suppressed the tumourigenicity of prostate cancer cells via the Hippo/ YAP pathway (Han et al., 2019).

It can be found that currently only AOS obtained by enzymatic hydrolysis has been reported as an antitumour agent and other forms of alginate oligosaccharides have not been reported. Also, the molecular mechanism of AOS in antitumour is not uniform and the structure–activity relationships are also not clear, so much more research is needed for analyzing the effects of AOS on antitumour.

2.6.6 Reducing obesity and resistance to diabetes

More than a third of the world's population is overweight or obese, putting them at risk of developing type 2 diabetes (Kleinert et al., 2018). Currently, anti-obesity drugs

on the market generally have side effects and are expensive. Using natural ingredients from food sources to control obesity is a promising project. Alginate supplementation as an adjunct to energy restriction could improve weight loss in obese subjects who complete a 12-week dietary intervention (Georg Jensen et al., 2012). It might be that alginate can form both acid and ionic gels in the stomach, leading to a decrease in the activity of digestive enzymes such as pancreatic lipase and satiation (Wilcox et al., 2014); (Houghton et al., 2015; Wilcox et al., 2021). Similarly, Guo et al. reported that the calcium carbonate-containing sodium alginate system formed a gel in stomach conditions, and the formation of the gel lowered the dextrin and whey protein isolate (WPI) hydrolysis rate *in vitro* (Guo et al., 2020). They also found that long-term feeding containing sodium alginate in the diet could reduce the food intake, body weight, apparent protein digestibility and blood glucose in rats, indicating that alginate could potentially be effective in the treatment of obesity (Guo et al., 2020). However, another study has reported that sustained consumption of alginate over a short period of time (10 days) has been proven to have no effect on gastric motor functions, satiation, appetite, or gut incorporation, questioning the use of short-term alginate treatment for weight loss (Odunsi et al., 2010).

Although there are no reports on satiety and other aspects of AOS, dietary supplementation of AOS can also achieve the effect of obesity intervention. In high-fat-diet (HFD)-induced obese zebrafish, AOS prepared by enzymatically depolymerized showed a marked anti-obesity effect, including reducing body weight, body mass index (BMI) and blood glucose level. Comparative proteomics showed that diets with AOS

suppressed obesity and pathophysiological disorders in HFD-fed zebrafish by modulating the lipid metabolism, suppressing inflammation, down-regulating apoptosis-related genes, and improving immune function by inhibiting stomatin-like protein 2 (STOML2) (Tran et al., 2019). Similar results were seen in high-fat diet fed C57BL/6J mice, in which AOS treatment improved lipid metabolism, such as reducing levels of triacylglycerol (TG) and LDL-C and inhibiting expression of lipogenesis genes and reducing the levels of fasting blood glucose and increasing the levels of serum insulin. Also, AOS treatment was found to lower the expression of markers of inflammation, including IL-1β and CD11c (Y. Wang et al., 2020). Low-molecular alginate from *Laminaria japonica* (L-LJA) could reduce the weight gain, fat accumulation in the liver and epididymal adipose tissue, lipid abnormality and inflammation in HFD-fed BALB/c mice (Zheng et al., 2021). Li et al. found that unsaturated AOS prepared by enzymatically depolymerized showed much more effective anti-obesity effects in HFD mouse models, including reduced body weight, reduced serum lipid, reduced liver weight, reduced liver TG and total cholesterol (TC), reduced serum alanine aminotransferase (ALT), reduced aspartate aminotransferase (AST) levels, reduced adipose mass, and reduced ROS formation and accumulation than those of saturated AOS prepared by acid hydrolyzed. AMP-activated protein kinase α (AMPKα) and acetyl-CoA carboxylase (ACC) phosphorylation in adipocytes was confirmed to play an important role in the anti-obesity effect of unsaturated AOS. Interestingly, the structural differences of M oligosaccharides and its C5 epimer G oligosaccharides did not cause significant functional differences (S. Li et al., 2019).

In HFD/streptozotocin (STZ)-induced type 2 diabetes mice, alginate from *Sargassum fusiforme* can effectively reduce fasting blood glucose (FBG), TG, and TC, while increasing HDL-c and improving glucose tolerance. In addition, administering alginate to diabetic mice moderately attenuated pathological changes in adipose, hepatic, and heart tissues as well as the skeletal muscles, and diminished oxidative stress (J. Liu et al., 2021). However, so far, no study has been found on the direct intervention of AOS in diabetes. Relevant literature can be found, mainly on the metal chelates of low-molecular-weight alginate derives, such as oligomannuronate-chromium (III) complexes (Hao, Hao, Wang, Han, et al., 2011; Hao, Hao, Wang, Li, et al., 2011; Hao et al., 2015).

2.6.7 Regulation of gut microbiota

Numerous studies have shown that gut microbes are linked to a variety of diseases, including the aforementioned food allergies (Lee et al., 2020), AD (Kesika et al., 2021), obesity (Rastelli et al., 2018; Singer-Englar et al., 2019). At present, there have been a lot of reports on the interaction between alginate and AOS and intestinal microbes, and the regulation of a variety of diseases. As mentioned above, oral alginate can restore the ovalbumin-induced gut microbiota disorder in a mouse model of egg allergy, recovering the richness and diversity of *Alloprevotella, Bacteroides*, *Parabacteroides* and *Rikenellaceae_RC9_gut_group* (Yao et al., 2021). Alginate from *Sargassum fusiforme* significantly increased some benign bacteria (*Lactobacillus*, *Bacteroides*, *Akkermansia Alloprevotella*, *Weissella* and *Enterorhabdus*), and significantly decreased harmful bacteria (*Turicibacter* and *Helicobacter*) in HFD/STZ-

induced type 2 diabetes mice. Meanwhile, alginate dramatically decreased branched-chain amino acids (BCAAs) and aromatic amino acids (AAAs) in the colons of type 2 diabetes mice, suggesting a positive benefit of alginate as an adjuvant agent for type 2 diabetes mice (J. Liu et al., 2021). Huang et al. found that alginate prepared from *Laminaria* increased the abundance of beneficial bacteria *(Lactobacillus, Roseburia, and Lachnospiraceae NK4A136) and* decreased pathogenic bacteria *(Helicobacter, Peptococcus, and Tyzzerella)* in the intestine of cyclophosphamide induced immunosuppressed BALB/c mice. Also, alginate treatment can reverse the intestinal mucosal injury and increase the intestinal permeability by upregulating the expression of tight junction proteins, indicating that alginate has potential application for enhancing immunity (J. Huang et al., 2021). Ejima found that diets with alginate could suppress HFD-induced metabolic syndrome (MetS) via an effect on the gut microbiota, including changing the gut microbiota composition and increasing the abundance of *Bacteroides* (Ejima et al., 2021). Similarly, alginate from *Laminaria japonica* could also increase the abundance of *Bacteroides* after fermenting with fresh fecal samples from healthy volunteers (Ai et al., 2019). Al-Najjar et al. found that when the calcium-crosslinked alginate aerogel was given to Wistar rats for 14 days with a daily dose of 250 mg, the *Clostridia* and *Bacteriodes* groups increased during the aerogels regime and continued to increase even after the aerogel was stopped, while other groups, such as *Erysipelotrichia*, and *Candidatus saccharibacteria*, increased during the aerogel treatment and then decreased again after one month (Al-Najjar et al., 2021).

Generally, alginate can avoid being digested by the upper digestive tract and reach

the colon where it can interact with the gut microbiota community and be used by gut microbes, degrading into short chain fatty acids (SCFAs), including acetate, propionate and butyrate acids, which can stimulate the growth of beneficial bacteria and suppress the growth of harmful bacteria (You et al., 2020). Also, SCFAs have the potential to be therapeutic targets for obesity and type II diabetes, maintaining the host health and preventing colonic diseases (Campos-Perez & Martinez-Lopez, 2021).

AOS has similar functions to alginate in microflora regulation. As mentioned above, L-LJA could reduce the obesity of HFD-fed BALB/c mice, it could also modulate the structure of gut microbiota, increase some *Bacteroidales* members, and reduce some *Clostridiales* members in mice, which were positively correlated with the improvement of physiological status (Zheng et al., 2021). As reported by Wang et al., the gut microbial modulation also contributed to the anti-obesity of AOS, in which AOS markedly prompted the growth of *Akkermansia muciniphila*, *Lactobacillus reuteri*, and *Lactobacillus gasseri*. Additionally, AOS intevention significantly increased concentrations of SCFAs, such as acetic acid, propionic acid, and butyric acid, as well as decreased levels of endotoxin (Y. Wang et al., 2020). In dextran sulfate sodium-induced colitis mice models, treatment with unsaturated AOS attributed to the maintenance of the mucosal barrier function and inhibition of immune injury by regulating the gut microbiota, including increased the abundance of phylum *Firmicutes* and *Actinobacteria*, and decreased the phylum *Bacteroidetes* (He et al., 2021). Zhang confirmed that AOS benefited gut microbiota and fecal microbiota transplantation (FMT) from AOS-dosed mice to busulfan-treated ICR male mice could

much more effectively recover the “beneficial” microbes such as *Leuconostocaceae* and *Lactobacillales* than those from control mice (Zhang et al., 2020). Also, FMT from AOS-dosed mice to busulfan-treated mice was beneficial to improve the fertility rate of this model (Cong Zhang et al., 2021; P. Zhang et al., 2021). Potassium alginate oligosaccharides (PAO) also possess the activity of gut microbiota regulation. Han et al. found that treatment with PAO could decrease the ratio of *Firmicutes* to *Bacteroidetes* by decreasing the abundance of *Prevotella* and *Phascolarctobacterium* bacteria, and reduce the plasma LPS level produced by Gram-negative bacteria, resulting in lowering blood pressure (Han et al., 2021).

For more comprehensive recognition of alginate and AOS as prebiotics, more research efforts should be put into the influences on whole gut microbiota after the administration by multiple disease models. So far, no studies have been found on the structure-activity of alginate and AOS in regulating bacterial flora. A large number of studies have found that alginate and AOS can upregulate *Bacteroidetes*, which may play an important role in achieving the bioactivity of alginate and AOS *in vivo*.

2.7 Conclusion and prospects

Alginate and AOS are important in both the food and pharmaceutical industries due to their physical and chemical properties, multiple health benefits and safety. A range of preparation methods, including acid hydrolysis, irradiation, enzymatic digestion, oxidative-reductive degradation, and thermal degradation, as well as organic and biosynthetic strategies, have been applied to the production of AOS. Among them,

enzymatic methods using alginate lyases are most widely employed due to their being affordable and environmentally friendly. Also, AOS formed from enzymatic digestion generally is more bioactive with lower degrees of polymerization and a stable structure. In the field of traditional food, they can be used for the preparation of food colloid and for the delivery of nutrients. In addition, they have immunomodulatory, antioxidative, neuroprotective antibacterial and antitumour activities, as well as reducing obesity, resistance to diabetes and gut microbiota regulation. Despite this research progress toward production and the elucidation of mechanisms for bioactivity, additional investigations are required. Although progress has been made in the AOS preparation, the bioactivity mechanism and the structure-activity relationship of alginate and AOS, further investigation is needed. Also, the improved separation and analysis methods, and the guarantee of safety are prerequisites for the application as a functional food material or drug. There is no doubt that the research in the above has provided an improved basis for the production and application of alginate and AOS.

Chapter 3 Unsaturated mannuronate oligosaccharide ameliorates β-amyloid pathology through autophagy in Alzheimer's disease cell models

3.1 Abstract

Unsaturated mannuronate oligosaccharide (MOS) is an enzymatic depolymerization product from alginate-derived polymannuronate (PM). In this study, we investigated for the first time the potential therapeutic effect of MOS on Alzheimer's disease (AD) and its molecular mechanism in N2a-sw cells and 3×Tg-AD primary cortex neurons. Our results showed that MOS ranges from mannuronate dimer to mannuronate undecamer (M2-M11) with an unsaturated nonreducing terminal structure and with a double bond and 1,4-glycosidic linkages. It significantly inhibited the aggregation of amyloid-β $(Aβ)_{1-42}$ oligomer, decreased expression of $Aβ_{1-42}$ and reduced levels of amyloid precursor protein (APP) and BACE1. It promoted the autophagy, which involves the inactivation of mTOR signaling pathway and the facilitation of the fusion of autophagosomes and lysosomes. Finally, autophagy inhibitors blocked MOS' anti-AD actions, confirming the involvement of autophagy. In conclusion, MOS from seaweed alginate might be a promising nutraceutical or natural medicine for AD therapy.

3.2 Keywords

unsaturated mannuronate oligosaccharide; alginate; Alzheimer's disease; amyloid-β; autophagy.

3.3 Introduction

Alzheimer's disease (AD) is the most common type of dementia in aged people with the disorder clinically characterized by the cognitive deficit including impairment of spatial and episodic memory, language and behaviors (Blennow et al., 2006). AD is currently an untreatable neurodegenerative disorder characterized by the extracellular senile plaques and neurofibrillary tangles in pathology (Jana & Pahan, 2010). Amyloid-β (Aβ) peptide is a 36-43 residue peptide cut from amyloid precursor protein (APP) by β- and γ-secretases orderly, which is the main component of senile plaques (Mattson, 2004). The main forms of Aβ peptide are $A\beta_{1-40}$ and $A\beta_{1-42}$ (Lazarov & Demars, 2012). After being cleaved, Aβ monomers spontaneously aggregate into oligomers and insoluble fibrils, and $A\beta_{1-42}$ oligomer is suggested as the most neurotoxic form (Pan et al., 2011). Therefore, APP, β-secretase and γ-secretase exert neurotoxic character mainly due to the generation of Aβ. In normal life, the production of Aβ and clearance are in a dynamic balance (Nixon, 2013). However, the failure of clearing Aβ is regarded as an important mechanism to promote Aβ accumulation in neuronal cells and exacerbates the pathological process of AD (Pickford et al., 2008).

Autophagy is a primary cellular degradation process which is responsible for the degradation and clearance of aggregated proteins and damaged organelles to maintain cellular homeostasis depending on the fusion of autophagosomes and lysosomes (Menzies et al., 2015). Autophagy is activated by starvation (Onodera & Ohsumi, 2005), NAD-dependent deacetylase SIRT1 (Lee et al., 2008), reduction of myo-inositol-1,4,5-trisphosphate (IP_3) (Sarkar et al., 2005) and adenosine

monophosphate activated protein kinase (AMPK) (Alers et al., 2012; Kim et al., 2011), and inhibited by the mammalian target of the rapamycin (mTOR) (Kim et al., 2011; Pantovic et al., 2013). It has been reported that inordinate autophagy promotes presenilin-1 expression and γ-secretase activity, thus affecting the clearance of Aβ (Nixon, 2013; Ohta et al., 2010) and then facilitating the pathogenesis of AD. Furthermore, the promotion of autophagy initiation and autolysosome formation can reduce the aggregate-prone proteins aggregation and its neurotoxicity in AD model (Nixon, 2013). As reported, autophagy enhancers, such as rapamycin and carbamazepine, or the overexpression of autophagy-related genes, such as *Beclin-1*, can ameliorate pathological processes of AD through Aβ clearance in the AD mouse model (Caccamo et al., 2010; Li et al., 2013; Pickford et al., 2008).

Alginate is a natural carbohydrate polymer and acidic polysaccharide comprised of β-D-mannuronate and its C-5 epimer α-L-guluronate with 1,4-glycosidic linkages (Haug et al., 1967). It exists widely in various brown seaweeds such as *Macrocystis pyrifera, Laminaria hyperborean*, *Ascophyllum nodosum*, and *Undaria pinnatifida* (Onsøyen, 1997) (Park et al., 2009). Alginate and alginate-derived polymannuronate (PM) and polyguluronate (PG) can be further depolymerized into alginate oligosaccharides (AOS) with various structures through enzymatic digestion, acid hydrolysis and oxidative reductive free radical depolymerization (Xu et al., 2016; Xu, Wu, et al., 2014). AOS display a wide variety of physiological activities, such as immunomodulatory (Fang et al., 2017; Xu et al., 2015; Xu, Bi, et al., 2014), neuroprotective (Bi, Lai, Han, et al., 2018; Bi et al., 2019; Zhou, Shi, Bi, et al., 2015), anti-inflammatory (Bi, Lai, Cai, et al., 2018;

Zhou, Shi, Gao, et al., 2015) and anti-oxidant effects (Tusi et al., 2011), and structure-activity relationship studies have shown that AOS with different structures possesses different pharmacological effects. In this study, we prepared a kind of AOS, unsaturated mannuronate oligosaccharide (MOS), from PM using alginate lyase, and determined the structure of MOS using electrospray ionization mass spectrometry (ESI-MS). The anti-AD activity of MOS and the corresponding molecular mechanism was then investigated. The experimental results obtained from this study could provide key insights into how MOS intervenes in the pathological process of AD.

3.4 Materials and Methods

3.4.1 Materials

Sodium alginate, Thioflavin T (ThT), dimethylsulfoxide (DMSO) and 4',6-diamidino-2-phenylindole (DAPI) were obtained from Sigma-Aldrich (St. Louis, MO, USA). DMEM medium, Opti-MEM medium, Neurobasal-A medium, B-27 Supplement (50X), penicillin, streptomycin and G418 were purchased from Gibco (Grand Island, NY, USA). Foetal bovine serum (FBS) was obtained from Biological Industries (Beit-Haemek, Israel). Aβ 6E10 antibody was obtained from BioLegend (San Diego, CA, USA). $A\beta_{1-42}$, APP and BACE1 antibody were purchased from Abcam (Cambridge, UK). Antibodies against LC3, mTOR, p-mTOR, p70 S6K, p-p70 S6K, Beclin-1, p62, Cat-D antibody were obtained from Cell Signaling Technology (Beverly, MA, USA). 3-methyladenine (3-MA) and Bafilomycin A1 (Baf A1) were obtained from InvivoGen (San Diego, CA, USA). Other chemicals were obtained from Macklin Biochemical Technology (Shanghai, China).

3.4.2 Measurement of the number average molecular weight (Mn) and weighted average molecular weight (Mw) of alginate

The Mn and Mw of the alginate were determined by a High performance liquid chromatography System coupled with a multi-angle laser scattering (MALLS) detector (Wyatt, Santa Barbara, CA, USA) and a refractive index (RI) detector (Agilent, Palo Alto, CA, USA). The value of dn/dc was set at 0.138 mL/g. The separation was performed on a chromatographic column (ACQUITY UPLC Protein BEH 125 Å, 1.7 µm, 4.6 × 300 mm, Waters, Milford, MA, USA) at 0.1 mL/min and 25°C. The injection volume was 20 mL, and the mobile phase was 20% methanol and 80% 80 mM ammonium acetate.

3.4.3 Preparation of unsaturated MOS

Homopolymerized PM was prepared from sodium alginate based on the method of Haug *et al.* (Haug et al., 1967). The homogeneity of PM was confirmed by the analysis of the circular dichroic (CD) spectrum using a spectropolarimeter (J-815; Jasco, Inc., Tokyo, Japan) coupled with a data processor according to the method of Morris *et al.* (Morris et al., 1980). MOS was prepared from PM with alginate lyase, which was purified from *Pseudoalteromonas* sp. strain 272 (Xu et al., 2003).

3.4.4 Fourier Transform Infrared (FT-IR) Spectroscopy Analysis

The chemical structures of MOS were characterized using an FT-IR spectrophotometer (Thermo Scientific, Rochester, NY, USA) with a scanning range of 4,000 to 600 cm^{-1}. MOS (2 mg) were mixed with potassium bromide (KBr) and pressed into thin discs for analysis.

3.4.5 Mass spectrometry analysis

Electrical spray ionization mass spectrometry (ESI-MS) analysis was performed using an ion trap time-of-flight mass spectrometer (Shimadzu, Tokyo, Japan) in the negative mode. MOS was dissolved in 1 mM $NH_3 \cdot H_2O$ in 50% aqueous methanol solution and diluted to a final concentration of 1 mg/mL. The oligosaccharide was infused into the mass spectrometer using a built-in syringe pump at a flow rate of 10 μL/min.

3.4.6 ThT fluorescence analysis

$A\beta_{1-42}$ peptide (Chinapeptides Co. Ltd., Guangdong, China) was dissolved in hexafluoroisopropanol (HFIP) to a concentration of 0.5 mg/mL and incubated at room temperature (RT) with shaking overnight. After sonicated in a water bath for 15-20 min, the $A\beta_{1-42}$ peptide was dried by N_2 gas to get $A\beta_{1-42}$ oligomer. $A\beta_{1-42}$ was finally dissolved in DMSO to a concentration of 5 mM and sonicated in a water bath for another 15-20 min and then stocked in -80°C.

To investigate the effects of MOS on $A\beta_{1-42}$ fibrillation, the ThT fluorescence analysis that is widely used to detect Aβ aggregation was used. In brief, 20 μM freshly prepared $A\beta_{1-42}$ oligomer was diluted in PBS (pH 7.4) containing 20 mM ThT and 100 mM NaCl, and 1 mg/mL MOS in Phosphate Buffer Saline (PBS) was added to the above system. Then, 150 μL of the solution mentioned above was added to 96-well plates and incubated at 37°C for 10 h. The ThT fluorescence intensity of each group was recorded using a microplate reader (Fluoroskan Ascent FL, Thermo Scientific, Rochester, NY, USA) with 444/485 nm excitation/emission filters at different time points.

3.4.7 Cell and neuron culture

N2a-sw cells are murine neuroblastoma N2a cells stably transfected with human Swedish mutant APP695. N2a-sw cells were cultured in DMEM medium supplemented with 50% Opti-MEM, 5% FBS, 1% antibiotic (penicillin and streptomycin) and 0.5% G418 at 37°C with 5% CO_2.

Triple-transgenic (3×Tg, transfected mutant human *APPsw*, and *tauP301L* genes and the mutant mouse *PS1M146V* gene) AD mice and wild type mice were fed under the standard laboratory conditions: 12-h light and 12-h dark cycle, the temperature at 22 ± 2°C. All experiments were approved by the Regional Ethical Committee for Animal Experimentation at Shenzhen University. Primary cortex neurons were obtained from postnatal (P_0-P_1) pups of 3×Tg-AD or wild type mice. Briefly, cortexes were stripped from the brain and triturated. After digested with 2 mg/mL papain at 37°C for 30 min, the tissue was transferred to the new DMEM medium with 10% FBS. After 3 min stewing, digested tissue was pipetted into the neurobasal-A medium with 2% B27 supplement, 0.5% L-glutamine and 1% penicillin-streptomycin. After shocking, the primary cortex neurons separated from cortex tissue were cultured in poly-$_D$-lysine coated 6-well plates at a density of 5×10^5 cells/well. The medium was changed completely after 4 h, and then, half replaced every 3 days. At day 10, neurons were treated with 1 mg/mL MOS for 24 h.

3.4.8 RNA isolation and RT-PCR

N2a-sw cells (1×10^6 cells/well) in 6-well plates were treated with 1 mg/mL MOS for

24 h. Then total RNA was separated using RNAfast2000 Kit (Fastagen, Shanghai, China). After reverse transcribed to cDNA, PCR reactions were performed using the following parameters: 1 cycle for 180 s at 95°C; 26 cycles for 55 s at 93°C, 45 s at 60°C, and 40 s at 72°C; and 1 cycle for 100 s at 72°C in a 20 μl reaction mixtures containing 20 μM forward and reverse primers using Premix Taq (TaKaRa Biotechnology, Co., Ltd., Liaoning, China). The primer sequences for APP and β-actin were as follows: APP, Forward 5′-ACCCACTGATGGTAATGCT-3′, Reverse 5′-TCTCTCTCGGTGCTTGG-3′; and β-actin, Forward 5′-GGAGAAGATCTGGCACCACACC-3′, Reverse 5′-CCTGCTTGCTGATCCACATCTGCTGG-3′. Last, the PCR product was separated by 1% agarose gel.

3.4.9 Western blot analysis

N2a-sw cells (1×10^6 cells/well) and primary cortex neurons (5×10^5 cells/well) in 6-well plates were treated with 1 mg/mL MOS for 24 h. The protein was collected using RIPA buffer containing a protease and phosphatase inhibitor cocktail (Selleck, Shanghai, China). Then 20 μg of protein was separated by SDS-PAGE and transferred to PVDF membranes. After being blocked with 5% (w/v) skim milk at RT for 2 h, the membranes were probed with primary antibodies (1:1000) at 4°C overnight and HRP-conjugated secondary antibody (1:5000) at RT for 1 h. After rinsing, the proteins on the membranes were visualized using an ECL kit (Thermo Scientific, Rochester, NY, USA) on a luminescent image analyser (Fujifilm Life Science, Tokyo, Japan), and the density of each band was quantified using the Quantity One software (Bio-Rad, Richmond, CA, USA).

3.4.10 Immunofluorescence analysis

N2a-sw cells (1×10^6 cells/well) seeded in a glass-bottom culture dish were treated with 1 mg/mL MOS for 24 h. After fixed using 4% formaldehyde for 30 min and permeabilized using 0.2% (w/v) Triton X-100 for 10 min, cells were blocked with 10% (w/v) goat serum at RT for 1 h. Cells were then incubated with anti-Aβ(6E10) or LC3 primary antibody at 4°C overnight. After washed, the cells were incubated with Alexa Fluor 488 conjugated secondary antibody, DAPI or LysoTracker Red DND-99 at RT for 2 h. After additional washes, cells were observed by confocal microscopy (Carl Zeiss Jena Gmbh, Jena, Germany) and analysed using the ImageJ software (US National Institutes of Health, Bethesda, MD, USA).

3.4.11 Statistical analysis

Each experiment was repeated at least three times and data were presented as means ± standard deviation (SD). The results were analysed using the two-tailed Student's *t*-test to determine any significant differences by GraphPad Prism 5.01 software (GraphPad Software, Inc., La Jolla, CA, USA). A value of $P < 0.05$ was considered statistically significant.

3.5 Results

3.5.1 Preparation and structural analysis of MOS

The Mn and Mw of alginate used in this study was 2.39×10^6 ±14.30% Da and 3.28×10^6±12.14% Da, respectively. The homogeneity of PM was confirmed by the analysis of the CD spectrum. According to Figure S3.1, the peak and trough of CD

spectrum of PM appeared at 200 nm and 216 nm respectively, indicating that the homogeneity of PM was over 90%.

The FT-IR spectra of MOS in the range of 4,000 to 600 cm^{-1} are presented in Figure 3.1. The characteristic at 3,405 and 2,929 cm^{-1} were assigned to the asymmetric stretching vibration of -OH and -CH groups, respectively. The absorption bands at 1,607 and 1,414 cm^{-1} were due to the symmetric and asymmetric stretching vibrations of -COOH groups. Three absorption s from 1,200 to 1,000 cm^{-1} were indicative of pyranoid saccharides, and the weak absorption at 819 cm^{-1} was unique to the mannuronic acid residues.

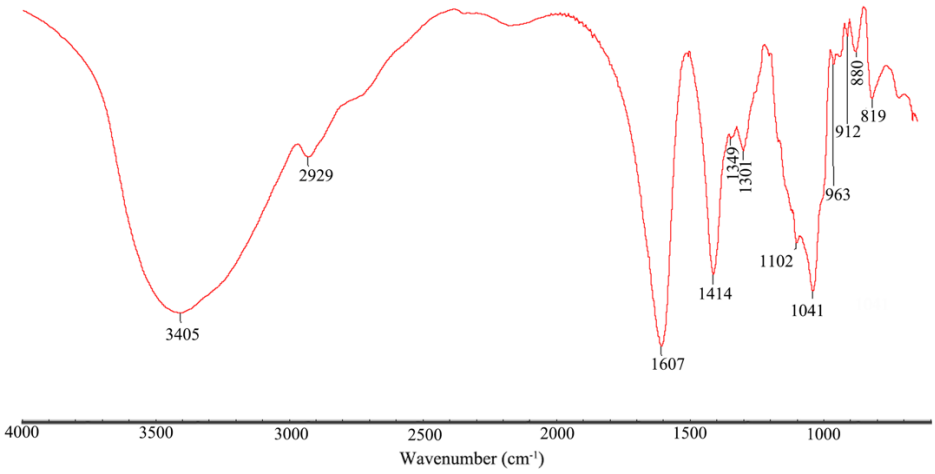

Figure 3.1 FT-IR spectra of MOS.

As shown in Figure 3.2A, multiply charged ions associated with different amounts of sodium or potassium adducts were observed. The Mw and degree of polymerization (DP) of MOS were determined precisely by assigning their corresponding peaks. The charge states of the ions were deduced based on their isotopic distribution profiles, and their Mw was calculated. As listed in Table 3.1 and Figure 3.2B, the MS results revealed that the sizes of primary MOS ranged from mannuronate dimer to

mannuronate undecamer (M2-M11).

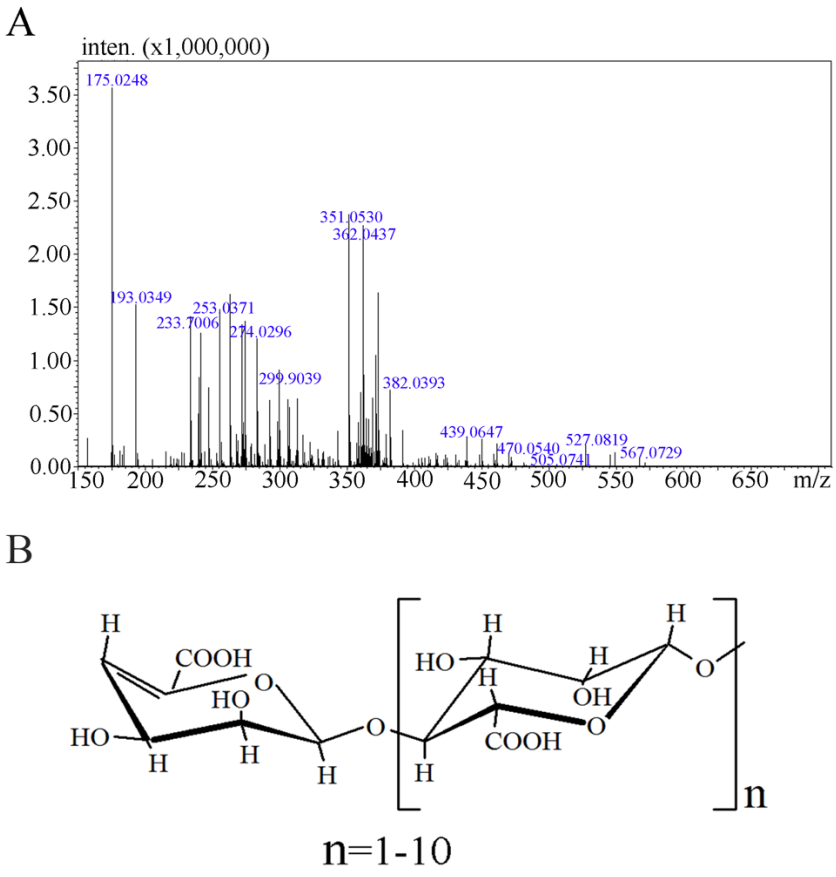

Figure 3.2 The electrospray ionization mass spectrometry (ESI-MS) and structure of MOS. (A) The spectrum was acquired in the negative ion mode with a high-resolution hybrid time-of-flight mass spectrometer. The ions were present in the form of $[M+xNa(K)-(x+n)H]^{n-}$. The corresponding Mw and DP were then calculated using the monoisotopic peaks and charge states of each group of ions. (B) Stereo-image of structure of MOS.

Table 3. 1 Ions observed in the mass spectrometry analysis of MOS.

m/z	Charge state	Ion format	Corresponding DP[a]	Mw[b]
351	1	$[M-H]^-$	2	352
263	2	$[M-2H]^{2-}$	3	528

274	2	$[M+Na-3H]^{2-}$	3	528
282	2	$[M+K-3H]^{2-}$	3	528
571	1	$[M+2Na-3H]^{-}$	3	528
351	2	$[M-2H]^{2-}$	4	704
362	2	$[M+Na-3H]^{2-}$	4	704
373	2	$[M+2Na-4H]^{2-}$	4	704
439	2	$[M-2H]^{2-}$	5	880
450	2	$[M+Na-3H]^{2-}$	5	880
461	2	$[M+2Na-4H]^{2-}$	5	880
472	2	$[M+3Na-5H]^{2-}$	5	880
527	2	$[M-2H]^{2-}$	6	1056
538	2	$[M+Na-3H]^{2-}$	6	1056
549	2	$[M+2Na-4H]^{2-}$	6	1056
424	3	$[M+2Na-5H]^{3-}$	7	1231
377	4	$[M+K+3Na-8H]^{4-}$	8	1408
406	4	$[M+2Na-6H]^{4-}$	9	1584
465	4	$[M+K+3Na-8H]^{4-}$	10	1760
407	5	$[M+K+3Na-9H]^{5-}$	11	1936

[a]DP = degree of polymerization; [b]Mw = molecular weight.

3.5.2 Effects of MOS on $A\beta_{1-42}$ aggregation *in vitro*

A ThT fluorescence-based analysis was used to examine the aggregation of $A\beta_{1-42}$. The fibrillization process of $A\beta_{1-42}$ was continuously monitored by a microplate reader. As shown in Figure 3.3A, a fast increase in ThT fluorescence was observed in accordance with a typical two-phase growth curve. When $A\beta_{1-42}$ was incubated with 1 mg/mL MOS, the maximal ThT fluorescence value decreased more than two folds

compared with the negative control (NC). The epigallocatechin gallate (EGCG) was chosen as a positive control (PC). These results suggest that MOS could inhibit aggregation of $A\beta_{1-42}$ *in vitro*.

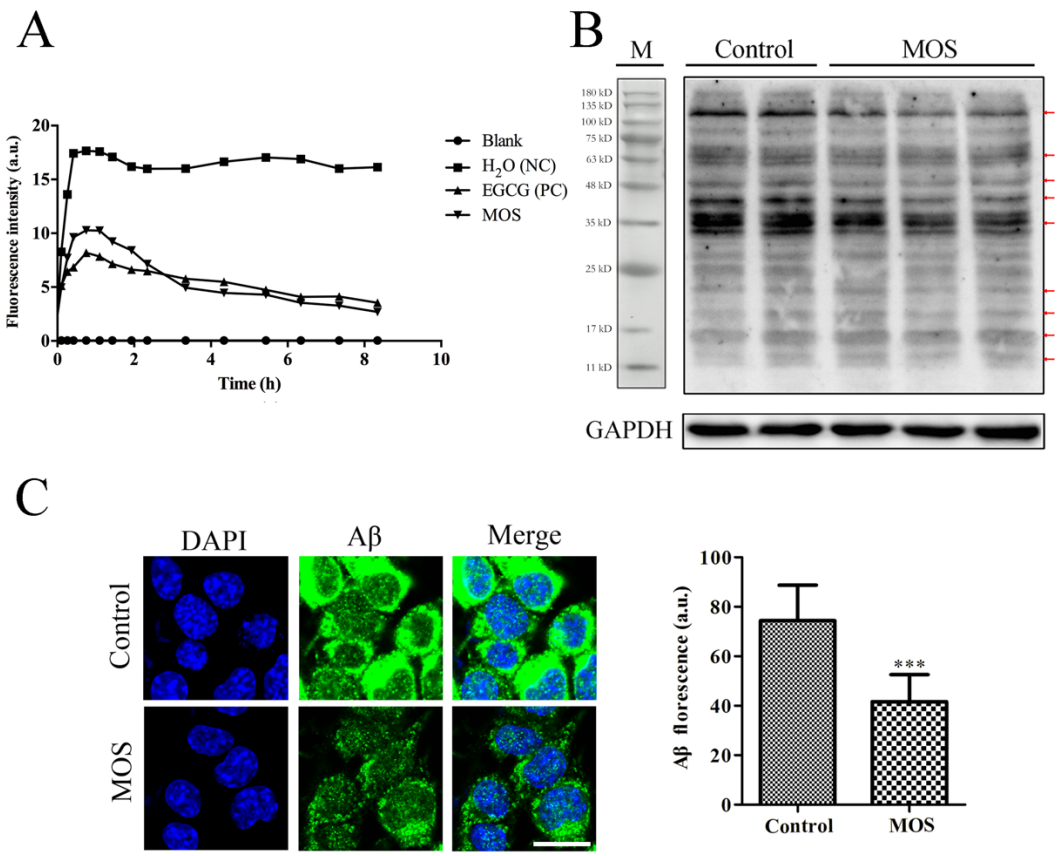

Figure 3.3 The effects of MOS on Aβ aggregation *in vitro* and production in N2a-sw cells. (A) 20 μM freshly prepared $A\beta_{1-42}$ oligomer was diluted in PBS (pH 7.4) containing 20 mM ThT and 100 mM NaCl co-incubated with 1 mg/mL MOS at 37°C. ThT fluorescence intensity of each group was recorded using a microplate reader with 444/485 nm excitation/emission filters at different time points. N2a-sw cells treated with MOS for 24 h, Aβ expression was evaluated via Western blot analysis (B) and immunofluorescence analysis and statistically analysed using the ImageJ software (C)

using the specific antibody 6E10. Representative images and results from three independent experiments are shown. Scale bar = 20 μm. NS, no significance. ***P < 0.001.

3.5.3 Effects of MOS on the Aβ pathway in AD cell models

The influence of MOS on the Aβ expression and deposition in the N2a-sw cells was examined by Western blot and immunofluorescence analyses using the specific antibody 6E10 after treatment with 1 mg/mL MOS for 24 h. From Figure 3.3B, it can be seen that MOS treatment notably decreased the expression of Aβ oligomers in N2a-sw cells, although there were no significant differences in low polymerization degree Aβ oligomers expression (< 36 kDa). Furthermore, the results from immunofluorescence analysis confirmed that MOS treatment could significantly reduce the Aβ expression and deposition in N2a-sw cells (Figure 3.3C). MOS treatment decreased 45% Aβ expression in N2a-sw cells compared with the control group (Figure 3.3C) based on the fluorescence intensity.

To explore the mechanisms of reduced expression and deposition of Aβ by MOS treatment, the amyloidogenic APP processing pathway was investigated in N2a-sw cells and 3×Tg-AD primary cortex neurons. As shown in Figure 3.4A and Figure S3.2, the expression levels of APP decreased significantly in a dose-dependent manner after the MOS treatment in N2a-sw cells. BACE1/β-secretase is responsible for the initiation of Aβ generation in the amyloidogenic pathway (Xie et al., 2017). MOS treatment notably reduced the protein expression levels of BACE1 and $A\beta_{1-42}$ in the N2a-sw cells

(Figure 3.4A and Figure S3.2).

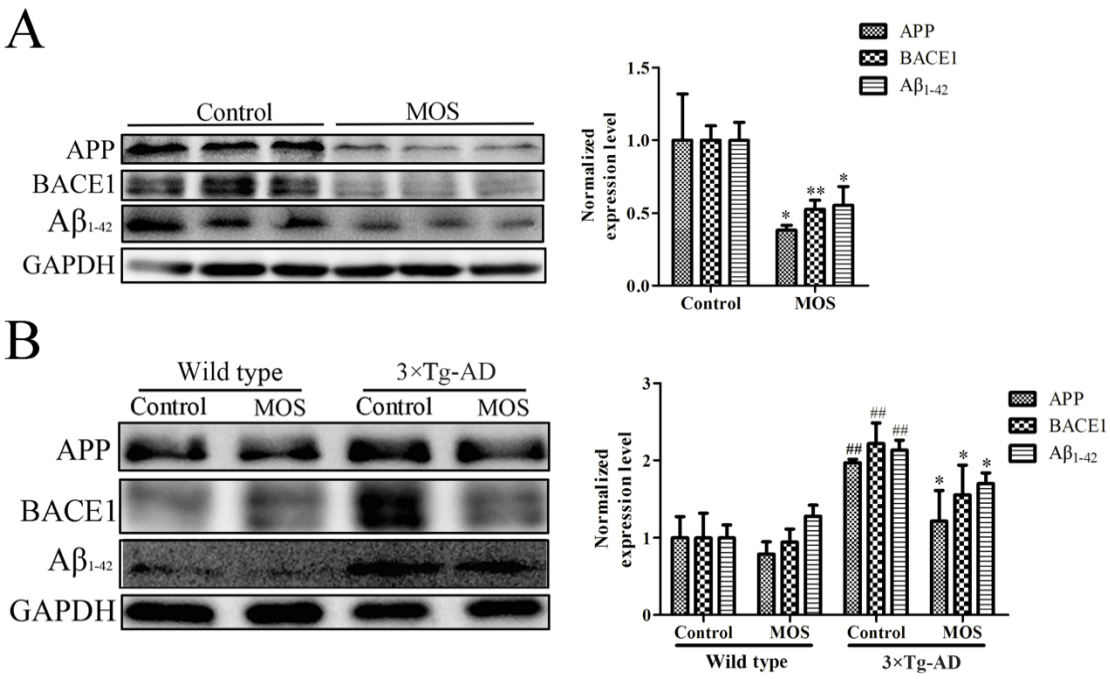

Figure 3.4 MOS inhibits APP pathway. (A) N2a-sw cells treated with MOS for 24 h, the levels of APP, BACE1 and $A\beta_{1-42}$ were evaluated via Western blot analysis and analysed using the ImageJ software. (B) Wild type and 3×Tg-AD primary cortex neurons treated with MOS for 24 h, the levels of APP, BACE1 and $A\beta_{1-42}$ were evaluated via Western blot analysis and statistically analysed using the ImageJ software. Representative images and results from three independent experiments are shown. NS, no significance. *Indicates significant differences between the control and MOS-treated groups. *P < 0.05, **P < 0.01; #Indicates significant differences between the 3×Tg-AD primary cortex neurons and wild type primary cortex neurons. ##P < 0.01.

As presented in Figure 3.4B, in the primary cortex neurons, the production of APP, BACE1 and $A\beta_{1-42}$ was much higher in the AD groups than that in the wild type groups. A similar tendency was seen in 3×Tg-AD primary cortex neurons after treated by MOS

that MOS treatment also could significantly decrease the expression of those protein, including APP, BACE1 and $A\beta_{1-42}$, in 3×Tg-AD primary cortex neurons (Figure 3.4B). Therefore, MOS treatment inhibited the generation and deposition of Aβ by down-regulating the expression of both APP and BACE1.

3.5.4 Effects of MOS on LC3 level in AD cell models

Generally, the decrease of APP might be the consequence of inhibition of the transcription of the APP gene or the clearance of overexpressed APP protein. However, it was seen that MOS treatment did not affect the mRNA expression of APP compared with the control group in N2a-sw cells (Figure 3.5A), suggesting that the reduction of APP induced by MOS might be due to the promotion of clearance mechanism to its protein, instead of the inhibition of the transcription of the APP gene.

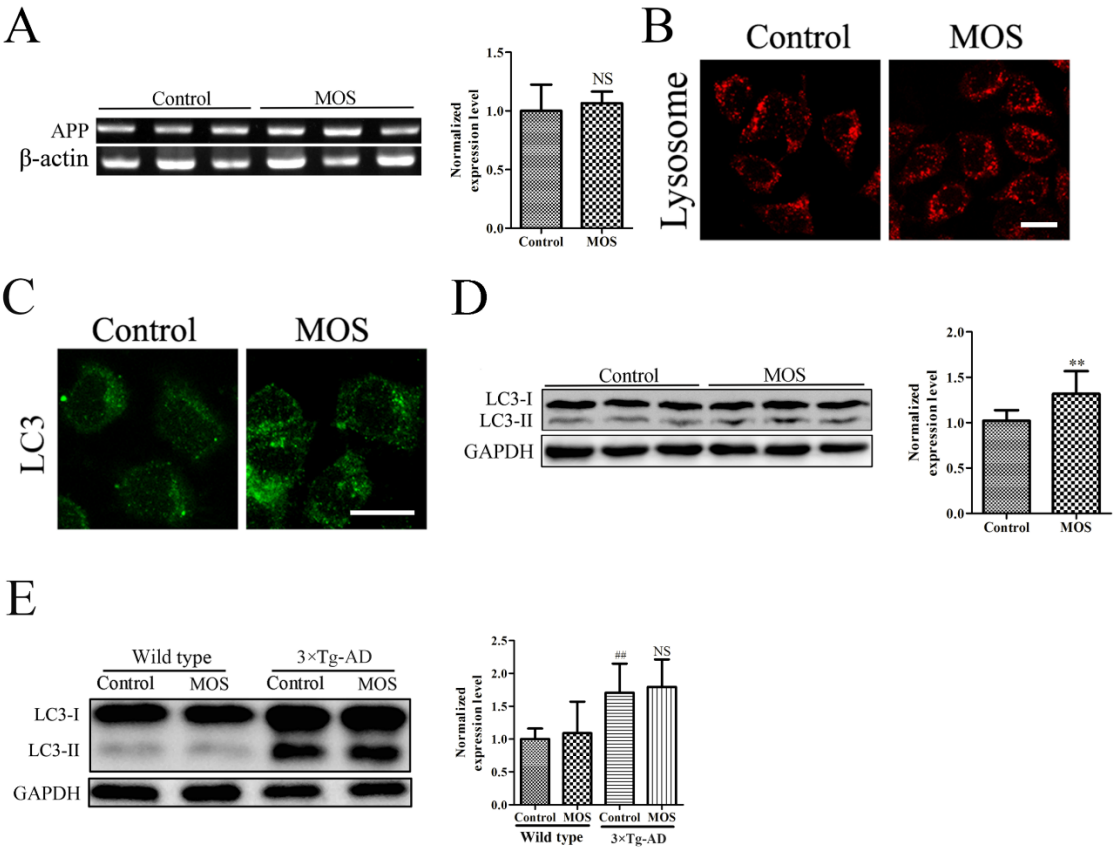

Figure 3.5 MOS affects LC3 expression. (A) N2a-sw cells treated with MOS for 24 h, APP mRNA levels were evaluated via RT-PCR. (B-D) N2a-sw cells treated with MOS for 24 h, the lysosome in N2a-sw cells was labeled LysoTracker Red DND-99 (B) and the LC3-II level was detected using immunofluorescence (C) and Western blot analysis (D). (E) Wild type and 3×Tg-AD primary cortex neurons were treated with MOS for 24 h, the LC3 level was detected using Western blot analysis. The gray value was statistically analysed using the ImageJ software. Representative images and results from three independent experiments are shown. Scale bar = 20 μm, NS, no significance. *Indicates significant differences between the control and MOS-treated groups, **P < 0.01; #Indicates significant differences between the 3×Tg-AD primary cortex neurons and wild type primary cortex neurons, ##P < 0.01.

Autophagy is a vital catabolic process in cells, and also a primary driving force for degradation of abnormal and aggregated proteins in autolysosome (Menzies et al., 2015). Light chain protein 3 (LC3) is commonly used as a marker of autophagy (Nixon, 2013). Although there was no influence on lysosome which labeled with LysoTracker Red DND-99 (Figure 3.5B), the levels of LC3 protein were significantly improved by the treatment from the immunofluorescence analysis in MOS treated N2a-sw cells (Figure 3.5C). Meanwhile, the expression of LC3-II, an active form as autophagy receptor converted from LC3-I during the formation of the autophagosome, was tested using Western blot analysis. As shown in Figure 3.5D, MOS treatment could improve the LC3-II levels in N2a-sw cells. These results suggest that MOS treatment could promote autophagy in N2a-sw cells.

It should be noted that a block in the fusion of autophagosomes and lysosomes would reduce the LC3 and p62 accumulation in the AD mouse model (Lee et al., 2014). As illustrated in Figure 3.5E, the expression level of LC3-II in 3×Tg-AD primary cortex neurons was much higher than that in the wild type primary cortex neurons, while there was not any effect of LC3-II expression in 3×Tg-AD primary cortex neurons after MOS treatment.

3.5.5 Effects of MOS on mTOR signaling pathway in AD cell models

The initiation of autophagy is mediated through a protein complex which was comprised ULK1 or ULK2, autophagy proteins (ATG)13, ATG101 and the focal adhesion kinase family interacting protein of 200 kDa (FIP200) (Menzies et al., 2015) and

regulated by mTOR (Kim et al., 2011; Pantovic et al., 2013). It was shown that the phosphorylation of mTOR as well as its downstream p70 S6K and its upstream Akt was decreased significantly after MOS treatment compared with the control group in N2a-sw cells (Figure 3.6A and Figure S3.3). Meanwhile, the phosphorylation of mTOR and p70 S6K was much higher in the 3×Tg-AD primary cortex neurons compared with those in the wild type primary cortex neurons (Figure 3.6B), indicating that autophagy initiated signaling pathway was blocked in 3×Tg-AD primary cortex neurons rather than in wild type primary cortex neurons. Meanwhile, the phosphorylation of mTOR and p70 S6K in 3×Tg-AD primary cortex neurons was reduced obviously after MOS treatment (Figure 3.6B). Our results suggest that MOS treatment could activate the mTOR signaling pathway in N2a-sw cells and 3×Tg-AD primary cortex neurons and promote the initiation of autophagy.

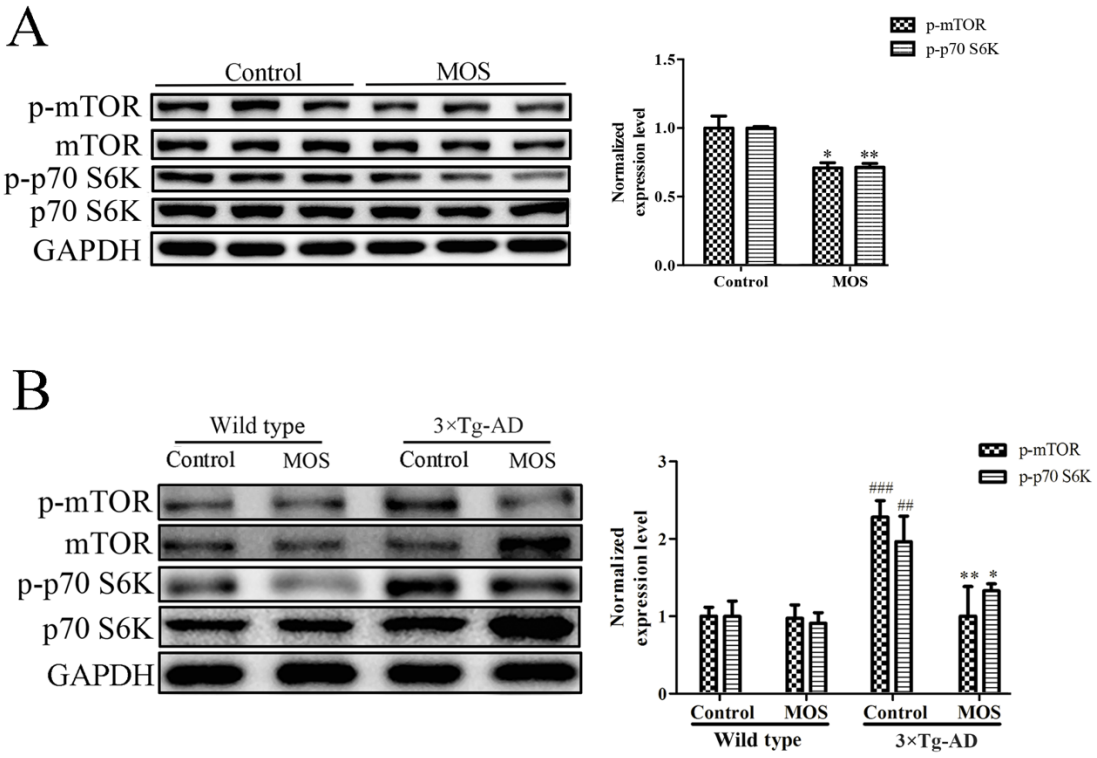

Figure 3.6 The effects of MOS on mTOR signaling pathway. (A) N2a-sw cells treated with MOS for 24 h, the levels of p-p70 S6K and p70 S6K were evaluated via Western blot analysis and analysed using the ImageJ software. (B) Wild type and 3×Tg-AD primary cortex neurons treated with MOS for 24 h, the levels of p-p70 S6K and p70 S6K were evaluated via Western blot analysis and statistically analysed using the ImageJ software. Representative images and results from three independent experiments are shown. NS, no significance. *Indicates significant differences between the control and MOS-treated groups. *P < 0.05, **P < 0.01; #Indicates significant differences between the 3×Tg-AD primary cortex neurons and wild type primary cortex neurons, ##P < 0.01, ###P < 0.001.

3.5.6 Effects of MOS on autophagy initiation and autophagy-lysosomal pathway in AD cell models

To confirm the effects of MOS on autophagy initiation and the fusion of autophagosomes and lysosomes, the protein levels of Beclin-1, p62 and Cathepsin D (Cat-D) were determined using Western blot analysis. As displayed in Figure 3.7A, MOS treatment could significantly increase the Beclin-1 production, attenuate p62 level and elevate mature Cat-D expression in N2a-sw cells. A similar phenomenon was observed in 3×Tg-AD primary cortex neurons after treated with MOS. Our results demonstrated that the Beclin-1 level in 3×Tg-AD primary cortex neurons was much lower than that in wild type primary cortex neurons and was significantly recovered after treated with MOS (Figure 3.7B). Furthermore, the extraordinarily elevated p62 expression in 3×Tg-AD primary cortex neurons was suppressed statistically with the MOS treatment accordingly (Figure 3.7B). However, there was no apparent difference for mature Cat-D expression between in 3×Tg-AD primary cortex neurons and in wild type primary cortex neurons, while MOS treatment could increase the level of mature Cat-D of 3×Tg-AD primary cortex neurons (Figure 3.7B). These results indicate that MOS treatment could promote the initiation of autophagy and autophagy-lysosomal pathway effectively not only in N2a-sw cells but also in 3×Tg-AD primary cortex neurons.

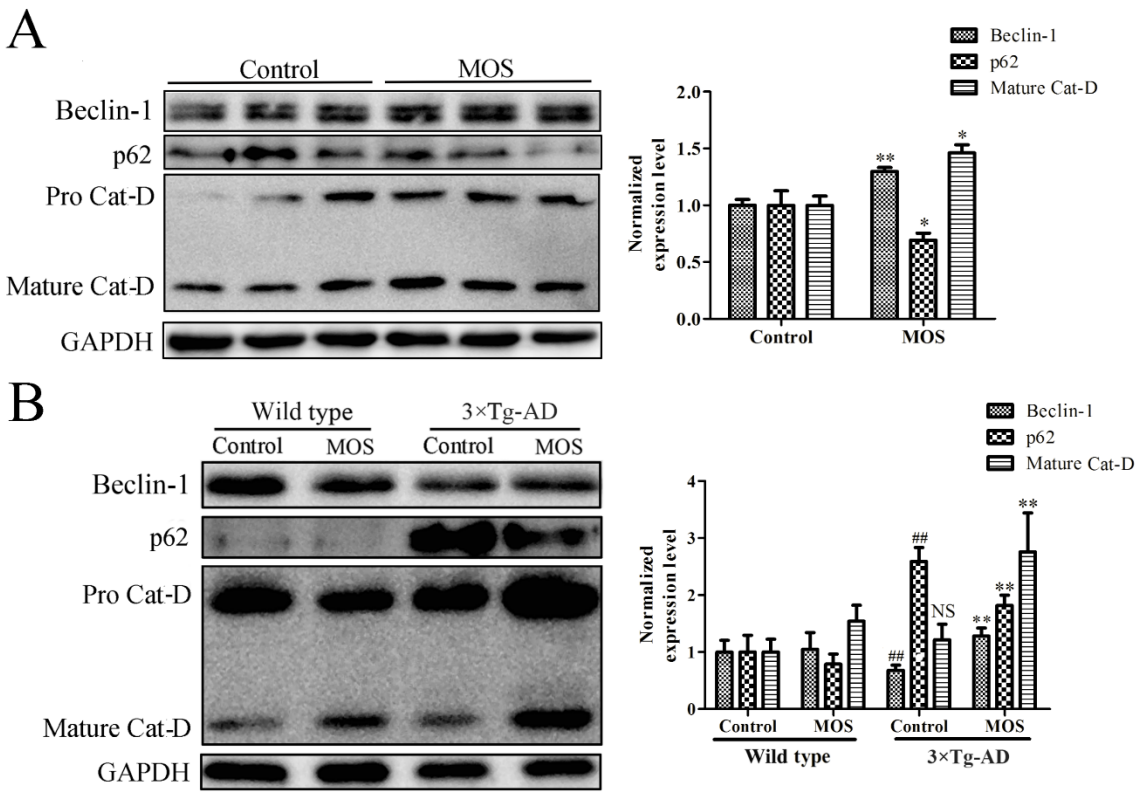

Figure 3.7 The effects of MOS on autophagy. (A) N2a-sw cells treated with MOS for 24 h, the levels of Beclin-1, p62 and Cat-D were evaluated via Western blot analysis and analysed using the ImageJ software. (B) Wild type and 3×Tg-AD primary cortex neurons treated with MOS for 24 h, the levels of Beclin-1, p62 and Cat-D were evaluated via Western blot analysis and statistically analysed using the ImageJ software. Representative images and results from three independent experiments are shown. NS, no significance. *Indicates significant differences between the control and MOS-treated groups. *P < 0.05, **P < 0.01; #Indicates significant differences between the 3×Tg-AD primary cortex neurons and wild type primary cortex neurons. ##P < 0.01.

3.5.7 Effect of autophagy inhibitors on MOS-induced the decrease of APP and Aβ expression in AD cell models

3-MA is the inhibitor of PI3K complex and inhibits the formation of autophagosomes, and Baf A1 is an autophagic flux inhibitor that blocks the fusion of autophagosomes with the lysosome, thereby inhibiting the autophagic degradation of proteins. To confirm the relationship between MOS-triggered the reduction of APP and Aβ expression and enhancement of autophagy, the APP and Aβ protein levels in MOS treated N2a-sw cells and 3×Tg-AD primary cortex neurons which were supplemented with above two autophagy inhibitors were evaluated using Western blot analysis. As the results indicated, the decline of APP and $A\beta_{1-42}$ expression in N2a-sw cells induced by MOS was recovered near to and even exceeded that in the control group while co-incubated with 3-MA (3.5 mM) and Baf A1 (0.1 μM) respectively (Figure 3.8A and B). And interestingly, Baf A1 increased the APP expression in N2a-sw cells, suggesting that autophagy inhibitors also affect the degradation of overexpressed APP (Figure 3.8B). In addition, a similar tendency was observed in 3×Tg-AD primary cortex neurons. As shown in Figure 3.8C and D, MOS treatment reduced the production of APP and $A\beta_{1-42}$, which effectively restored after co-incubation with 3-MA (0.35 mM) and Baf A1 (0.01μM) respectively. Taken together, MOS treatment could suppress APP and Aβ expressions in N2a-sw cells and 3×Tg-AD primary cortex neurons closely related to the autophagy process.

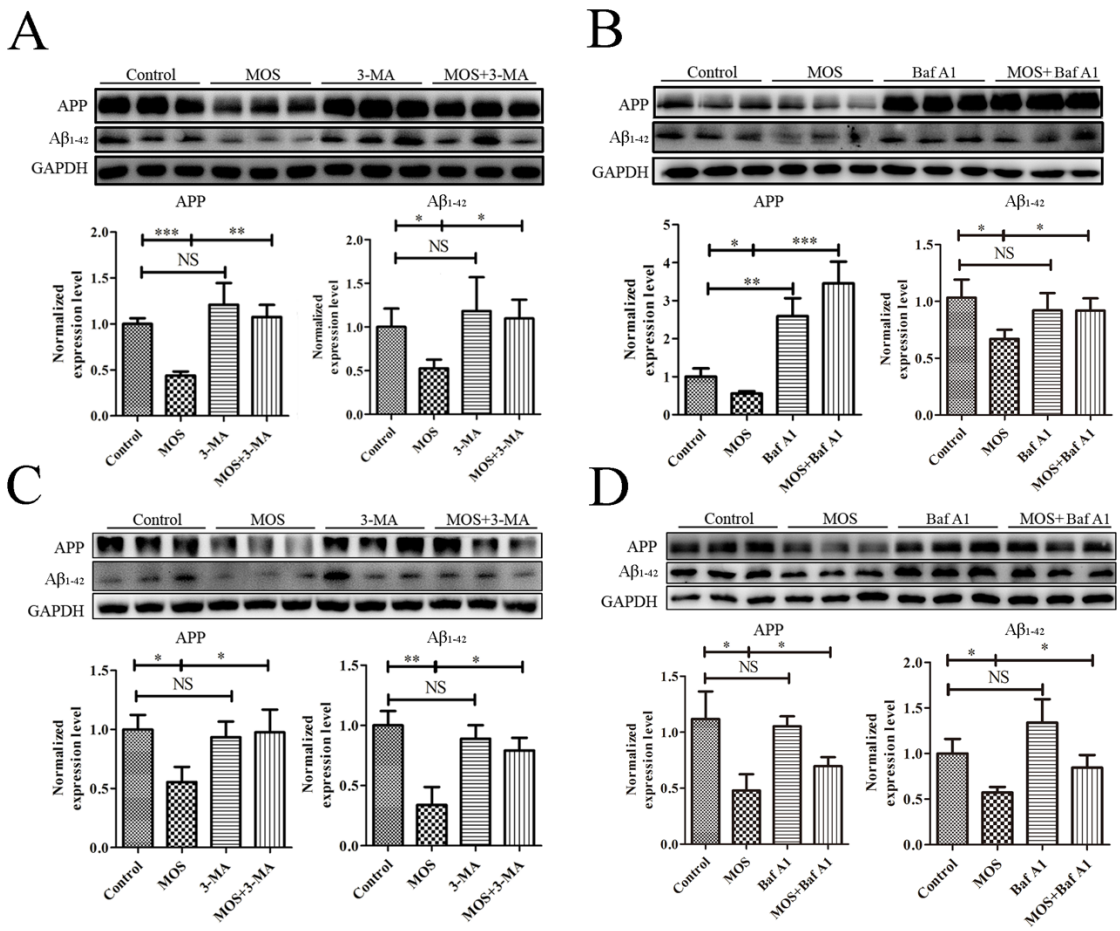

Figure 3.8 Effect of autophagy inhibitor on MOS-reduced the expression of APP and Aβ levels via autophagy. (A) N2a-sw cells co-treated with 1 mg/mL MOS and 3-MA (3.5 mM) or Baf A1 (0.1 μM) for 24 h, the levels of APP and $A\beta_{1\text{-}42}$ were evaluated via Western blot analysis and statistically analysed using the ImageJ software. (B) 3×Tg-AD primary cortex neurons co-treated with 1 mg/mL MOS and 3-MA (0.35 mM) or Baf A1 (0.01 μM) for 24 h, the levels of APP and $A\beta_{1\text{-}42}$ were evaluated via Western blot analysis and analysed using the ImageJ software. Representative images and results from three independent experiments are shown. NS, no significance. *P < 0.05, **P < 0.01, ***P < 0.001.

3.6 Discussion

AD is a progressive neurodegenerative disease which holds cognitive decline and memory loss as major clinically pathological indicators, and is a severe social and medical problem for human health and social stability because of its high disability rate (Blennow et al., 2006). However, to date, there is no radical cure and current medication only offers limited symptom relief (Xie et al., 2017). Although what contributes to the pathogenesis of AD is multifaceted, inhibiting the Aβ production and promoting Aβ clearance is still a valuable therapeutic target (Sikanyika et al., 2019). Many inhibitors or medicines have been proven to be useless in clinical experiments. For example, semagacestat, the inhibitor of γ-secretase, was dropped in Phase III studies due to its failure to improve the cognitive function of AD patients (Doody et al., 2013). Solanezumab, an anti-amyloid monoclonal antibody binding soluble Aβ, has also been reported to fail in Phase III trials because of non-significant differences in improving cognitive impairment compared with vehicle in patients with mild Alzheimer's disease (Sacks et al., 2017). More researchers have focused on searching valuable natural products in AD prevention and cure, such as EGCG (Cheng et al., 2013) and methylene blue (Brunden et al., 2009), which are in the process of entering clinical trials.

Recently, some polysaccharides and oligosaccharides from seaweeds have been reported to possess anti-AD activity. Fucoidan, isolated from a brown alga *Sargassum fusiforme* grown in Dongtou, China, could improve the cognitive dysfunction of the scopolamine-, ethanol-, and sodium nitrite-treated mice (Hu et al., 2016). Fucoidan

collected from the coast of Dalian, China, could prevent PC12 cells from apoptosis induced by $A\beta_{25–35}$, and improve learning and memory impairment in the AD mouse model (Wei et al., 2017). It has been reported that trehalose could decrease the lysosomal metabolism of AD-related APP and Aβ by altering its vesicular endocytic transport in human neuroglioma H4 cells and human neuroblastoma SH-SY5Y cells (Tien et al., 2016). In addition, κ-carrageenan-derived pentasaccharide (KCP) extracted from marine red algae possesses significant neuroprotection activity against $A\beta_{25-35}$-induced neurotoxicity in SH-SY5Y cells (Liu et al., 2017). It should be noticed that acidic oligosaccharide sugar chain (AOSC), a marine-derived acidic oligosaccharide extracted from brown algae, could pass the blood-brain barrier (BBB) easily to exert excellent inhibition effects on $A\beta_{1-40}$ aggregation and attenuate scopolamine induced memory impairment *in vivo* (Guo et al., 2006; J. Hu et al., 2004); (Fan et al., 2005). In our study, enzymatically depolymerized oligosaccharide from alginate, i.e., MOS, was prepared, which ranges from dimer to undecamer (M2-M11). We confirmed its structure using ESI-MS detection (Figure 3.2 and Table 3.1), and confirmed that MOS could effectively intervene in AD through inhibiting $A\beta_{1-42}$ aggregation and Aβ production and promoting Aβ clearance.

Examined by ThT fluorescence assay, MOS exhibited satisfactory results in inhibiting aggregation of $A\beta_{1-42}$ that is the main toxic form of Aβ in the brain (Figure 3.3A). We speculate that the inhibitory effects are due to the binding of MOS to $A\beta_{1-42}$, which would be analogous to heparin binding (J. Hu et al., 2004).

Utilizing two AD cell models, N2A-sw cells and 3×Tg-AD primary cortex neurons, we

examined the effectiveness of MOS on the Aβ pathway. We found that MOS treatment significantly reduced the levels of APP and BACE1, and followed by a decrease of Aβ production, suggesting that MOS could affect the Aβ production (Figure 3.4). Regarding its mechanism, we propose that MOS might inhibit the transcription of BACE1 similar to that of EGCG (Z.-X. Zhang et al., 2017). As for APP, we speculate that there is a clearance mechanism to eliminate the overproduced APP and even Aβ, because there was no apparent alteration of APP mRNA expression after MOS treatment in N2a-sw cells (Figure 3.5A).

Autophagy is an essential degradation pathway which is occupied in the digestion and recycling of nutrients by autophagosomes to maintain cellular homeostasis (Menzies et al., 2015). The process is primary for cell survival during nutrient starvation and is also a major pathway for the degradation of overexpressed and aggregate-prone proteins and even intracellular damaged organelles (Menzies et al., 2015). It has been reported that disordered autophagy plays an essential role in the pathogenesis of AD (Nixon, 2013). As shown in Figure 3.5D and 7B, the levels of LC3-II and p62 in the 3×Tg-AD primary cortex neurons are much higher than those in the wild type primary cortex neurons, and it might be the consequences of blocked autophagy pathway (Lee et al., 2014). Although there is no change of LC3-II level after MOS treatment, the p62 level decreased and the mature Cat-D level increased significantly, which indicates that treatment with MOS could alleviate the fusion of autophagosomes and lysosomes, promote the fusion of autophagosome and lysosomes, and then make the promotion of LC3 levels to dynamic balance. A similar phenomenon was observed in N2a-sw cells

(Figure 3.7A). Those results suggest that MOS treatment promotes the fusion of autophagosomes and lysosomes and enhances digestion. Therefore, we conclude that the decrease of APP after MOS treatment might be the result of autophagy activation and promotion of the fusion of autophagosomes and lysosomes, as well as Aβ.

Autophagy initiation is regulated by mTOR and AMPK signaling pathways, which are sensitive to amino acids (Alers et al., 2012; Kim et al., 2011). The activated mTOR signaling pathway blocks the initiation of autophagy by inhibitory interaction of ULK1/ULK2-Atg13-FIP200 protein complex (Alers et al., 2012; Kim et al., 2011). The activated ULK1/ULK2-Atg13-FIP200 protein complex is the director of the PI3K complex, which regulates the formation of autophagosomes (Menzies et al., 2015). In 3×Tg-AD primary cortex neurons, the activation of mTOR signaling pathways was much stronger than those in wild type primary cortex neurons individually (Figure 3.6B). Beclin-1, a primary component of the PI3K complex, was presented at a low level in 3×Tg-AD primary cortex neurons (Figure 3.7B). These results suggest that the transmission of the autophagy signaling pathway and the autophagy initiation in AD are blocked. In MOS treated 3×Tg-AD primary cortex neurons and N2a-sw cells, the activated mTOR signaling pathway was suppressed significantly and the level of Beclin-1 increased significantly (Figure 3.6 and 3.7)., Autophagy receptor, p62, binds to the ubiquitylated protein and then target LC3 family members on autophagosomes through their LC3-interacting region motifs. It has been identified as a specific substrate which could degrade through the autophagy-lysosomal pathway (Menzies et al., 2015). Cat-D, an essential lysosomal aspartyl protease in the lysosome, could be

activated by proteolysis to format a mature form (Menzies et al., 2015). We found that the p62 level in MOS-treated N2A-sw cells and 3×Tg-AD primary cortex neurons reduced significantly compared with that in the vehicle-treated group. In contrast, the activated Cat-D level increased significantly (Figure 3.7). It is therefore suggested that MOS is able to activate the autophagy-lysosomal pathway effectively. Taken all together, MOS treatment can promote not only the initiation of autophagosomes but also the fusion of autophagosomes and lysosomes.

In AD, inordinate APP processing is associated with an increase of Aβ levels. Autophagy enhancers have been proven to ameliorate Aβ deposition in AD mice (Li et al., 2013; Pickford et al., 2008). In this study, to confirm the relationship between the decrease of APP and Aβ levels and the autophagy, autophagy inhibitors 3-MA and Baf A1 were used. As expected, that the expression of APP and Aβ in the existence of autophagy inhibitors elevated significantly compared with those treated by MOS alone in N2a-sw cells and 3×Tg-AD primary cortex neurons. This demonstrated that autophagy inhibitors could disturb the attenuation of APP and Aβ levels induced by MOS (Figure 3.8). These findings can verify the involvement of autophagy in the MOS-activated Aβ pathway.

Why could MOS up-regulate the levels of autophagy in AD cell models? We speculate that MOS inhibits the expression and aggregation of Aβ and then blocks the oxidative stress induced by Aβ oligomer to cells. Oxidative stress is a principal reason to break the function and structure of lysosome via inhibiting lysosome enzyme (such as Cat-D) function, damaging lysosome membrane and increasing lysosomal pH

(Hensley & Harris-White, 2015; Pivtoraiko et al., 2009). It has been reported that alginate oligosaccharides by enzymatic depolymerization can combine with radical and then remove free radicals on account of its conjugated alkene acid structure (Falkeborg et al., 2014). MOS, derived from alginate using enzymatic depolymerization, has a conjugated alkene acid structure. We have found that acidic polysaccharides and oligosaccharides have valuable regulating effects on homeostasis to life in our previous study (Xu et al., 2015). Therefore, we suggest that MOS maintains the homeostasis of life and exerts anti-AD activity because of its special characteristic structure.

In conclusion, our present study demonstrates that MOS treatment inhibits Aβ oligomer aggregation and reduces Aβ levels via inhibiting the production BACE1, and enhances autophagy to promote clearance of APP and Aβ in AD cell models. These data shed light on a novel application prospect of MOS as a promising functional food or a natural medication for the treatment or the assistance of the treatment of AD.

3.7 Supplementary data

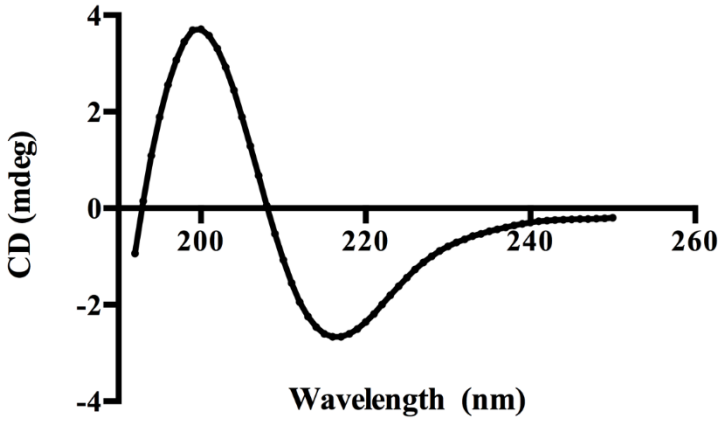

Figure S3.1 CD spectrum of PM.

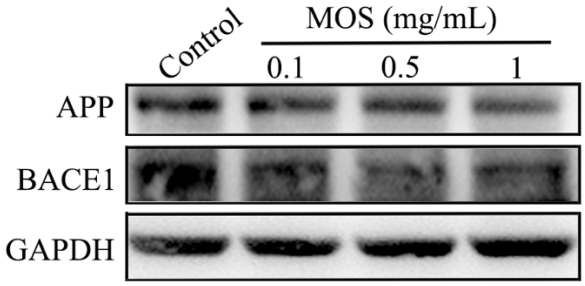

Figure S3.2 MOS inhibits APP and BACE1 production in a dose-dependent manner. N2a-sw cells treated with 0.1, 0.5 and 1 mg/mL MOS for 24 h, the levels of APP and BACE1 were evaluated via Western blot analysis.

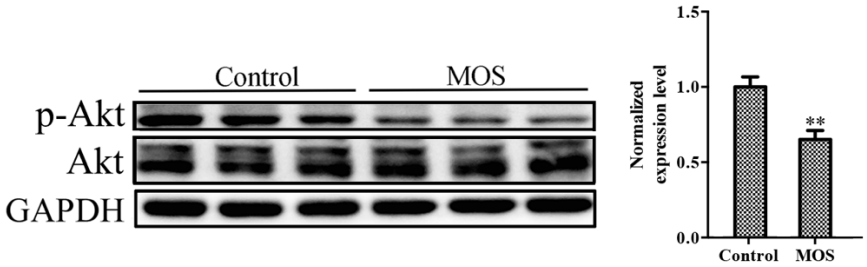

Figure S3.3 MOS inhibits p-Akt production. N2a-sw cells treated with MOS for 24 h, the levels of p-Akt and Akt were evaluated via Western blot analysis and analysed using

the ImageJ software. **P < 0.01.

Chapter 4 Alginate-derived mannuronate oligosaccharide attenuates tauopathy through enhancing autophagy

4.1 Abstract

Polymannuronate (PM) is an acidic polysaccharide prepared from alginate, contained in edible brown seaweeds. Unsaturated mannuronate oligosaccharide (MOS) is an enzymatically depolymerized oligosaccharide prepared from PM. The effects of MOS on attenuating tauopathy was studied in HEK293/Tau cells and primary triple transgenic (3×Tg) neurons. MOS inhibited heparin-induced aggregation of Tau-K18 oligomer and suppressed the levels of phosphorylated Tau protein. MOS treatment reduced the activity of glycogen synthase kinase-3β (GSK-3β) by decreasing its phosphorylation levels on the sites of Y216 and increasing phosphorylation levels on the sites of S9. MOS treatment increased the ratio of LC3-II/LC3-I levels and reduced the expression of p62, indicating an increase of autophagy. Finally, MOS-induced decrease of Tau protein expression was attenuated by the addition of autophagy inhibitor, confirming the involvement of autophagy. These data support MOS as a promising functional food or potential pharmaceutics for attenuating Tau protein related disease.

4.2 Keywords

Unsaturated mannuronate oligosaccharide (MOS); tauopathy; Tau protein; autophagy

4.3 Introduction

Tauopathies are progressive neurodegenerative disorders with the pathological feature of Tau protein aggregation in the brain, including Alzheimer's disease (AD), corticobasal syndrome, progressive supranuclear palsy, and some frontotemporal dementias (Orr et al., 2017). Tau protein, first discovered in 1975, is a microtubule-associated protein encoded by the *MAPT* gene located on chromosome 17 and critical for microtubule assembly and stabilization (Weingarten et al., 1975). Under disease conditions, Tau protein is phosphorylated by kinase easily, and then detaches from microtubule and aggregates into oligomers (Wang & Mandelkow, 2016). Tau protein oligomers aggregate paired helical filaments (PHFs) and neurofibrillary tangles (NFTs) and then deposit in the brain (Orr et al., 2017). This is a major pathological hallmark of tauopathy. The phosphorylation site of Tau protein is specific and mainly occurs at serine or threonine residues(Wang & Mandelkow, 2016). There are approximately 45 potential phosphorylation sites that have been observed in the longest Tau protein form experimentally, including Ser396, Ser404, Thr231, and Thr235. Furthermore, those sites are the targets of proline-directed protein kinases including glycogen synthase kinase 3β (GSK3β), mitogen-activated protein kinases (MAPKs), and cyclin-dependent kinase 5 (CDK5) (Brunden et al., 2009).

Autophagy, as a vital cellular degradation process for the recycling of nutrients, is crucial for the digestion and clearance of damaged organelles and aggregated proteins (Menzies et al., 2015). During autophagy, a double-membrane sequestering compartment termed autophagosome is formed, which involves multiple proteins and

the conversion of LC3 from LC3-I to membrane-associated LC3-II form (Feng et al., 2014). Then, the p62 carrying cargo targets for binding to LC3-II through their LC3-interacting region motifs. An autolysosome subsequently forms via the fusion of autophagosomes and lysosomes, and the cargo is digested by lysosomal enzymes in the autolysosome (Menzies et al., 2015). Inordinate autophagy affects the clearance of pathological Tau proteins and facilitates the pathogenesis of tauopathy (Schaeffer et al., 2012). Autophagy enhancers, such as rapamycin (Ozcelik et al., 2013), trehalose (Schaeffer et al., 2012), and methylene blue (Congdon et al., 2012) can suppress Tau protein induced neurotoxicity and may be alternative approaches to ameliorate pathological process of tauopathy.

Alginate, a common food hydrocolloid, is a natural acidic polysaccharide which presents mainly as the calcium salt of alginic acid in the cell walls of many brown algae. The main components of alginate are β-D-mannuronic acid and its C-5 epimer α-L-guluronic acid (Haug et al., 1967). Alginate can be further depolymerized by alginate lyase, HCl, or H_2O_2 into alginate oligosaccharide (AOS) with various structures (Xu, Wu, et al., 2014). We have found that AOS and its derivatives from chemical modification exert diverse biological activities, including neuroprotective (Bi et al., 2019; Zhou, Shi, Bi, et al., 2015), immunomodulatory (Bi et al., 2017; Fang et al., 2017), and anti-inflammatory (Bi, Lai, Cai, et al., 2018; Zhou, Shi, Gao, et al., 2015) activities. An alginate-derived acidic oligosaccharide, acidic oligosaccharide sugar chain (AOSC) prepared from brown algae *Echlonia kurome* Okam through enzymatic depolymerization shows significant intervention effects on neurodegeneration disease

(J. Hu et al., 2004). In our previous study, we have found that unsaturated mannuronate oligosaccharide (MOS), a structural analogue of AOSC, present marked anti-AD activities with amelioration of β-amyloid pathology through autophagy in AD cell models (Bi, Yao, et al., 2021).

In this study, we hypothesize that the carbohydrate polymer MOS may be able to attenuate tauopathy via Tau protein intervention. Hence, the effects of MOS on the phosphorylation and clearance of Tau protein in cell models of HEK293/Tau and 3×Tg mice primary cortex neurons were investigated, in order to explore the mechanism of action of MOS in tauopathy's pathological process.

4.4 Materials and methods

4.4.1 Materials

Thioflavin T (ThT) and Alginate were purchased from Sigma-Aldrich (St. Louis, MO, USA). Neurobasal-A medium, Dulbecco's modified eagle medium (DMEM), penicillin, B-27 supplement (50×), streptomycin and G418 were supplied by Gibco (Grand Island, NY, USA). Fetal bovine serum (FBS) and Bafilomycin A1 (Baf A1) were supplied by Biological Industries (Beit-Haemek, Israel) and InvivoGen (San Diego, CA, USA), respectively. Antibodies against p-S404-Tau, p-S396-Tau, p-S262-Tau, p-S202-Tau, GSK-3β, Tau 5, p-S9 GSK-3β, p-Y216 GSK-3β, LC3, p62, horseradish peroxidase (HRP)-conjugated secondary antibody and Alexa Fluor 488-conjugated secondary antibody were obtained from Cell Signaling Technology (Beverly, MA, USA). Antibody against human tau 7 (HT7) and antibody against Microtubule Associated Protein 2 (Map 2)

were purchased from Thermo Scientific (Rochester, NY, USA) and Abcam (Cambridge, UK), respectively. Other chemicals were supplied by Macklin Biochemical Technology (Shanghai, China).

4.4.2 Preparation of MOS

Polymannuronate (PM) was prepared from alginate using a previously published method (Haug et al., 1967). In brief, 10 g alginate was dissolved in 0.5 M HCl of 500 mL and heated for 7 h at 90 °C. Solution was centrifuged at 2000 *g* for 10 min, and the sediment was removed and then re-dissolved in 8% $NaHCO_3$ at pH 2.85. The solution was centrifuged, and then 95% ethyl alcohol (1:3, v:v) was added to the solution to make PM precipitate. After centrifugation, the precipitate of white color was re-dissolved in pure water and freeze-dried. PM was obtained after freeze drying. After confirmed the homogeneity using circular dichroic spectrum (J-815; Jasco, Inc., Tokyo, Japan), PM (500 mg in 20 mL 5 mM phosphate buffer, pH=6.5) was mixed with 20 μL alginate lyase (0.3 mg/mL), purified from of *Pseudoalteromonas sp. strain 272*. After incubating in a water bath for 2 h at 37°C, equal enzyme solution was added and incubated for a further 18 h. MOS was obtained after filtration and freeze drying.

4.4.3 ThT fluorescence analysis

Tau-K18 is a truncated form of human Tau containing only the four microtubule binding repeats, the aggregation of which could be monitored by ThT (Zhang et al., 2019). To investigate the effect of MOS on Tau-K18 fibrillation, 200 μM Tau-K18 was diluted in Tris buffer (pH 7.4) containing 20 mM ThT and 16 μM heparin, and then MOS

(final concentration 1 mg/mL) in Tris buffer was added. Solution of 200 μL each well was added to the wells of black 96-well plates and incubated for 20 h at 37°C. ThT fluorescence was measured at different time points by using a microplate reader (Thermo Scientific, Hudson, NH, USA) with excitation/emission set at 444/485 nm.

4.4.4 Cell and neuronal culture

Human embryonic kidney 293 (HEK293) cells was from the Shanghai Cell Bank of the Chinese Academy of Sciences (Shanghai, China). HEK293/Tau cells are HEK293 cells were transfected with the longest human Tau protein (Tau441). The culture conditions for HEK293/Tau cells were: DMEM supplemented with 10% FBS, 0.5% G418, 1% antibiotics (penicillin and streptomycin), temperature 37°C and 5% CO_2. HEK293/Tau cells (1×10^6 cells/well) treated with 1 mg/mL MOS were incubated in 6-well plates for 24 h.

Wild type or 3×Tg mice were hosted under the standard laboratory conditions with 12-12 light-dark cycle, 22 ± 2°C temperature and food *ad libitum*. Mice (3×Tg) were supplied by the Jackson Laboratory (hybrid 129/C57BL6 background, JAX order number 3591206), with overexpressed human mutant P301L-Tau and multi-site hyperphosphorylated. All experiments were approved by the Shenzhen University Regional Ethical Committee for Animal Experimentation (2014-12-012). Primary cortex neurons were dissected from the brain of postnatal (P_0-P_1) 3×Tg or wild type mouse pups. In brief, cortex was dissected from the brain and digested in DMEM containing 2 mg/mL papain at 37°C for 30 min. After 3 min terminating digestion in new DMEM

with 10% FBS, the cortex tissue was added to neurobasal-A medium containing 2% B-27, 1% penicillin-streptomycin and 0.5% L-glutamine. After shaking slightly, 5×10^5 dissociated neurons were transferred to poly-D-lysine coated 6-well plates or glass-bottom culture dish to be cultured. After 4h, the medium was changed completely, and thereafter, half-replacement change was carried out once every 3 days. At day 10, MOS (1 mg/mL) treatment was applied to cultured neurons for 24 h.

4.4.5 RNA isolation and reverse transcription-polymerase chain reaction (RT-PCR)

Total RNA was extracted from MOS-treated HEK293/Tau cells using the RNAfast2000 RNA Extraction Kit (Fastagen, Shanghai, China). After reverse transcription to cDNA, PCR procedures were done with the following conditions: 1 cycle for 180 s at 95°C; 26 cycles for 55 s at 93°C, 45 s at 60°C, and 40 s at 72°C; and 1 cycle for 100 s at 72°C using Premix Taq Kit (TaKaRa Biotechnology Co., Ltd., Liaoning, China). The sequences of primers for Tau protein and β-actin were:

Tau protein,

Forward: 5’- TCGCAGTCACCGCCACCCAC-3’,

Reverse: 5’- TGTCATCGCTTCCAGTCCCGTC-3’;

β-actin,

Forward: 5’-GGAGAAGATCTGGCACCACACC-3’,

Reverse: 5’-CCTGCTTGCTGATCCACATCTGCTGG-3’.

Each PCR reaction product was resolved on a 1% agarose gel and analyzed using a

G-box imaging system (Syngene, Cambridge, UK), and the band density was quantified using the Quantity One software (Bio-Rad, Richmond, CA, USA).

4.4.6 Western blot analysis

After MOS treatment, the HEK293/Tau cells or primary cortex neurons were obtained and lysed on ice using Western and IP cell lysis buffer (Beyotime Institute of Biotechnology, Jiangsu, China) containing protease and phosphatase inhibitor cocktail (Selleck, Shanghai, China). After detecting the protein content using a BCA Protein Quantitation Kit (Beyotime Biotechnology), 20 μg protein of each sample was resolved by 12% or 15% SDS-PAGE and transferred to a 0.45 μM PVDF membrane (Merck Millipore Ltd, Darmstade, Germany). Then membranes were blocked in 5% (w/v) skim milk at room temperature (RT) for 2 h and primary antibodies (1:1000) was probed with samples overnight at 4°C. After subsequent three washes using TBST, membranes were incubated with HRP-conjugated secondary antibody (1:5000) at RT for 1 h. After rinsing, the protein bands on the membranes were sanned by the luminescent image analyzer (LAS3000; Fujifilm Life Science, Tokyo, Japan) which required an ECL kit to run (Thermo Scientific, Hudson, NH, USA). The density of bands was quantitated by using the Quantity One software.

4.4.6 Immunofluorescence analysis

After MOS treatment, the primary cortex neurons on the glass were fixed with 4% formaldehyde for 30 min at RT. After 0.2% (w/v) Triton X-100 (in PBS) treatment for 10 min, cells were blocked with 10% (w/v) goat serum (in PBS) for 2 h at RT. Cells were

then incubated with p-S396-Tau, p-S404-Tau or MAP2 primary antibody overnight at 4°C. Washed by PBS, the cells were incubated with Alexa Fluor 488 or 594 conjugated secondary antibody for 2 h at RT. After additional washes, cells were imaged under a confocal microscope (Carl Zeiss Jena Gmbh, Jena, Germany).

4.4.7 Statistical analysis

The data for all the experiments were means of triplicate assays in any given single experiment, and presented as means ± standard deviation (SD). Data were tested for distribution. Log transformation was applied to those data with large variation and not normally distributed. Two-tailed Student's t-test was used to analyze data and determine if there were any significant differences by using GraphPad Prism 7 (GraphPad Software, Inc., La Jolla, CA, USA).

4.5 Results

4.5.1 Chemical Characterization of PM and MOS

The homogeneity of PM and MOS was analyzed by the CD spectrum (J-815; Jasco, Inc., Tokyo, Japan). CD spectrum of PM and MOS appeared at 197 nm as a peak and at 215 nm as a trough, respectively (Figure 4.1A). Based on our previous report, the Mw of PM was 4.11 kDa and the degree of polymerization MOS obtained from PM using alginate lyase ranged from mannuronate dimer to mannuronate undecamer (M2-M11) (Figure 4.1B) (Bi et al., 2020; Bi, Yao, et al., 2021).

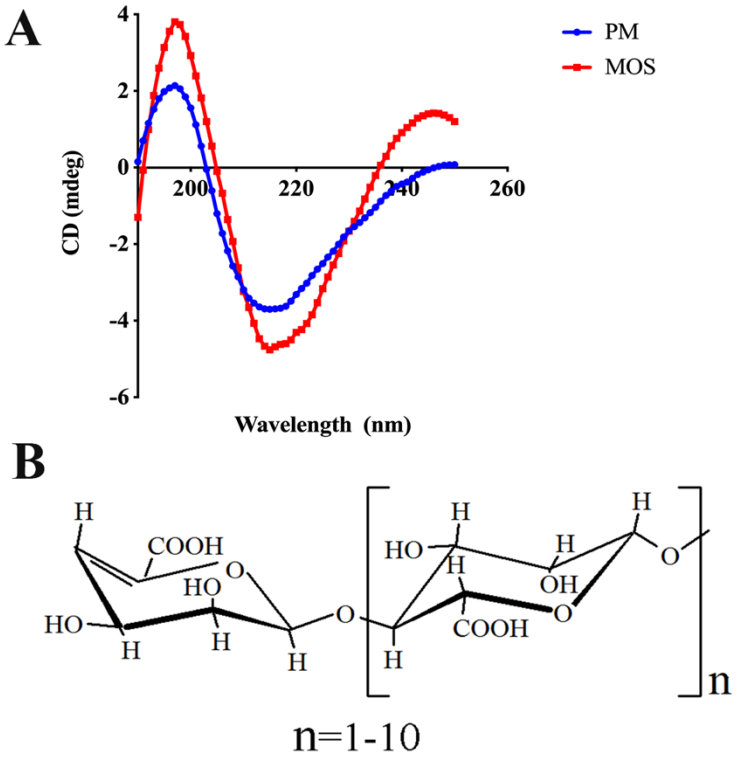

Figure 4.1 Chemical characterization of PM and MOS. (A) CD spectrum of PM and MOS. (B) Stereo-image of structure of MOS.

4.5.2 MOS inhibits fibrillation of Tau-K18 *in vitro.*

A fluorescence-based analysis of ThT was used to monitor the aggregation of Tau-K18 monomer. As shown in Figure 4.2, an increase of ThT fluorescence was observed in only heparin-treated Tau-K18 group, but the maximal ThT fluorescence value was decreased by the addition of MOS (1 mg/mL) in heparin more than five folds compared with the only heparin-induced group.

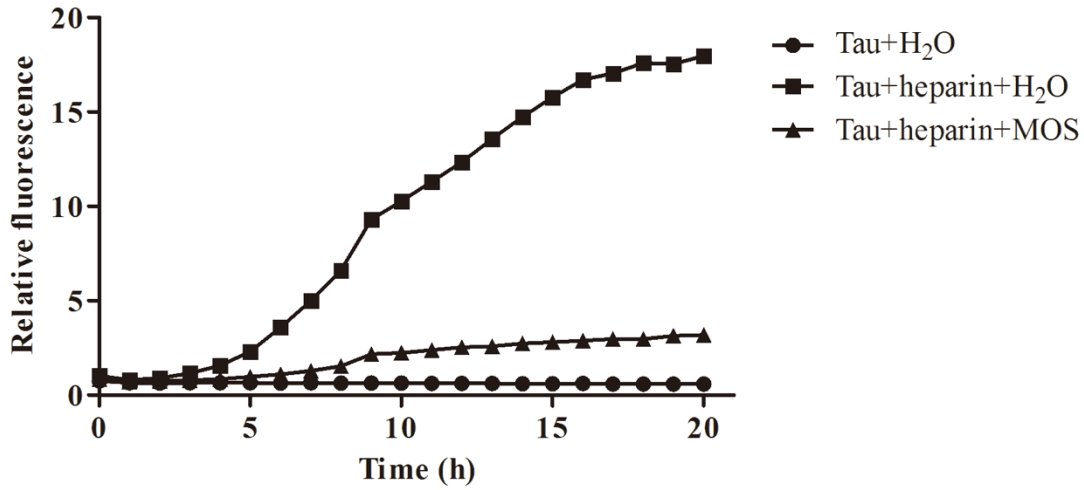

Figure 4.2 The effects of MOS on Aβ aggregation *in vitro*. Tau-K18 of 200 μM was diluted in Tris buffer (pH 7.4) containing 20 mM ThT and 16 μM heparin incubated with MOS of 1 mg/mL at 37°C. Fluorescence intensity of ThT in each group was measured at different time points by using a microplate reader with excitation/emission set at 444/485 nm.

4.5.3 MOS inhibits phosphorylation of Tau protein.

The effects of MOS on the Tau protein phosphorylation were examined by Western blotting and analysis immunofluorescence in HEK293/Tau cells and in primary cortex neurons. MOS treatment decreased the phosphorylation levels of Tau protein on the sites of Ser404, Ser396, Ser262 and Ser202 as well as total Tau protein level (Figure 4.3A). A similar trend was seen in primary cortex neurons. As presented in Figure 4.3B, phosphorylation levels and total expression of Tau protein were much higher in primary cortex neurons of 3×Tg mice than that of wild type mice. After treated with MOS, phosphorylation levels of Tau protein on the sites of Ser404, Ser396, Ser262 and Ser202 were significantly decreased. However, expression of the total Tau protein in

primary cortex neurons of 3×Tg mice did not change after MOS treatment (Figure 4.3B). In addition, immunofluorescence analysis also confirmed there was a significant reduction in Tau protein phosphorylation in the primary cortex neurons of MOS treated 3×Tg mice (Figure 4.3C).

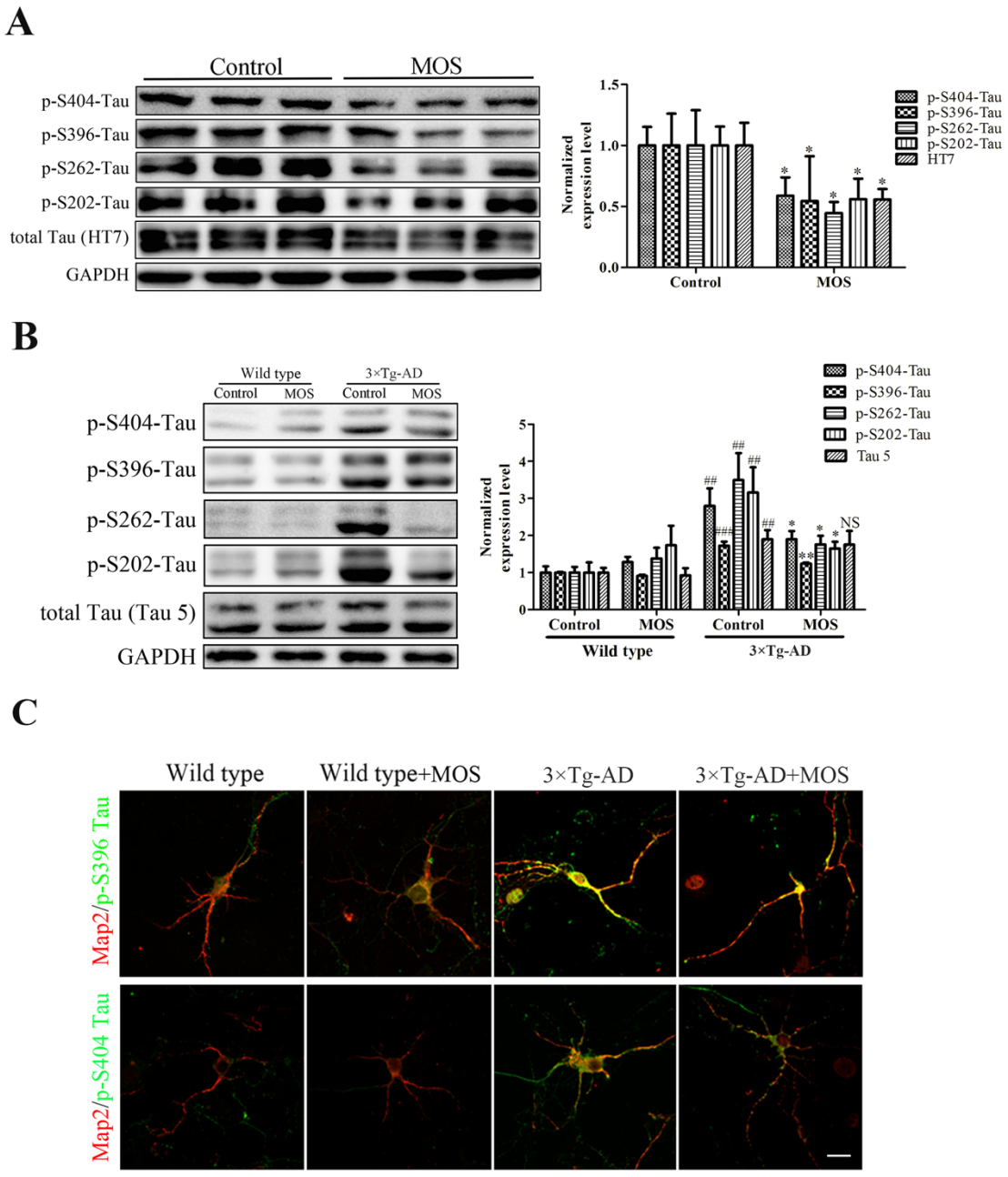

Figure 4.3 The effects of MOS on Tau protein production. (A) HEK293/Tau cells treated with MOS for 24 h, the levels of p-S202-Tau, p-S262-Tau, p-S396-Tau, p-S404-Tau and

total Tau protein were evaluated via Western blot analysis and analysed using the ImageJ software. Wild type and 3×Tg-AD primary cortex neurons treated with MOS for 24 h, (B) the levels of p-S202-Tau, p-S262-Tau, p-S396-Tau, p-S404-Tau and total Tau protein were evaluated via Western blot analysis and statistically analysed using the ImageJ software, and (C) the levels of p-S396-Tau and p-S404-Tau were evaluated via immunofluorescence analysis. Only representative Western blot images are shown. NS, no significance. *Indicates significant differences between the control and MOS-treated groups. *P < 0.05, **P < 0.01; #Indicates significant differences between wild type primary cortex neurons and the 3×Tg-AD primary cortex neurons. ##P < 0.01, ###P < 0.001. Scale bar = 20 μm.

4.5.4 MOS inhibits GSK-3β signaling pathway.

To further investigate the mechanism why Tau protein phosphorylation levels was reduced by MOS treatment, the level of a protein kinase, GSK-3β, which regulates this post-translational modification, was evaluated. The activity of GSK-3β is regulated via phosphorylation at different amino acid sites. It is inhibited by the phosphorylation at residue Ser9 and improved by the phosphorylation at residue Tyr216 (Shaw et al., 1997). Figure 4.4A shows that the phosphorylation levels were significantly increased at Ser9 site of GSK-3β, and in contrast, was decreased remarkably at Tyr216 site in MOS-treated HEK293/Tau cells, showing that MOS could effectively inhibit the GSK-3β activity. The GSK-3β expression in primary cortex neurons was also determined using Western blot analysis and the similar trend was observed in Figure 4.4B. MOS treatment did not show any statistically significant effect on the GSK-3β activity in wild

type neurons (Figure 4.4B). However, the phosphorylation levels at Ser9 site of GSK-3β in primary cortex neurons of 3×Tg mice was much lower than the neurons of wild type, and the phosphorylation levels at Tyr216 site of GSK-3β was much higher in primary cortex neurons of 3×Tg mice than that of wild type, showing the GSK-3β activity primary cortex neurons of 3×Tg mice is over-activated (Figure 4.4B). Then, significant changes of GSK-3β phosphorylation level in primary cortex neurons of 3×Tg mice were observed between the MOS-treated and control groups, including the increased phosphorylation levels at Ser9 site of GSK-3β and the decreased phosphorylation levels at Tyr216 site after MOS treatment (Figure 4.4B), showing MOS treatment inhibited the activity of GSK-3β in neurons.

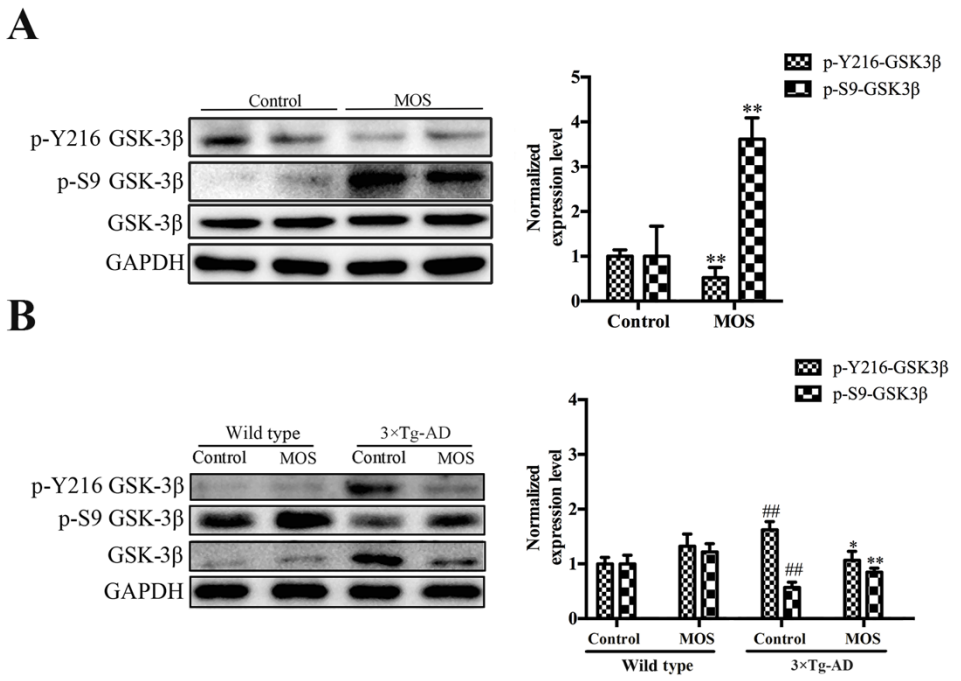

Figure 4.4 The effects of MOS on GSK-3β pathway. (A) HEK293/Tau cells treated with MOS for 24 h, the levels of p-Y216-GSK-3β, p-S9-GSK-3β and GSK-3β were evaluated via Western blot analysis and analysed using the ImageJ software. (B) Wild type and

3×Tg-AD primary cortex neurons treated with MOS for 24 h, the levels of p-Y216-GSK-3β, p-S9-GSK-3β and GSK-3β were evaluated via Western blot analysis and analysed using the ImageJ software. Only representative Western blot images are shown. *Indicates significant differences between the control and MOS-treated groups. *P < 0.05, **P < 0.01; #Indicates significant differences between the 3×Tg-AD primary cortex neurons and wild type primary cortex neurons. ##P < 0.01.

4.4.5 MOS increases cell autophagy to decrease the levels of Tau protein.

A significant reduction of total Tau protein by MOS treatment was shown in HEK293/Tau cells (Figure 4.3A). The reason may be that blocking of the transcription of Tau gene or promotion the elimination of overexpressed Tau protein was caused by MOS treatment. However, MOS treatment did not make any change to Tau protein mRNA expression in comparison with the control group in HEK293/Tau cells (Figure 4.5A), which suggests that the decrease of Tau protein might be related to an elimination mechanism. Autophagy, an intracellular degradation pathway, is responsible for the clearance of abnormal proteins in autolysosome (Menzies et al., 2015). The expression level of LC3 and p62 were assayed using Western blot to assess the extent of autophagy. As shown in Figure 4.5B, MOS treatment improved the expression ratio of LC3-II/LC3-I. It also decreased the p62 protein level in HEK293/Tau cells, demonstrating that MOS treatment promoted the autophagy level.

Baf A1 is an autophagic inhibitor which blocks the fusion of autophagosomes with lysosome. It was used to investigate the relationship between the MOS-triggered autophagy and Tau protein reduction. As the results presented, the decline of total Tau

protein and p-Ser404-Tau protein induced by MOS were recovered while Baf A1 was co-incubated in HEK293/Tau cells (Figure 4.5C). Taken together, the MOS-triggered suppression of total Tau protein and phosphorylated Tau protein might be entwined in the autophagy process.

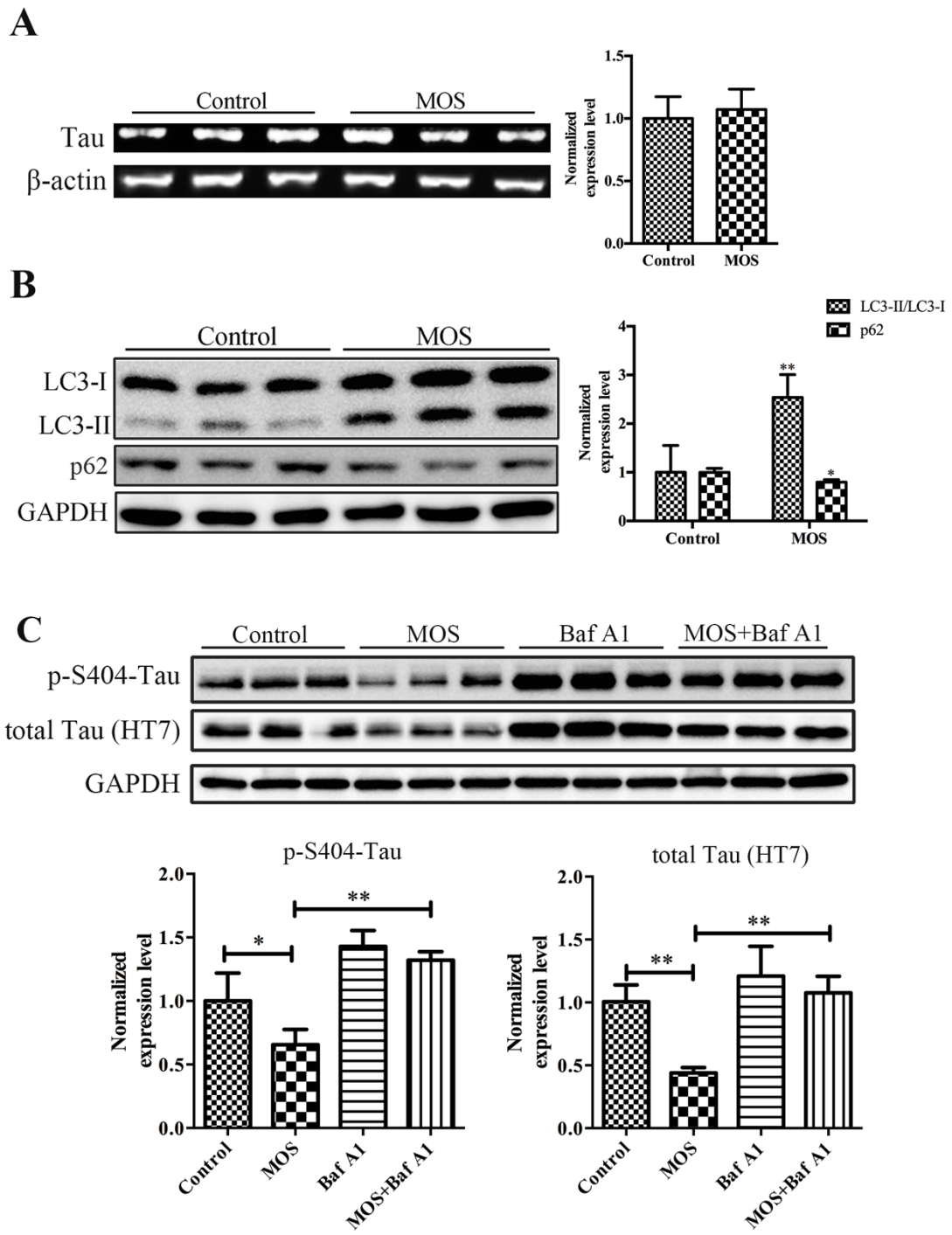

Figure 4.5 The effects of MOS on autophagy. (A) HEK293/Tau cells treated with MOS for 24 h, Tau mRNA levels were evaluated via RT-PCR and analysed using the ImageJ software. (B) HEK293/Tau cells treated with MOS for 24 h, the levels of LC3 and p62 were evaluated via Western blot analysis and analysed using the ImageJ software. (C)

HEK293/Tau cells co-treated with 1 mg/mL MOS and Baf A1 (0.1 μM) for 24 h, the levels of p-S404-Tau and total Tau protein were evaluated via Western blot analysis and statistically analyzed using the ImageJ software. Representative images and results from three independent experiments are shown. *P < 0.05, **P < 0.01.

4.6 Discussion

Tau protein, which aggregates and accumulate to form NFTs in the brains of patients with tauopathies while it is hyperphosphorylated, is an important target for the prevention/treatment of tauopathies (Orr et al., 2017). Many researches have reported that the toxicity of Tau protein is mainly from the oligomers form, instead of the monomer and fibril (Lasagna-Reeves et al., 2010). Therefore, a compound which could inhibit the Tau protein aggregation has the potentially to be developed into tauopathy treatment. Epigallocatechin gallate (EGCG), a green tea polyphenol being studied in the clinical trials for AD, suppresses the aggregation of Tau K18ΔK280 into toxic oligomers, thereby rescuing its toxicity (Wobst et al., 2015). Methylene blue which is being studied in clinical trials can change the structure of existing PHFs isolated from tauopathy patients' brains (Wischik et al., 1996). In our previous study, we found that MOS could effectively inhibit the aggregation of β-amyloid (Aβ) (Bi, Yao, et al., 2021), which is a major content of senile plaques in brains of AD patients. Now, the inhibition of Tau protein aggregation by MOS was determined in this study (Figure 4.2). This positive result suggests that MOS may become a candidate to attenuate tauopathy.

What make Tau protein aggregate in tauopathies are not fully clear. However, a post-

translational modification that could alter the Tau properties is hyperphosphorylation which occurs in all tauopathies (Brunden et al., 2009). As the microtubule-associated protein, Tau protein is normally phosphorylated at multiple serine and threonine residues and the function of Tau protein is to maintain stability of microtubules and inhibit dissociation of microtubule protein molecules (Alonso et al., 1996). Hyperphosphorylated Tau protein monomer would fall from microtubules and then self-aggregate. In this study, MOS treatment has been found to effectively decrease hyperphosphorylated Tau protein levels in HEK293/Tau cells and primary cortex neurons of 3×Tg mice (Figure 4.3). A hyperactivation in protein kinases is the direct cause for Tau protein hyperphosphorylation. GSK-3β can phosphorylate Tau protein at multiple residues in a site-specific manner. Our study shows that MOS treatment could effectively inhibit the activation of GSK-3β in HEK293/Tau cells and primary cortex neurons of 3×Tg mice (Figure 4.4). It suggests that MOS could decrease Tau phosphorylation levels via regulating the protein kinase activation. Some results in HEK293/Tau cells were inconsistent with those of 3×Tg mice primary cortex neurons, which might be caused by the presence of other mutated genes interfering with Tau pathway in the 3×Tg mice primary cortex neurons.

It has been reported that the reduction of endogenous murine Tau in adult mice improves the neuroanatomical abnormalities (DeVos et al., 2013), indicating the possibility of a Tau lowering therapy. Furthermore, the misfolded proteins in neurodegenerative disease, such as Tau protein and synuclein, were targeted by autophagy (Z. Zhang et al., 2017). It has been shown that promotion of autophagy can

increase life span in yeast and mice (Harrison et al., 2009; Kaeberlein et al., 2005). Enhancement of autophagy in SH-SY5Y cells also are beneficial for inhibiting 6-hydroxydopamine (Lin & Tsai, 2017), Aβ (Hung et al., 2009), or Tau (Jiang et al., 2014) induced toxicity. Our previous study has shown that MOS is a significant autophagy enhancer (Bi, Yao, et al., 2021). In the present study, MOS showed no effect on the Tau gene expression in HEK293/Tau cells indicating that the reduction of total Tau by MOS in HEK293/Tau cells might be the Tau clearance via autophagy. LC3 is an important marker which usually used in assessing the cell autophagy levels and LC3-II is an active form converted from LC3-I during the autophagosome formation (Feng et al., 2014). In contrast, p62 expression is negatively correlated with autophagy levels (Komatsu et al., 2007). The increase of LC3-II/LC3-I ratio and decrease of p62protein level in MOS-treated HEK293/Tau cells in our current study showed that MOS effectively increased the level of autophagy in HEK293/Tau cells (Figure 4.5B). Applying autophagy inhibitor prevented the increase of autophay, confirming our hypothesis that MOS-induced Tau reduction is associated with autophagy (Figure 4.5C).

Many marine resources, especially seaweed polysaccharide extracts are attracting attentions in various research fields including drug and functional foods development (Bi, Yu, et al., 2018). As early as the sixteenth century, seaweed polysaccharides was used for medicinal purposes in China (Jiang et al., 2011). It has been reported that AOSC, an alginate derivative exhibits excellent effects in anti-AD (J. Hu et al., 2004). Pentasaccharide prepared from κ-carrageenan possesses significant neuroprotection activity (Liu et al., 2017). A common problem for new brain diseases drugs is whether

they can pass the blood-brain barrier (BBB). Our previous study reported that the saccharides with the molecular weight < 2.2 kDa could pass through the BBB easily (Bi, Lai, Han, et al., 2018). It has also been found that AOSC with the molecular weight of 1.3 kDa could also pass the BBB easily (Guo et al., 2006). We have revealed that the degree of polymerization MOS ranged from M2-M11 (Figure 4.1). Based on the information above, MOS should be able to pass BBB, laying a foundation for it to be further developed as a candidate for the treatment of brain diseases.

Many failed clinical trials suggest that single target-based drugs to neurodegenerative disease, especial to AD, may not be sufficiently effective, such as Semagacestat (Doody et al., 2013) and Solanezumab (Sacks et al., 2017). Therefore, researchers are searching for multi-targeted natural compounds in neurodegenerative disease prevention and treatment. GV-971 is an alginate-derived oligosaccharide and has successfully passed phase III clinical trials. It is a multi-target drug (Gao et al., 2019). Previous study has proven that MOS can not only reduce Aβ levels via the inhibition of BACE1 but also enhance autophagy to increase Aβ clearance in AD cell models (Bi, Yao, et al., 2021). This suggests that MOS, also derived from brown seaweed alginate, is a multi-target compound which has the potential to be used in the treatment and/or prevention of neurodegenerative diseases.

In conclusion, we have revealed that MOS treatment not only inhibits the Tau protein aggregation, but also attenuates the phosphorylation of Tau protein and promotes its clearance through autophagy in tauopathy cell models in this report. Our results suggest that MOS has the potential to be developed further for the

treatment/prevention or to become a promising nutraceutical of neurodegenerative diseases such as tauopathy.

Chapter 5 Conclusion

5.1 Overall conclusion

AD is the most common type of dementia in aged people with the disorder clinically characterized by cognitive deficits. In November 2019, GV-971 was approved by the China Food and Drugs Administration for the treatment of mild to moderate patients diagnosed with Alzheimer's disease to improve cognitive function. However, there are still no significantly effective drugs or other therapeutic drugs that can be used to completely prevent or delay the progression of AD, and no effective biomarkers can be directly used for the early diagnosis and early detection of AD.

In this study, a variety of analytical methods, including HPLC, IR spectroscopy, CD spectroscopy, and ESI-MS, were applied to the structural analysis of alginate and alginate-derived MOS, which confirmed that the degree of polymerization of MOS ranged from mannuronate dimer to mannuronate undecamer (M2- M11). Then, the inhibitory effects of MOS on the aggregation of the $A\beta_{1-42}$ oligomer and Tau-K18 oligomer *in vitro* were confirmed. In multiple AD cell models, MOS treatment prevented the Aβ pathway and tau pathway through inactivation of BACE1 and GSK-3β, respectively. Additionally, MOS treatment promoted Aβ and tau protein clearance through activation of autophagy. These results confirmed the involvement of autophagy in the anti-AD activity of MOS.

5.2 Significance

This study investigated for the first time the potential therapeutic effect of MOS on

AD and its molecular mechanism. The results show that there is an interaction between MOS and Aβ and the tau oligomer. Furthermore, MOS treatment prevents the Aβ and tau pathways and enhances autophagy to promote the clearance of Aβ and tau proteins in AD cell models. These data shed light on a novel application prospect of MOS as a promising functional food or a natural medication for the treatment or assistance of the treatment of AD.

5.3 Prospects

In this study, it was found that MOS could inhibit the aggregation of Aβ and Tau oligomers *in vitro*. In the later stage, the interaction mechanism between MOS and Aβ and the tau oligomer will be further studied by using UV spectroscopy, fluorescence spectroscopy, CD spectroscopy, isothermal titration heating, surface plasmon resonance, NMR and other biophysical methods.

Additionally, this study found that MOS had significant anti-AD activity, but its mechanism was not thoroughly studied. In addition, the current studies are all conducted at the cellular level, and the pathology and mechanism of MOS anti-AD will be further studied in AD animal models in the future.

.

Reference

Abd El-Mohdy, H. (2017). Radiation-induced degradation of sodium alginate and its plant growth promotion effect. *Arabian Journal of Chemistry*, *10*, S431-S438.

Ai, C., Jiang, P., Liu, Y., Duan, M., Sun, X., Luo, T., . . . Song, S. (2019). The specific use of alginate from Laminaria japonica by Bacteroides species determined its modulation of the Bacteroides community. *Food & Function*, *10*(7), 4304-4314.

Al-Najjar, M. A., Athamneh, T., AbuTayeh, R., Basheti, I., Leopold, C., Gurikov, P., & Smirnova, I. (2021). Evaluation of the orally administered calcium alginate aerogel on the changes of gut microbiota and hepatic and renal function of Wistar rats. *PloS One*, *16*(4), e0247633.

Alers, S., Löffler, A. S., Wesselborg, S., & Stork, B. (2012). Role of AMPK-mTOR-Ulk1/2 in the regulation of autophagy: Cross talk, shortcuts, and feedbacks. *Molecular and Cellular Biology*, *32*(1), 2-11.

Alonso, A. d. C., Grundke-Iqbal, I., & Iqbal, K. (1996). Alzheimer's disease hyperphosphorylated tau sequesters normal tau into tangles of filaments and disassembles microtubules. *Nature Medicine*, *2*(7), 783-787.

An, Q. D., Zhang, G. L., Wu, H. T., Zhang, Z. C., Zheng, G. S., Luan, L., . . . Li, X. (2009). Alginate-deriving oligosaccharide production by alginase from newly isolated Flavobacterium sp. LXA and its potential application in protection against pathogens. *Journal of applied microbiology*, *106*(1), 161-170.

Ariyo, B., Tamerler, C., Bucke, C., & Keshavarz, T. (1998). Enhanced penicillin production by oligosaccharides from batch cultures of Penicillium chrysogenum in stirred-tank reactors. *FEMS microbiology letters*, *166*(1), 165-170.

Ariyo, B. T., Bucke, C., & Keshaverz, T. (1997). Alginate oligosaccharides as enhancers of penicillin

production in cultures of Penicillium chrysogenum. *Biotechnology and bioengineering*, *53*(1), 17-20.

Assis, J., Serrão, E. Á., Coelho, N. C., Tempera, F., Valero, M., & Alberto, F. (2018). Past climate changes and strong oceanographic barriers structured low-latitude genetic relics for the golden kelp Laminaria ochroleuca. *Journal of Biogeography*, *45*(10), 2326-2336.

Atkins, E., Nieduszynski, I., Mackie, W., Parker, K., & Smolko, E. (1973). Structural components of alginic acid. II. The crystalline structure of poly-α-L-guluronic acid. Results of X-ray diffraction and polarized infrared studies. *Biopolymers: Original Research on Biomolecules*, *12*(8), 1879-1887.

Bachurin, S. O., Bovina, E. V., & Ustyugov, A. A. (2017). Drugs in clinical trials for Alzheimer's disease: the major trends. *Medicinal Research Reviews*, *37*(5), 1186-1225.

Baddeley, T. C., McCaffrey, J., Storey, J. M., Cheung, J. K., Melis, V., Horsley, D., . . . Wischik, C. M. (2015). Complex disposition of methylthioninium redox forms determines efficacy in tau aggregation inhibitor therapy for Alzheimer's disease. *Journal of Pharmacology Experimental Therapeutics*, *352*(1), 110-118.

Baker, M., Mackenzie, I. R., Pickering-Brown, S. M., Gass, J., Rademakers, R., Lindholm, C., . . . Rollinson, S. (2006). Mutations in progranulin cause tau-negative frontotemporal dementia linked to chromosome 17. *Nature*, *442*(7105), 916-919.

Balakrishnan, B., Lesieur, S., Labarre, D., & Jayakrishnan, A. (2005). Periodate oxidation of sodium alginate in water and in ethanol–water mixture: a comparative study. *Carbohydrate Research*, *340*(7), 1425-1429.

Bhatia, V., & Sharma, S. (2021). Role of mitochondrial dysfunction, oxidative stress and autophagy in progression of Alzheimer's disease. *Journal of the neurological sciences*, *421*, 117253.

Bi, D., Lai, Q., Cai, N., Li, T., Zhang, Y., Han, Q., . . . Bao, W. (2018). Elucidation of the molecular-mechanisms and in vivo evaluation of the anti-inflammatory effect of alginate-derived Seleno-polymannuronate. *Journal of Agricultural and Food Chemistry*, *66*(9), 2083-2091.

Bi, D., Lai, Q., Han, Q., Cai, N., He, H., Fang, W., . . . Li, X. (2018). Seleno-polymannuronate attenuates neuroinflammation by suppressing microglial and astrocytic activation. *Journal of Functional Foods*, *51*, 113-120.

Bi, D., Lai, Q., Li, X., Cai, N., Li, T., Fang, W., . . . Xu, X. (2019). Neuroimmunoregulatory potential of seleno-polymannuronate derived from alginate in lipopolysaccharide-stimulated BV2 microglia. *Food Hydrocolloids*, *87*, 925-932.

Bi, D., Li, X., Li, T., Li, X., Lin, Z., Yao, L., . . . Zhang, Z. (2020). Characterization and neuroprotection potential of seleno-polymannuronate. *Frontiers in Pharmacology*, *11*, 21.

Bi, D., Xiao, S., Lin, Z., Yao, L., Fang, W., Wu, Y., . . . Xu, X. (2021). Alginate-derived mannuronate oligosaccharide attenuates tauopathy through enhancing autophagy. *Journal of Agricultural and Food Chemistry*, *69*, 4438-4445.

Bi, D., Yao, L., Lin, Z., Chi, L., Li, H., Xu, H., . . . Xu, X. (2021). Unsaturated mannuronate oligosaccharide ameliorates β-amyloid pathology through autophagy in Alzheimer's disease cell models. *Carbohydrate Polymers*, *251*, 117124.

Bi, D., Yu, B., Han, Q., Lu, J., White, W. L., Lai, Q., . . . Li, S. (2018). Immune activation of RAW264. 7 macrophages by low molecular weight fucoidan extracted from New Zealand Undaria pinnatifida. *Journal of Agricultural Food Chemistry*, *66*(41), 10721-10728.

Bi, D., Zhou, R., Cai, N., Lai, Q., Han, Q., Peng, Y., . . . Xu, X. (2017). Alginate enhances Toll-like receptor 4-mediated phagocytosis by murine RAW264. 7 macrophages. *International Journal of*

Biological Macromolecules, *105*, 1446-1454.

Blennow, K., Mony J De, L., & Zetterberg, H. (2006). Alzheimer's disease. *Lancet*, *368*(9533), 387-403.

Boucelkha, A., Petit, E., Elboutachfaiti, R., Molinié, R., Amari, S., & Zaidi-Yahaoui, R. (2017). Production of guluronate oligosaccharide of alginate from brown algae Stypocaulon scoparium using an alginate lyase. *Journal of Applied Phycology*, *29*(1), 509-519.

Brownlee, I., Allen, A., Pearson, J., Dettmar, P., Havler, M., Atherton, M., & Onsøyen, E. (2005). Alginate as a source of dietary fiber. *Critical reviews in food science and nutrition*, *45*(6), 497-510.

Brunden, K. R., Trojanowski, J. Q., & Lee, V. M. Y. (2009). Advances in Tau-focused drug discovery for Alzheimer's disease and related tauopathies. *Nature Reviews Drug Discovery*, *8*(10), 783-793.

Bulic, B., Pickhardt, M., Schmidt, B., Mandelkow, E. M., Waldmann, H., & Mandelkow, E. (2009). Development of tau aggregation inhibitors for Alzheimer's disease. *Angewandte Chemie International Edition*, *48*(10), 1740-1752.

Burana-osot, J., Hosoyama, S., Nagamoto, Y., Suzuki, S., Linhardt, R. J., & Toida, T. (2009). Photolytic depolymerization of alginate. *Carbohydrate Research*, *344*(15), 2023-2027.

Caccamo, A., Majumder, S., Richardson, A., Strong, R., & Oddo, S. (2010). Molecular interplay between mammalian target of rapamycin (mTOR), amyloid-β, and tau effects on cognitive impairments. *Journal of Biological Chemistry*, *285*(17), 13107-13120.

Campos-Perez, W., & Martinez-Lopez, E. (2021). Effects of short chain fatty acids on metabolic and inflammatory processes in human health. *Biochimica et Biophysica Acta (BBA)-Molecular and Cell Biology of Lipids*, 158900.

Chang, L., Li, F., Chen, X., Xu, S., Wang, C., Chen, H., & Wang, Q. (2014). Effects of acidic oligosaccharide sugar chain on amyloid oligomer-induced impairment of synaptic plasticity in rats. *Metabolic*

brain disease, *29*(3), 683-690.

Chen, J., Hu, Y., Zhang, L., Wang, Y., Wang, S., Zhang, Y., . . . Wang, Y. (2017). Alginate oligosaccharide DP5 exhibits antitumor effects in osteosarcoma patients following surgery. *Frontiers in Pharmacology*, *8*, 623.

Chen, Y., Dou, W., Li, H., Shi, J., & Xu, Z. (2018). The alginate lyase from Isoptericola halotolerans CGMCC 5336 as a new tool for the production of alginate oligosaccharides with guluronic acid as reducing end. *Carbohydrate Research*, *470*, 36-41.

Cheng, B., Gong, H., Xiao, H., Petersen, R. B., Zheng, L., & Huang, K. (2013). Inhibiting toxic aggregation of amyloidogenic proteins: a therapeutic strategy for protein misfolding diseases. *Biochimica ET Biophysica Acta- General Subjects*, *1830*(10), 4860-4871.

Cheng, H., Wen, C., Zhang, C., & Kwapong, W. (2020). The use of GV-971 induces liver injury in an Alzheimer's disease patient. *Authorea Preprints*.

Ching, S. H., Bansal, N., & Bhandari, B. (2017). Alginate gel particles–A review of production techniques and physical properties. *Critical reviews in food science and nutrition*, *57*(6), 1133-1152.

Congdon, E. E., Wu, J. W., Myeku, N., Figueroa, Y. H., Herman, M., Marinec, P. S., . . . Duff, K. E. (2012). Methylthioninium chloride (methylene blue) induces autophagy and attenuates tauopathy in vitro and in vivo. *Autophagy*, *8*(4), 609-622.

da Silva Bastos, D., de Lima Araújo, K. G., & da Rocha Leão, M. H. M. (2009). Ascorbic acid retaining using a new calcium alginate-Capsul based edible film. *Journal of Microencapsulation*, *26*(2), 97-103.

Deng, Z., Li, J., Song, R., Zhou, B., Li, B., & Liang, H. (2021). Carboxymethylpachymaran/alginate gel entrapping of natural pollen capsules for the encapsulation, protection and delivery of probiotics with enhanced viability. *Food Hydrocolloids*, 106855.

DeVos, S. L., Goncharoff, D. K., Chen, G., Kebodeaux, C. S., Yamada, K., Stewart, F. R., . . . Rigo, F. (2013). Antisense reduction of tau in adult mice protects against seizures. *Journal of Neuroscience*, *33*(31), 12887-12897.

Dische, Z. (1947). A new specific color reaction of hexuronic acids. *Journal of Biological Chemistry*, *167*(1), 189-198.

Doody, R., Raman, R., Farlow, M., Iwatsubo, T., Vellas, B., Joffe, S., . . . Aisen, P. (2013). A phase 3 trial of semagacestat for treatment of Alzheimer's disease. *New England Journal of Medicine*, *369*(4), 341-350.

Dou, L., Li, B., Zhang, K., Chu, X., & Hou, H. (2018). Physical properties and antioxidant activity of gelatin-sodium alginate edible films with tea polyphenols. *International Journal of Biological Macromolecules*, *118*, 1377-1383.

Draget, K., Bræk, G. S., & Smidsrød, O. (1994). Alginic acid gels: the effect of alginate chemical composition and molecular weight. *Carbohydrate Polymers*, *25*(1), 31-38.

Ebere, E., Obinna, I., & Wirnkor, V. (2019). Applications of column, paper, thin layer and ion exchange chromatography in purifying samples: Mini review. *SF Journal of Pharmaceutical and Analytical Chemistry*, *2*, 1018.

Eftekharzadeh, B., Khodagholi, F., Abdi, A., & Maghsoudi, N. (2010). Alginate protects NT2 neurons against H2O2-induced neurotoxicity. *Carbohydrate Polymers*, *79*(4), 1063-1072.

Ejima, R., Akiyama, M., Sato, H., Tomioka, S., Yakabe, K., Kimizuka, T., . . . Fukuda, S. (2021). Seaweed Dietary Fiber Sodium Alginate Suppresses the Migration of Colonic Inflammatory Monocytes and Diet-Induced Metabolic Syndrome via the Gut Microbiota. *Nutrients*, *13*(8), 2812.

Ermund, A., Recktenwald, C. V., Skjåk-Bræk, G., Meiss, L. N., Onsøyen, E., Rye, P. D., . . . Hansson, G. C.

(2017). OligoG CF-5/20 normalizes cystic fibrosis mucus by chelating calcium. *Clinical and Experimental Pharmacology and Physiology*, *44*(6), 639-647.

Falkeborg, M., Cheong, L., Gianfico, C., Sztukiel, K. M., Kristensen, K., Glasius, M., . . . Guo, Z. (2014). Alginate oligosaccharides: enzymatic preparation and antioxidant property evaluation. *Food Chemistry*, *164*, 185-194.

Fan, Y., Hu, J., Li, J., Zhao, Y., Xin, X., Wang, J., . . . Geng, M. (2005). Effect of acidic oligosaccharide sugar chain on scopolamine-induced memory impairment in rats and its related mechanisms. *Neuroscience Letters*, *374*(374), 222-226.

Fang, W., Bi, D., Zheng, R., Cai, N., Xu, H., Zhou, R., . . . Xu, X. (2017). Identification and activation of TLR4-mediated signalling pathways by alginate-derived guluronate oligosaccharide in RAW264. 7 macrophages. *Scientific Reports*, *7*(1), 1663.

Feng, W., Hu, Y., An, N., Feng, Z., Liu, J., Mou, J., . . . Mao, Y. (2020). Alginate oligosaccharide alleviates monocrotaline-induced pulmonary hypertension via anti-oxidant and anti-inflammation pathways in rats. *International heart journal*, *61*(1), 160-168.

Feng, W., Liu, J., Wang, S., Hu, Y., Pan, H., Hu, T., . . . Mao, Y. (2021). Alginate oligosaccharide alleviates D-galactose-induced cardiac ageing via regulating myocardial mitochondria function and integrity in mice. *Journal of Cellular and Molecular Medicine*, *25*(15), 7157-7168.

Feng, W., Yang, X., Feng, M., Pan, H., Liu, J., Hu, Y., . . . Mao, Y. (2021). Alginate oligosaccharide prevents against D-galactose-mediated cataract in C57BL/6J mice via regulating oxidative stress and antioxidant system. *Current Eye Research*, *46*(6), 802-810.

Feng, Y., He, D., Yao, Z., & Klionsky, D. (2014). The machinery of macroautophagy. *Cell Research*, *24*(1), 24.

Flórez-Fernández, N., Torres, M. D., González-Muñoz, M. J., & Domínguez, H. (2019). Recovery of bioactive and gelling extracts from edible brown seaweed Laminaria ochroleuca by non-isothermal autohydrolysis. *Food Chemistry*, *277*, 353-361.

Franco, J. N., Tuya, F., Bertocci, I., Rodríguez, L., Martínez, B., Sousa-Pinto, I., & Arenas, F. (2018). The 'golden kelp'Laminaria ochroleuca under global change: Integrating multiple eco-physiological responses with species distribution models. *Journal of Ecology*, *106*(1), 47-58.

Fujihara, M., Iizima, N., Yamamoto, I., & Nagumo, T. (1984). Purification and chemical and physical characterisation of an antitumour polysaccharide from the brown seaweed Sargassum fulvellum. *Carbohydrate Research*, *125*(1), 97-106.

Fujihara, M., & Nagumo, T. (1992). The effect of the content of D-mannuronic acid and L-guluronic acid blocks in alginates on antitumor activity. *Carbohydrate Research*, *224*, 343-347.

Fujihara, M., & Nagumo, T. (1993). An influence of the structure of alginate on the chemotactic activity of macrophages and the antitumor activity. *Carbohydrate Research*, *243*(1), 211-216.

Gacesa, P., Squire, A., & Winterburn, P. J. (1983). The determination of the uronic acid composition of alginates by anion-exchange liquid chromatography. *Carbohydrate Research*, *118*, 1-8.

Gao, Y., Zhang, L., & Jiao, W. (2019). Marine glycan-derived therapeutics in China. *Progress in Molecular Biology Translational Science*, *163*, 113-134.

Georg Jensen, M., Kristensen, M., & Astrup, A. (2012). Effect of alginate supplementation on weight loss in obese subjects completing a 12-wk energy-restricted diet: a randomized controlled trial. *The American journal of clinical nutrition*, *96*(1), 5-13.

Gordon, S. (2002). Pattern recognition receptors: doubling up for the innate immune response. *Cell*, *111*(7), 927-930.

Grasdalen, H., Larsen, B., & Smidsrød, O. (1979). A pmr study of the composition and sequence of uronate residues in alginates. *Carbohydrate Research*, *68*(1), 23-31.

Grasdalen, H., Larsen, B., & Smisrod, O. (1981). 13C-NMR studies of monomeric composition and sequence in alginate. *Carbohydrate Research*, *89*(2), 179-191.

Guo, J., Ma, L., Shi, H., Zhu, J., Wu, J., Ding, Z., . . . Ge, J. (2016). Alginate oligosaccharide prevents acute doxorubicin cardiotoxicity by suppressing oxidative stress and endoplasmic reticulum-mediated apoptosis. *Marine Drugs*, *14*(12), 231.

Guo, J., Xu, F., Li, Y., Li, J., Liu, X., Wang, X., . . . An, Y. (2017). Alginate oligosaccharide alleviates myocardial reperfusion injury by inhibiting nitrative and oxidative stress and endoplasmic reticulum stress-mediated apoptosis. *Drug design, development and therapy*, *11*, 2387.

Guo, L., Goff, H. D., Xu, F., Liu, F., Ma, J., Chen, M., & Zhong, F. (2020). The effect of sodium alginate on nutrient digestion and metabolic responses during both in vitro and in vivo digestion process. *Food Hydrocolloids*, *107*, 105304.

Guo, X., Xin, X., Gan, L., Nie, Q., & Geng, M. (2006). Determination of the accessibility of acidic oligosaccharide sugar chain to blood-brain barrier using surface plasmon resonance. *Biological and Pharmaceutical Bulletin*, *29*(1), 60-63.

Guttman, A. (1997). Analysis of monosaccharide composition by capillary electrophoresis. *Journal of Chromatography A*, *763*(1-2), 271-277.

Han, Y., Zhang, L., Yu, X., Wang, S., Xu, C., Yin, H., & Wang, S. (2019). Alginate oligosaccharide attenuates α2, 6-sialylation modification to inhibit prostate cancer cell growth via the Hippo/YAP pathway. *Cell death & disease*, *10*(5), 1-14.

Han, Z., Chen, M., Fu, X., Yang, M., Hrmova, M., Zhao, Y., & Mou, H. (2021). Potassium Alginate

Oligosaccharides Alter Gut Microbiota, and Have Potential to Prevent the Development of Hypertension and Heart Failure in Spontaneously Hypertensive Rats. *International Journal of Molecular Sciences*, *22*(18), 9823.

Hanger, D. P., Anderton, B. H., & Noble, W. (2009). Tau phosphorylation: the therapeutic challenge for neurodegenerative disease. *Trends in Molecular Medicine*, *15*(3), 112-119.

Hao, C., Hao, J., Wang, W., Han, Z., Li, G., Zhang, L., . . . Yu, G. (2011). Insulin sensitizing effects of oligomannuronate-chromium (III) complexes in C2C12 skeletal muscle cells. *PloS One*, *6*(9), e24598.

Hao, C., Hao, J., Wang, W., Li, G., Zeng, Y., Wang, P., . . . Yu, G. (2011). Oligomannuronate-chromium (III) complex ameliorates insulin resistance in C57BL/KsJ-db/db mice. *Journal of Ocean University of China*, *10*(4), 336-342.

Hao, J., Hao, C., Zhang, L., Liu, X., Zhou, X., Dun, Y., . . . An, Y. (2015). OM2, a novel oligomannuronate-chromium (III) complex, promotes mitochondrial biogenesis and lipid metabolism in 3T3-L1 adipocytes via the AMPK-PGC1α pathway. *PloS One*, *10*(7), e0131930.

Hardy, J., & Allsop, D. (1991). Amyloid deposition as the central event in the aetiology of Alzheimer's disease. *Trends in pharmacological sciences*, *12*, 383-388.

Harrison, D. E., Strong, R., Sharp, Z. D., Nelson, J. F., Astle, C. M., Flurkey, K., . . . Carter, C. S. (2009). Rapamycin fed late in life extends lifespan in genetically heterogeneous mice. *Nature*, *460*(7253), 392.

Haug, A. (1964). Composition and properties of alginates. In Report No. 30. Norwegian Institute of Seaweed Research.

Haug, A., & Larsen, B. (1966). A study on the constitution of alginic acid by partial acid hydrolysis.

Proceedings of the Fifth International Seaweed Symposium, Halifax, August 25–28, 1965,

Haug, A., & Larsen, B. (1971). Biosynthesis of alginate: Part II. Polymannuronic acid C-5-epimerase from Azotobacter vinelandii (Lipman). *Carbohydrate Research*, *17*(2), 297-308.

Haug, A., Larsen, B., & Smidsrod, O. (1967). Studies on the sequence of uronic acid residues in alginic acid. *Acta Chemica Scandinavica*, *21*(3), 691-704.

He, N., Yang, Y., Wang, H., Liu, N., Yang, Z., & Li, S. (2021). Unsaturated alginate oligosaccharides (UAOS) protects against dextran sulfate sodium-induced colitis associated with regulation of gut microbiota. *Journal of Functional Foods*, *83*, 104536.

He, X., Hwang, H.-m., Aker, W. G., Wang, P., Lin, Y., Jiang, X., & He, X. (2014). Synergistic combination of marine oligosaccharides and azithromycin against Pseudomonas aeruginosa. *Microbiological research*, *169*(9-10), 759-767.

Hensley, K., & Harris-White, M. E. (2015). Redox regulation of autophagy in healthy brain and neurodegeneration. *Neurobiology of Disease*, *84*, 50-59.

Hien, N. Q., Nagasawa, N., Tham, L. X., Yoshii, F., Dang, V. H., Mitomo, H., . . . Kume, T. (2000). Growth-promotion of plants with depolymerized alginates by irradiation. *Radiation Physics and Chemistry*, *59*(1), 97-101.

Holme, H. K., Davidsen, L., Kristiansen, A., & Smidsrød, O. (2008). Kinetics and mechanisms of depolymerization of alginate and chitosan in aqueous solution. *Carbohydrate Polymers*, *73*(4), 656-664.

Holme, H. K., Lindmo, K., Kristiansen, A., & Smidsrød, O. (2003). Thermal depolymerization of alginate in the solid state. *Carbohydrate Polymers*, *54*(4), 431-438.

Holtan, S., Zhang, Q., Strand, W. I., & Skjåk-Bræk, G. (2006). Characterization of the hydrolysis

mechanism of polyalternating alginate in weak acid and assignment of the resulting MG-oligosaccharides by NMR spectroscopy and ESI− mass spectrometry. *Biomacromolecules*, *7*(7), 2108-2121.

Houghton, D., Wilcox, M. D., Chater, P. I., Brownlee, I. A., Seal, C. J., & Pearson, J. P. (2015). Biological activity of alginate and its effect on pancreatic lipase inhibition as a potential treatment for obesity. *Food Hydrocolloids*, *49*, 18-24.

Hu, F., Cao, S., Li, Q., Zhu, B., & Yao, Z. (2021). Construction and biochemical characterization of a novel hybrid alginate lyase with high activity by module recombination to prepare alginate oligosaccharides. *International Journal of Biological Macromolecules*, *166*, 1272-1279.

Hu, F., Zhu, B., Li, Q., Yin, H., Sun, Y., Yao, Z., & Ming, D. (2020). Elucidation of a unique pattern and the role of carbohydrate binding module of an alginate lyase. *Marine Drugs*, *18*(1), 32.

Hu, J., Geng, M., Li, J., Xin, X., Wang, J., Tang, M., . . . Ding, J. (2004). Acidic oligosaccharide sugar chain, a marine-derived acidic oligosaccharide, inhibits the cytotoxicity and aggregation of amyloid beta protein. *Journal of Pharmacological Sciences*, *95*(2), 248-255.

Hu, P., Li, Z., Chen, M., Sun, Z., Ling, Y., Jiang, J., & Huang, C. (2016). Structural elucidation and protective role of a polysaccharide from Sargassum fusiforme on ameliorating learning and memory deficiencies in mice. *Carbohydrate Polymers*, *139*, 150-158.

Hu, T., Li, C., Zhao, X., Li, G., Yu, G., & Guan, H. (2013). Preparation and characterization of guluronic acid oligosaccharides degraded by a rapid microwave irradiation method. *Carbohydrate Research*, *373*, 53-58.

Hu, X., Jiang, X., Hwang, H., Liu, S., & Guan, H. (2004). Antitumour activities of alginate-derived oligosaccharides and their sulphated substitution derivatives. *European Journal of Phycology*,

39(1), 67-71.

Huang, G., Wen, S., Liao, S., Wang, Q., Pan, S., Zhang, R., . . . Huang, S. (2019). Characterization of a bifunctional alginate lyase as a new member of the polysaccharide lyase family 17 from a marine strain BP-2. *Biotechnology letters*, *41*(10), 1187-1200.

Huang, H., Li, S., Bao, S., Mo, K., Sun, D., & Hu, Y. (2021). Expression and Characterization of a Cold-Adapted Alginate Lyase with Exo/Endo-Type Activity from a Novel Marine Bacterium Alteromonas portus HB161718T. *Marine Drugs*, *19*(3), 155.

Huang, J., Huang, J., Li, Y., Wang, Y., Wang, F., Qiu, X., . . . Li, H. (2021). Sodium Alginate Modulates Immunity, Intestinal Mucosal Barrier Function, and Gut Microbiota in Cyclophosphamide-Induced Immunosuppressed BALB/c Mice. *Journal of Agricultural and Food Chemistry*, *69*, 7064-7073.

Hung, S.-Y., Huang, W.-P., Liou, H.-C., & Fu, W.-M. (2009). Autophagy protects neuron from Aβ-induced cytotoxicity. *Autophagy*, *5*(4), 502-510.

Ismillayli, N., Hadi, S., Dharmayani, N. K. T., Sanjaya, R. K., & Hermanto, D. (2020). Characterization of alginate-chitosan membrane as potential edible film. IOP Conference Series: Materials Science and Engineering,

Itoh, T., Nakagawa, E., Yoda, M., Nakaichi, A., Hibi, T., & Kimoto, H. (2019). Structural and biochemical characterisation of a novel alginate lyase from Paenibacillus sp. str. FPU-7. *Scientific Reports*, *9*(1), 1-14.

Iwamoto, M., Kurachi, M., Nakashima, T., Kim, D., Yamaguchi, K., Oda, T., . . . Muramatsu, T. (2005). Structure–activity relationship of alginate oligosaccharides in the induction of cytokine production from RAW264. 7 cells. *FEBS Letters*, *579*(20), 4423-4429.

Iwamoto, Y., Iriyama, K., Osatomi, K., Oda, T., & Muramatsu, T. (2002). Primary structure and chemical modification of some amino acid residues of bifunctional alginate lyase from a marine bacterium Pseudoalteromonas sp. strain No. 272. *Journal of protein chemistry*, *21*(7), 455-463.

Iwamoto, Y., Xu, X., Tamura, T., Oda, T., & Muramatsu, T. (2003). Enzymatically depolymerized alginate oligomers that cause cytotoxic cytokine production in human mononuclear cells. *Bioscience Biotechnology and Biochemistry*, *67*(2), 258-263.

Jack, A. A., Khan, S., Powell, L. C., Pritchard, M. F., Beck, K., Sadh, H., . . . Rye, P. D. (2018). Alginate oligosaccharide-induced modification of the lasI-lasR and rhlI-rhlR quorum-sensing systems in Pseudomonas aeruginosa. *Antimicrobial agents and chemotherapy*, *62*(5), e02318-02317.

Jack, A. A., Nordli, H. R., Powell, L. C., Farnell, D. J., Pukstad, B., Rye, P. D., . . . Hill, K. E. (2019). Cellulose nanofibril formulations incorporating a low-molecular-weight alginate oligosaccharide modify bacterial biofilm development. *Biomacromolecules*, *20*(8), 2953-2961.

Jana, A., & Pahan, K. (2010). Fibrillar amyloid-β-activated human astroglia kill primary human neurons via neutral sphingomyelinase: implications for Alzheimer's disease. *Journal of Neuroscience*, *30*(38), 12676-12689.

Jeong, H., Lee, S., Moon, P., Na, H., Park, R., Um, J., . . . Hong, S. (2006). Alginic acid has anti-anaphylactic effects and inhibits inflammatory cytokine expression via suppression of nuclear factor-κB activation. *Clinical & Experimental Allergy*, *36*(6), 785-794.

Jiang, F., Yang, L., Wang, S., Ying, X., Ling, J., & Ouyang, X. k. (2021). Fabrication and characterization of zein-alginate oligosaccharide complex nanoparticles as delivery vehicles of curcumin. *Journal of Molecular Liquids*, 116937.

Jiang, R., Du, X., Zhang, X., Wang, X., Hu, D., Meng, T., . . . Shen, J. (2013). Synthesis and bioassay of β-

(1, 4)-D-mannans as potential agents against Alzheimer's disease. *Acta Pharmacologica Sinica*, *34*(12), 1585-1591.

Jiang, T., Yu, J.-T., Zhu, X.-C., Zhang, Q.-Q., Cao, L., Wang, H.-F., . . . Zhang, Y.-D. (2014). Temsirolimus attenuates tauopathy in vitro and in vivo by targeting tau hyperphosphorylation and autophagic clearance. *Neuropharmacology*, *85*, 121-130.

Jiang, Z., Guo, Y., Wang, X., Li, H., Ni, H., Li, L., . . . Zhu, Y. (2019). Molecular cloning and characterization of AlgL17, a new exo-oligoalginate lyase from Microbulbifer sp. ALW1. *Protein expression and purification*, *161*, 17-27.

Jiang, Z., Okimura, T., Yamaguchi, K., & Oda, T. (2011). The potent activity of sulfated polysaccharide, ascophyllan, isolated from Ascophyllum nodosum to induce nitric oxide and cytokine production from mouse macrophage RAW264. 7 cells: Comparison between ascophyllan and fucoidan. *Nitric Oxide*, *25*(4), 407-415.

Kaeberlein, M., Powers, R. W., Steffen, K. K., Westman, E. A., Hu, D., Dang, N., . . . Kennedy, B. K. (2005). Regulation of yeast replicative life span by TOR and Sch9 in response to nutrients. *Science*, *310*(5751), 1193-1196.

Kazemi, S. M., & Rezaei, M. (2015). Antimicrobial effectiveness of gelatin–alginate film containing oregano essential oil for fish preservation. *Journal of food safety*, *35*(4), 482-490.

Kelishomi, Z. H., Goliaei, B., Mahdavi, H., Nikoofar, A., Rahimi, M., Moosavi-Movahedi, A. A., . . . Bigdeli, B. (2016). Antioxidant activity of low molecular weight alginate produced by thermal treatment. *Food Chemistry*, *196*, 897-902.

Kesika, P., Suganthy, N., Sivamaruthi, B. S., & Chaiyasut, C. (2021). Role of gut-brain axis, gut microbial composition, and probiotic intervention in Alzheimer's disease. *Life sciences*, *264*, 118627.

Khan, S., Tøndervik, A., Sletta, H., Klinkenberg, G., Emanuel, C., Onsøyen, E., . . . Hill, K. E. (2012). Overcoming drug resistance with alginate oligosaccharides able to potentiate the action of selected antibiotics. *Antimicrobial agents and chemotherapy*, *56*(10), 5134-5141.

Kim, J., Kundu, M., Viollet, B., & Guan, K. L. (2011). AMPK and mTOR regulate autophagy through direct phosphorylation of Ulk1. *Nature Cell Biology*, *13*(2), 132-141.

Kleinert, M., Clemmensen, C., Hofmann, S. M., Moore, M. C., Renner, S., Woods, S. C., . . . Schürmann, A. (2018). Animal models of obesity and diabetes mellitus. *Nature Reviews Endocrinology*, *14*(3), 140-162.

Knutson, C. A., & Jeanes, A. (1968a). Determination of the composition of uronic acid mixtures. *Analytical biochemistry*, *24*(3), 482-490.

Knutson, C. A., & Jeanes, A. (1968b). A new modification of the carbazole analysis: application to heteropolysaccharides. *Analytical biochemistry*(3), 470-481.

Komatsu, M., Waguri, S., Koike, M., Sou, Y.-s., Ueno, T., Hara, T., . . . Murata, S. (2007). Homeostatic levels of p62 control cytoplasmic inclusion body formation in autophagy-deficient mice. *Cell*, *131*(6), 1149-1163.

Kuan, Y. L., Sivanasvaran, S. N., Pui, L. P., Yusof, Y. A., & Senphan, T. (2020). Physicochemical Properties of Sodium Alginate Edible Film Incorporated with Mulberry (Morus australis) Leaf Extract. *Pertanika Journal of Tropical Agricultural Science*, *43*(3).

Kuklenyik, Z., Boyer, A. E., Lins, R., Quinn, C. P., Gallegos-Candela, M., Woolfitt, A., . . . Barr, J. R. (2011). Comparison of MALDI-TOF-MS and HPLC-ESI-MS/MS for endopeptidase activity-based quantification of anthrax lethal factor in serum. *Analytical chemistry*, *83*(5), 1760-1765.

Kumar, S., & Nayak, S. K. (2019). Purification Techniques For Biological Proteins. *Think India Journal*,

22(30), 1057-1077.

Kurachi, M., Nakashima, T., Miyajima, C., Iwamoto, Y., Muramatsu, T., Yamaguchi, K., & Oda, T. (2005). Comparison of the activities of various alginates to induce TNF-α secretion in RAW264. 7 cells. *Journal of infection and chemotherapy*, *11*(4), 199-203.

Lamela, M., Anca, J., Villar, R., Otero, J., & Calleja, J. (1989). Hypoglycemic activity op several seaweed extracts. *Journal of ethnopharmacology*, *27*(1-2), 35-43.

Lane, C., Hardy, J., & Schott, J. (2018). Alzheimer's Disease. *European journal of neurology*, *25*(1), 59-70.

Larsen, B. (1962). Quantitative determination of the uronic acid composition of alginates. *Acta Chemica Scandinavica*, *16*(8).

Larsen, B., & Haug, A. (1971a). Biosynthesis of alginate: Part I. Composition and structure of alginate produced by Azotobacter vinelandii (Lipman). *Carbohydrate Research*, *17*(2), 287-296.

Larsen, B., & Haug, A. (1971b). Biosynthesis of alginate: Part III. Tritium incorporation with polymannuronic acid 5-epimerase from Azotobacter vinelandii. *Carbohydrate Research*, *20*(2), 225-232.

Lasagna-Reeves, C. A., Castillo-Carranza, D. L., Guerrero-Muñoz, M. J., Jackson, G. R., & Kayed, R. (2010). Preparation and characterization of neurotoxic tau oligomers. *Biochemistry*, *49*(47), 10039-10041.

Lazarov, O., & Demars, M. P. (2012). All in the family: how the APPs regulate neurogenesis. *Frontiers in Neuroscience*, *6*, 81.

Lee, D. W., Choi, W. S., Byun, M. W., Park, H. J., Yu, Y.-M., & Lee, C. M. (2003). Effect of γ-irradiation on degradation of alginate. *Journal of Agricultural and Food Chemistry*, *51*(16), 4819-4823.

Lee, I. H., Cao, L., Mostoslavsky, R., Lombard, D. B., Liu, J., Bruns, N. E., . . . Finkel, T. (2008). A role for

the NAD-dependent deacetylase Sirt1 in the regulation of autophagy. *Proceedings of the National Academy of Sciences*, *105*(9), 3374-3379.

Lee, J. K., Jin, H. K., Min, H. P., Kim, B., Lee, P. H., Nakauchi, H., . . . Bae, J. (2014). Acid sphingomyelinase modulates the autophagic process by controlling lysosomal biogenesis in Alzheimer's disease. *Journal of Cell Biology*, *211*(8), 1551-1570.

Lee, K. H., Song, Y., Wu, W., Yu, K., & Zhang, G. (2020). The gut microbiota, environmental factors, and links to the development of food allergy. *Clinical and Molecular Allergy*, *18*(1), 1-11.

Li, H., Wang, S., Zhang, Y., & Chen, L. (2018). High-level expression of a thermally stable alginate lyase using pichia pastoris, characterization and application in producing brown alginate oligosaccharide. *Marine Drugs*, *16*(5), 158.

Li, L., Zhang, S., Zhang, X., Li, T., Tang, Y., Liu, H., . . . Le, W. (2013). Autophagy enhancer carbamazepine alleviates memory deficits and cerebral amyloid-β pathology in a mouse model of Alzheimer's disease. *Current Alzheimer Research*, *10*(4), 433-441.

Li, Q., Hu, F., Zhu, B., Sun, Y., & Yao, Z. (2019). Biochemical characterization and elucidation of action pattern of a novel polysaccharide lyase 6 family alginate lyase from marine bacterium Flammeovirga sp. NJ-04. *Marine Drugs*, *17*(6), 323.

Li, S., He, N., & Wang, L. (2019). Efficiently Anti-obesity effects of unsaturated alginate oligosaccharides (UAOS) in high-fat diet (HFD)-fed mice. *Marine Drugs*, *17*(9), 540.

Li, X., Xu, A., Xie, H., Yu, W., Xie, W., & Ma, X. (2010). Preparation of low molecular weight alginate by hydrogen peroxide depolymerization for tissue engineering. *Carbohydrate Polymers*, *79*(3), 660-664.

Li, Y., Lu, J., Tian, X., Xu, Z., Huang, L., Xiao, H., . . . Kong, Q. (2021). Alginate with citrus pectin and

pterostilbene as healthy food packaging with antioxidant property. *International Journal of Biological Macromolecules*, *193*, 2093-2102.

Lim, L., Tan, H., & Pui, L. (2021). Development and characterization of alginate-based edible film incorporated with hawthorn berry (Crataegus pinnatifida) extract. *Journal of Food Measurement and Characterization*, *15*(3), 2540-2548.

Lin, C.-Y., & Tsai, C.-W. (2017). Carnosic acid attenuates 6-hydroxydopamine-induced neurotoxicity in SH-SY5Y cells by inducing autophagy through an enhanced interaction of Parkin and Beclin1. *Molecular Neurobiology*, *54*(4), 2813-2822.

Linker, A., & Evans, L. R. (1984). Isolation and characterization of an alginase from mucoid strains of Pseudomonas aeruginosa. *Journal of Bacteriology*, *159*(3), 958-964.

Linker, A., & Jones, R. S. (1964). A polysaccharide resembling alginic acid from a Pseudomonas micro-organism. *Nature*, *204*(4954), 187-188.

Linker, A., & Jones, R. S. (1966). A new polysaccharide resembling alginic acid isolated from pseudomonads. *Journal of Biological Chemistry*, *241*(16), 3845-3851.

Liu, J., Kennedy, J. F., Zhang, X., Heng, Y., Chen, W., Chen, Z., . . . Wu, X. (2020). Preparation of alginate oligosaccharide and its effects on decay control and quality maintenance of harvested kiwifruit. *Carbohydrate Polymers*, *242*, 116462.

Liu, J., Wu, S., Cheng, Y., Liu, Q., Su, L., Yang, Y., . . . Tong, H. (2021). Sargassum fusiforme Alginate Relieves Hyperglycemia and Modulates Intestinal Microbiota and Metabolites in Type 2 Diabetic Mice. *Nutrients*, *13*(8), 2887.

Liu, J., Yang, S., Li, X., Yan, Q., Reaney, M. J., & Jiang, Z. (2019). Alginate oligosaccharides: production, biological activities, and potential applications. *Comprehensive reviews in food science and*

food safety, *18*(6), 1859-1881.

Liu, M., Nie, Q., Xin, X., & Geng, M. (2008). Identification of AOSC-binding proteins in neurons. *Chinese Journal of Oceanology and Limnology*, *26*(4), 394-399.

Liu, Q., Xi, Y., Wang, Q., Liu, J., Li, P., Meng, X., . . . Liu, Z. (2021). Mannan oligosaccharide attenuates cognitive and behavioral disorders in the 5xFAD Alzheimer's disease mouse model via regulating the gut microbiota-brain axis. *Brain, Behavior, and Immunity*, *95*, 330-343.

Liu, Y., Jiang, L., & Li, X. (2017). κ-carrageenan-derived pentasaccharide attenuates Aβ25-35-induced apoptosis in SH-SY5Y cells via suppression of the JNK signaling pathway. *Molecular Medicine Reports*, *15*(1), 285-290.

Llanes, F., Ryan, D. H., & Marchessault, R. H. (2000). Magnetic nanostructured composites using alginates of different M/G ratios as polymeric matrix. *International Journal of Biological Macromolecules*, *27*(1), 35-40.

Lu, J., Yang, H., Hao, J., Wu, C., Liu, L., Xu, N., . . . Zhang, Z. (2015). Impact of hydrolysis conditions on the detection of mannuronic to guluronic acid ratio in alginate and its derivatives. *Carbohydrate Polymers*, *122*, 180-188.

Luan, L. Q., Ha, V. T. T., Uyen, N. H. P., Trang, L. T. T., & Hien, N. Q. (2012). Preparation of oligoalginate plant growth promoter by γ irradiation of alginate solution containing hydrogen peroxide. *Journal of Agricultural and Food Chemistry*, *60*(7), 1737-1741.

Mahcene, Z., Khelil, A., Hasni, S., Bozkurt, F., Goudjil, M. B., & Tornuk, F. (2021). Home-made cheese preservation using sodium alginate based on edible film incorporating essential oils. *Journal of Food Science and Technology*, *58*(6), 2406-2419.

Maizura, M., Fazilah, A., Norziah, M., & Karim, A. (2007). Antibacterial activity and mechanical

properties of partially hydrolyzed sago starch–alginate edible film containing lemongrass oil. *Journal of Food Science*, *72*(6), C324-C330.

Mak, W., Wang, S. K., Liu, T., Hamid, N., Li, Y., Lu, J., & White, W. L. (2014). Anti-proliferation potential and content of fucoidan extracted from sporophyll of New Zealand Undaria pinnatifida. *Frontiers in Nutrition*, *1*.

Mao, S., Zhang, T., Sun, W., & Ren, X. (2012). The depolymerization of sodium alginate by oxidative degradation. *Pharmaceutical development and technology*, *17*(6), 763-769.

Martínez-Molina, E. C., Freile-Pelegrín, Y., Ovando-Chacón, S. L., Gutiérrez-Miceli, F. A., Ruiz-Cabrera, M. Á., Grajales-Lagunes, A., . . . Abud-Archila, M. (2021). Development and characterization of alginate-based edible film from Sargassum fluitans incorporated with silver nanoparticles obtained by green synthesis. *Journal of Food Measurement and Characterization*, 1-11.

Mattson, M. P. (2004). Pathways towards and away from Alzheimer's disease. *Nature*, *430*(7000), 631-639.

Menzies, F. M., Fleming, A., & Rubinsztein, D. C. (2015). Compromised autophagy and neurodegenerative diseases. *Nature Reviews Neuroscience*, *16*(6), 345-357.

Ming, L., Lei, L., ZHANG, H.-f., Bao, Y., & Everaert, N. (2021). Alginate oligosaccharides preparation, biological activities and their application in livestock and poultry. *Journal of Integrative Agriculture*, *20*(1), 24-34.

Mørch, Ý. A., Donati, I., Strand, B. L., & Skjåk-Bræk, G. (2006). Effect of Ca2+, Ba2+, and Sr2+ on alginate microbeads. *Biomacromolecules*, *7*(5), 1471-1480.

Morris, E. R., Rees, D. A., & Thom, D. (1980). Characterisation of alginate composition and block-structure by circular dichroism. *Carbohydrate Research*, *81*(2), 305-314.

Mouton, A. J., Li, X., Hall, M. E., & Hall, J. E. (2020). Obesity, hypertension, and cardiac dysfunction: novel roles of immunometabolism in macrophage activation and inflammation. *Circulation research*, *126*(6), 789-806.

Nagasawa, N., Mitomo, H., Yoshii, F., & Kume, T. (2000). Radiation-induced degradation of sodium alginate. *Polymer Degradation and Stability*, *69*(3), 279-285.

Nixon, R. A. (2013). The role of autophagy in neurodegenerative disease. *Nature Medicine*, *19*(8), 983-997.

Oakley, J. L., Weiser, R., Powell, L. C., Forton, J., Mahenthiralingam, E., Rye, P. D., . . . Pritchard, M. F. (2021). Phenotypic and genotypic adaptations in Pseudomonas aeruginosa biofilms following long-term exposure to an alginate oligomer therapy. *Msphere*, *6*(1), e01216-01220.

Odunsi, S. T., Vázquez-Roque, M. I., Camilleri, M., Papathanasopoulos, A., Clark, M. M., Wodrich, L., . . . Burton, D. (2010). Effect of alginate on satiation, appetite, gastric function, and selected gut satiety hormones in overweight and obesity. *Obesity*, *18*(8), 1579-1584.

Ohta, K., Mizuno, A., Ueda, M., Li, S., Suzuki, Y., Hida, Y., . . . Kobori, M. (2010). Autophagy impairment stimulates PS1 expression and γ-secretase activity. *Autophagy*, *6*(3), 345-352.

Onodera, J., & Ohsumi, Y. (2005). Autophagy is required for maintenance of amino acid levels and protein synthesis under nitrogen starvation. *Journal of Biological Chemistry*, *280*(36), 31582-31586.

Onsøyen, E. (1997). Alginates. In *Thickening and Gelling Agents for Food* (pp. 22-44). Springer.

Orr, M. E., Sullivan, A. C., & Frost, B. (2017). A brief overview of tauopathy: causes, consequences, and therapeutic strategies. *Trends in pharmacological sciences*, *38*(7), 637-648.

Özbilenler, C., Altundağ, E. M., & Gazi, M. (2020). Synthesis of quercetin-encapsulated alginate beads

with their antioxidant and release kinetic studies. *Journal of Macromolecular Science, Part A*, *58*(1), 22-31.

Ozcelik, S., Fraser, G., Castets, P., Schaeffer, V., Skachokova, Z., Breu, K., . . . Goedert, M. (2013). Rapamycin attenuates the progression of tau pathology in P301S tau transgenic mice. *PloS One*, *8*(5), e62459.

Pan, H., Feng, W., Chen, M., Luan, H., Hu, Y., Zheng, X., . . . Mao, Y. (2021). Alginate Oligosaccharide Ameliorates D-Galactose-Induced Kidney Aging in Mice through Activation of the Nrf2 Signaling Pathway. *Biomed Research International*, *2021*.

Pan, X., Zhu, Y., Lin, N., Zhang, J., Ye, Q., Huang, H., & Chen, X. (2011). Microglial phagocytosis induced by fibrillar β-amyloid is attenuated by oligomeric β-amyloid: implications for Alzheimer's disease. *Molecular Neurodegeneration*, *6*(1), 45.

Pantovic, A., Krstic, A., Janjetovic, K., Kocic, J., Harhaji-Trajkovic, L., Bugarski, D., & Trajkovic, V. (2013). Coordinated time-dependent modulation of AMPK/Akt/mTOR signaling and autophagy controls osteogenic differentiation of human mesenchymal stem cells. *Bone*, *52*(1), 524-531.

Park, H., Kang, S., Kim, B., Mooney, D., & Lee, K. (2009). Shear-reversibly crosslinked alginate hydrogels for tissue engineering. *Macromolecular Bioscience*, *9*(9), 895-901.

Park, H. J., Ahn, J.-M., Park, R.-M., Lee, S.-H., Sekhon, S. S., Kim, S. Y., . . . Min, J. (2016). Effects of alginate oligosaccharide mixture on the bioavailability of lysozyme as an antimicrobial agent. *Journal of nanoscience and nanotechnology*, *16*(2), 1445-1449.

Penman, A., & Sanderson, G. (1972). A method for the determination of uronic acid sequence in alginates. *Carbohydrate Research*, *25*(2), 273-282.

Pickford, F., Masliah, E., Britschgi, M., Lucin, K., Narasimhan, R., Jaeger, P. A., . . . Levine, B. (2008). The

autophagy-related protein beclin 1 shows reduced expression in early Alzheimer disease and regulates amyloid β accumulation in mice. *Journal of Clinical Investigation*, *118*(6), 2190-2199.

Pillai, C. K., Paul, W., & Sharma, C. P. (2009). Chitin and chitosan polymers: Chemistry, solubility and fiber formation. *Progress in Polymer Science*, *34*(7), 641-678.

Pisoschi, A. M., Pop, A., Iordache, F., Stanca, L., Predoi, G., & Serban, A. I. (2021). Oxidative stress mitigation by antioxidants-an overview on their chemistry and influences on health status. *European Journal of Medicinal Chemistry*, *209*, 112891.

Pivtoraiko, V. N., Stone, S. L., Roth, K. A., & Shacka, J. J. (2009). Oxidative stress and autophagy in the regulation of lysosome-dependent neuron death. *Antioxidants and Redox Signaling*, *11*(3), 481-496.

Poo, M. (2020). New light on the horizon of Alzheimer's disease. In (pp. 831): Oxford University Press.

Powell, L. C., Pritchard, M. F., Emanuel, C., Onsøyen, E., Rye, P. D., Wright, C. J., . . . Thomas, D. W. (2014). A nanoscale characterization of the interaction of a novel alginate oligomer with the cell surface and motility of Pseudomonas aeruginosa. *American journal of respiratory cell and molecular biology*, *50*(3), 483-492.

Powell, L. C., Pritchard, M. F., Ferguson, E. L., Powell, K. A., Patel, S. U., Rye, P. D., . . . Copping, J. M. (2018). Targeted disruption of the extracellular polymeric network of Pseudomonas aeruginosa biofilms by alginate oligosaccharides. *NPJ biofilms and microbiomes*, *4*(1), 1-10.

Pritchard, M. F., Jack, A., Powell, L. C., Sadh, H., Rye, P. D., Hill, K. E., & Thomas, D. W. (2017). Alginate oligosaccharides modify hyphal infiltration of Candida albicans in an in vitro model of invasive human candidosis. *Journal of applied microbiology*, *123*(3), 625-636.

Pritchard, M. F., Oakley, J. L., Brilliant, C. D., Rye, P. D., Forton, J., Doull, I. J., . . . Lewis, P. D. (2019). Mucin

structural interactions with an alginate oligomer mucolytic in cystic fibrosis sputum. *Vibrational Spectroscopy*, *103*, 102932.

Pritchard, M. F., Powell, L. C., Jack, A. A., Powell, K., Beck, K., Florance, H., . . . Hill, K. E. (2017). A low-molecular-weight alginate oligosaccharide disrupts pseudomonal microcolony formation and enhances antibiotic effectiveness. *Antimicrobial agents and chemotherapy*, *61*(9), e00762-00717.

Pritchard, M. F., Powell, L. C., Khan, S., Griffiths, P. C., Mansour, O. T., Schweins, R., . . . Wright, C. J. (2017). The antimicrobial effects of the alginate oligomer OligoG CF-5/20 are independent of direct bacterial cell membrane disruption. *Scientific Reports*, *7*(1), 1-12.

Pritchard, M. F., Powell, L. C., Menzies, G. E., Lewis, P. D., Hawkins, K., Wright, C., . . . Dessen, A. (2016). A new class of safe oligosaccharide polymer therapy to modify the mucus barrier of chronic respiratory disease. *Molecular pharmaceutics*, *13*(3), 863-872.

Rahelivao, M. P., Andriamanantoanina, H., Heyraud, A., & Rinaudo, M. (2013). Structure and properties of three alginates from Madagascar seacoast algae. *Food Hydrocolloids*, *32*(1), 143-146.

Rastelli, M., Knauf, C., & Cani, P. D. (2018). Gut microbes and health: a focus on the mechanisms linking microbes, obesity, and related disorders. *Obesity*, *26*(5), 792-800.

Reddy, P. H., Manczak, M., Mao, P., Calkins, M. J., Reddy, A. P., & Shirendeb, U. (2010). Amyloid-β and mitochondria in aging and Alzheimer's disease: implications for synaptic damage and cognitive decline. *Journal of Alzheimer's disease*, *20*(s2), S499-S512.

Reddy, P. H., Tonk, S., Kumar, S., Vijayan, M., Kandimalla, R., Kuruva, C. S., & Reddy, A. P. (2017). A critical evaluation of neuroprotective and neurodegenerative MicroRNAs in Alzheimer's disease. *Biochemical Biophysical Research Communications*, *483*(4), 1156-1165.

Reyes-Avalos, M., Femenia, A., Minjares-Fuentes, R., Contreras-Esquivel, J., Aguilar-González, C., Esparza-Rivera, J., & Meza-Velázquez, J. (2016). Improvement of the quality and the shelf life of figs (Ficus carica) using an alginate–chitosan edible film. *Food and Bioprocess Technology*, *9*(12), 2114-2124.

Reyes-Avalos, M., Minjares-Fuentes, R., Femenia, A., Contreras-Esquivel, J., Quintero-Ramos, A., Esparza-Rivera, J., & Meza-Velázquez, J. (2019). Application of an alginate–chitosan edible film on figs (Ficus carica): Effect on bioactive compounds and antioxidant capacity. *Food and Bioprocess Technology*, *12*(3), 499-511.

Roberts, J. L., Khan, S., Emanuel, C., Powell, L. C., Pritchard, M., Onsøyen, E., . . . Hill, K. E. (2013). An in vitro study of alginate oligomer therapies on oral biofilms. *Journal of dentistry*, *41*(10), 892-899.

Ruan, C., Zhang, Y., Wang, J., Sun, Y., Gao, X., Xiong, G., & Liang, J. (2019). Preparation and antioxidant activity of sodium alginate and carboxymethyl cellulose edible films with epigallocatechin gallate. *International Journal of Biological Macromolecules*, *134*, 1038-1044.

Rumpel, C., & Dignac, M.-F. (2006). Gas chromatographic analysis of monosaccharides in a forest soil profile: Analysis by gas chromatography after trifluoroacetic acid hydrolysis and reduction–acetylation. *Soil Biology and Biochemistry*, *38*(6), 1478-1481.

Russell, R. C., Tian, Y., Yuan, H., Park, H. W., Chang, Y.-Y., Kim, J., . . . Guan, K.-L. (2013). ULK1 induces autophagy by phosphorylating Beclin-1 and activating VPS34 lipid kinase. *Nature Cell Biology*, *15*(7), 741-750.

Rye, P., Tøndervik, A., Sletta, H., Pritchard, M., Kristiansen, A., Dessen, A., & Thomas, D. (2018). Alginate oligomers and their use as active pharmaceutical drugs. In *Alginates and Their Biomedical*

Applications (pp. 237-256). Springer.

Sacks, C. A., Avorn, J., & Kesselheim, A. S. (2017). The failure of solanezumab—How the FDA saved taxpayers billions. *New England Journal of Medicine*, *376*(18), 1706-1708.

Sarkar, S., Floto, R. A., Berger, Z., Imarisio, S., Cordenier, A., Pasco, M., . . . Rubinsztein, D. C. (2005). Lithium induces autophagy by inhibiting inositol monophosphatase. *The Journal of cell biology*, *170*(7), 1101-1111.

Schaeffer, V., Lavenir, I., Ozcelik, S., Tolnay, M., Winkler, D. T., & Goedert, M. (2012). Stimulation of autophagy reduces neurodegeneration in a mouse model of human tauopathy. *Brain*, *135*(7), 2169-2177.

Şen, M., & Atik, H. (2012). The antioxidant properties of oligo sodium alginates prepared by radiation-induced degradation in aqueous and hydrogen peroxide solutions. *Radiation Physics and Chemistry*, *81*(7), 816-822.

Shaw, M., Cohen, P., & Alessi, D. R. (1997). Further evidence that the inhibition of glycogen synthase kinase-3β by IGF-1 is mediated by PDK1/PKB-induced phosphorylation of Ser-9 and not by dephosphorylation of Tyr-216. *FEBS Letters*, *416*(3), 307-311.

Shen, P., Gu, Y., Zhang, C., Sun, C., Qin, L., Yu, C., & Qi, H. (2021). Metabolomic approach for characterization of polyphenolic compounds in Laminaria japonica, Undaria pinnatifida, Sargassum fusiforme and Ascophyllum nodosum. *Foods*, *10*(1), 192.

Shimokawa, T., Yoshida, S., Takeuchi, T., Murata, K., Ishii, T., & Kusakabe, I. (1996). Preparation of two series of oligo-guluronic acids from sodium alginate by acid hydrolysis and enzymatic degradation. *Bioscience, biotechnology, and biochemistry*, *60*(9), 1532-1534.

Sikanyika, N. L., Parkington, H. C., Smith, A. I., & Kuruppu, S. (2019). Powering Amyloid Beta Degrading

Enzymes: A Possible Therapy for Alzheimer's Disease. *Neurochemical Research*, 1-8.

Singer-Englar, T., Barlow, G., & Mathur, R. (2019). Obesity, diabetes, and the gut microbiome: an updated review. *Expert review of gastroenterology & hepatology*, *13*(1), 3-15.

Soeda, Y., Saito, M., Maeda, S., Ishida, K., Nakamura, A., Kojima, S., & Takashima, A. J. J. o. A. s. D. (2019). Methylene blue inhibits formation of tau fibrils but not of granular tau oligomers: A plausible key to understanding failure of a clinical trial for Alzheimer's disease. *Journal of Alzheimer's Disease*, *68*(4), 1677-1686.

Soukaina, B., Zainab, E., Guillaume, P., Halima, R., Philippe, M., Cherkaoui, E. M., & Cédric, D. (2020). Radical Depolymerization of Alginate Extracted from Moroccan Brown Seaweed Bifurcaria bifurcata. *Applied Sciences*, *10*(12), 4166.

Stanford, E. (1881). Improvements in the manufacture of useful products from seaweeds. *British Patent*, *142*.

Stender, E. G., Andersen, C. D., Fredslund, F., Holck, J., Solberg, A., Teze, D., . . . Welner, D. H. (2019). Structural and functional aspects of mannuronic acid–specific PL6 alginate lyase from the human gut microbe Bacteroides cellulosilyticus. *Journal of Biological Chemistry*, *294*(47), 17915-17930.

Stokniene, J., Powell, L. C., Aarstad, O. A., Aachmann, F. L., Rye, P. D., Hill, K. E., . . . Ferguson, E. L. (2020). Bi-Functional Alginate Oligosaccharide–Polymyxin Conjugates for Improved Treatment of Multidrug-Resistant Gram-Negative Bacterial Infections. *Pharmaceutics*, *12*(11), 1080.

Tien, N. T., Karaca, I., Tamboli, I. Y., & Walter, J. (2016). Trehalose alters subcellular trafficking and the metabolism of the Alzheimer-associated amyloid precursor protein. *Journal of Biological Chemistry*, *291*(20), 10528-10540.

Tøndervik, A., Sletta, H., Klinkenberg, G., Emanuel, C., Powell, L. C., Pritchard, M. F., . . . Rye, P. D. (2014). Alginate oligosaccharides inhibit fungal cell growth and potentiate the activity of antifungals against Candida and Aspergillus spp. *PloS One*, *9*(11), e112518.

Tran, V., Cho, S., Kwon, J., & Kim, D. (2019). Alginate oligosaccharide (AOS) improves immuno-metabolic systems by inhibiting STOML2 overexpression in high-fat-diet-induced obese zebrafish. *Food & Function*, *10*(8), 4636-4648.

Tsukada, M., & Ohsumi, Y. (1993). Isolation and characterization of autophagy-defective mutants of Saccharomyces cerevisiae. *FEBS Letters*, *333*(1-2), 169-174.

Tusi, S. K., Khalaj, L., Ashabi, G., Kiaei, M., & Khodagholi, F. (2011). Alginate oligosaccharide protects against endoplasmic reticulum-and mitochondrial-mediated apoptotic cell death and oxidative stress. *Biomaterials*, *32*(23), 5438-5458.

Uddin, M. S., Kabir, M. T., Al Mamun, A., Barreto, G. E., Rashid, M., Perveen, A., & Ashraf, G. M. (2020). Pharmacological approaches to mitigate neuroinflammation in Alzheimer's disease. *International Immunopharmacology*, *84*, 106479.

Ueno, M., Cho, K., Nakazono, S., Isaka, S., Abu, R., Takeshita, S., . . . Oda, T. (2015). Alginate oligomer induces nitric oxide (NO) production in RAW264. 7 cells: elucidation of the underlying intracellular signaling mechanism. *Bioscience, biotechnology, and biochemistry*, *79*(11), 1787-1793.

Umaraw, P., & Verma, A. K. (2017). Comprehensive review on application of edible film on meat and meat products: An eco-friendly approach. *Critical reviews in food science and nutrition*, *57*(6), 1270-1279.

Uno, T., Hattori, M., & Yoshida, T. (2006). Oral administration of alginic acid oligosaccharide suppresses

IgE production and inhibits the induction of oral tolerance. *Bioscience Biotechnology and Biochemistry*, *70*(12), 3054-3057.

Ushasree, M. V., Lee, O. K., & Lee, E. Y. (2021). Alginate derived functional oligosaccharides: Recent developments, barriers, and future outlooks. *Carbohydrate Polymers*, 118158.

Voragen, A., Schols, H., De Vries, J., & Pilnik, W. (1982). High-performance liquid chromatographic analysis of uronic acids and oligogalacturonic acids. *Journal of Chromatography A*, *244*(2), 327-336.

Wan, J., Zhang, J., Chen, D., Yu, B., & He, J. (2017). Effects of alginate oligosaccharide on the growth performance, antioxidant capacity and intestinal digestion-absorption function in weaned pigs. *Animal Feed Science and Technology*, *234*, 118-127.

Wan, J., Zhang, J., Chen, D., Yu, B., Huang, Z., Mao, X., . . . He, J. (2018). Alginate oligosaccharide enhances intestinal integrity of weaned pigs through altering intestinal inflammatory responses and antioxidant status. *RSC Advances*, *8*(24), 13482-13492.

Wan, J., Zhang, J., Xu, Q., Yin, H., Chen, D., Yu, B., & He, J. (2021). Alginate oligosaccharide protects against enterotoxigenic Escherichia coli-induced porcine intestinal barrier injury. *Carbohydrate Polymers*, 118316.

Wan, J., Zhang, J., Yin, H., Chen, D., Yu, B., & He, J. (2020). Ameliorative effects of alginate oligosaccharide on tumour necrosis factor-α-induced intestinal epithelial cell injury. *International Immunopharmacology*, *89*, 107084.

Wang, H., Song, Z., Ciofu, O., Onsøyen, E., Rye, P. D., & Høiby, N. (2016). OligoG CF-5/20 disruption of mucoid Pseudomonas aeruginosa biofilm in a murine lung infection model. *Antimicrobial agents and chemotherapy*, *60*(5), 2620-2626.

Wang, P., Jiang, X., Jiang, Y., Hu, X., Mou, H., Li, M., & Guan, H. (2007). In vitro antioxidative activities of three marine oligosaccharides. *Natural Product Research*, *21*(7), 646-654.

Wang, S., Li, J., Xia, W., & Geng, M. (2007). A marine-derived acidic oligosaccharide sugar chain specifically inhibits neuronal cell injury mediated by β-amyloid-induced astrocyte activation in vitro. *Neurological Research*, *29*(1), 96-102.

Wang, X., Chen, X., Yang, X., Geng, M., & Wang, L. (2007). Acidic oligosaccharide sugar chain, a marine-derived oligosaccharide, activates human glial cell line-derived neurotrophic factor signaling. *Neuroscience Letters*, *417*(2), 176-180.

Wang, X., Sun, G., Feng, T., Zhang, J., Huang, X., Wang, T., . . . Wang, H. (2019). Sodium oligomannate therapeutically remodels gut microbiota and suppresses gut bacterial amino acids-shaped neuroinflammation to inhibit Alzheimer's disease progression. *Cell Research*, *29*(10), 787-803.

Wang, Y., Li, L., Ye, C., Yuan, J., & Qin, S. (2020). Alginate oligosaccharide improves lipid metabolism and inflammation by modulating gut microbiota in high-fat diet fed mice. *Applied microbiology and biotechnology*, *104*(8), 3541-3554.

Wang, Y., & Mandelkow, E. (2016). Tau in physiology and pathology. *Nature Reviews Neuroscience*, *17*(1), 22-35.

Wang, Z., Cao, M., Li, B., Ji, X., Zhang, X., Zhang, Y., & Wang, H. (2020). Cloning, secretory expression and characterization of a unique pH-stable and cold-adapted alginate lyase. *Marine Drugs*, *18*(4), 189.

Wei, H., Gao, Z., Zheng, L., Zhang, C., Liu, Z., Yang, Y., . . . Zou, X. (2017). Protective effects of fucoidan on Aβ25–35 and D-Gal-induced neurotoxicity in PC12 cells and D-Gal-induced cognitive dysfunction in mice. *Marine Drugs*, *15*(3), 77.

Weijers, C. A., Franssen, M. C., & Visser, G. M. (2008). Glycosyltransferase-catalyzed synthesis of bioactive oligosaccharides. *Biotechnology advances*, *26*(5), 436-456.

Weingarten, M. D., Lockwood, A. H., Hwo, S.-Y., & Kirschner, M. W. (1975). A protein factor essential for microtubule assembly. *Proceedings of the National Academy of Sciences*, *72*(5), 1858-1862.

Wilcox, M. D., Brownlee, I. A., Richardson, J. C., Dettmar, P. W., & Pearson, J. P. (2014). The modulation of pancreatic lipase activity by alginates. *Food Chemistry*, *146*, 479-484.

Wilcox, M. D., Chater, P. I., Stanforth, K. J., Woodcock, A. D., Dettmar, P. W., & Pearson, J. P. (2021). The rheological properties of an alginate satiety formulation in a physiologically relevant human model gut system. *Annals of Esophagus*, 1-9.

Wischik, C., Edwards, P., Lai, R., Roth, M., & Harrington, C. (1996). Selective inhibition of Alzheimer disease-like tau aggregation by phenothiazines. *Proceedings of the National Academy of Sciences*, *93*(20), 11213-11218.

Wobst, H. J., Sharma, A., Diamond, M. I., Wanker, E. E., & Bieschke, J. (2015). The green tea polyphenol (−)-epigallocatechin gallate prevents the aggregation of tau protein into toxic oligomers at substoichiometric ratios. *FEBS Letters*, *589*(1), 77-83.

Wong, T. Y., Preston, L. A., & Schiller, N. L. (2000). Alginate lyase: review of major sources and enzyme characteristics, structure-function analysis, biological roles, and applications. *Annual Reviews in Microbiology*, *54*(1), 289-340.

Xie, X., & Cheong, K. L. (2021). Recent advances in marine algae oligosaccharides: structure, analysis, and potential prebiotic activities. *Critical reviews in food science and nutrition*, 1-16.

Xie, Y., Tan, Y., Zheng, Y., Du, X., & Liu, Q. (2017). Ebselen ameliorates β-amyloid pathology, tau pathology, and cognitive impairment in triple-transgenic Alzheimer's disease mice. *Journal of Biological*

Inorganic Chemistry (5800), 1-15.

Xing, M., Cao, Q., Wang, Y., Xiao, H., Zhao, J., Zhang, Q., . . . Song, S. (2020). Advances in research on the bioactivity of alginate oligosaccharides. *Marine Drugs*, *18*(3), 144.

Xu, X., Bi, D., Li, C., Fang, W., Zhou, R., Li, S., . . . Shen, L. (2015). Morphological and proteomic analyses reveal that unsaturated guluronate oligosaccharide modulates multiple functional pathways in murine macrophage RAW264. 7 cells. *Marine Drugs*, *13*(4), 1798-1818.

Xu, X., Bi, D., & Wan, M. (2016). Characterization and Immunological Evaluation of Low-Molecular-Weight Alginate Derivatives. *Current Topics in Medicinal Chemistry*, *16*(8), 874-887.

Xu, X., Bi, D., Wu, X., Wang, Q., Wei, G., Chi, L., . . . Wan, M. (2014). Unsaturated guluronate oligosaccharide enhances the antibacterial activities of macrophages. *FASEB Journal*, *28*(6), 2645-2654.

Xu, X., Iwamoto, Y., Kitamura, Y., Oda, T., & Muramatsu, T. (2003). Root growth-promoting activity of unsaturated oligomeric uronates from alginate on carrot and rice plants. *Bioscience Biotechnology and Biochemistry*, *67*(9), 2022-2025.

Xu, X., Wu, X., Wang, Q., Cai, N., Zhang, H., Jiang, Z., . . . Oda, T. (2014). Immunomodulatory effects of alginate oligosaccharides on murine macrophage RAW264. 7 cells and their structure–activity relationships. *Journal of Agricultural and Food Chemistry*, *62*(14), 3168-3176.

Yamamoto, Y., Kurachi, M., Yamaguchi, K., & Oda, T. (2007a). Induction of multiple cytokine secretion from RAW264. 7 cells by alginate oligosaccharides. *Bioscience, biotechnology, and biochemistry*, *71*(1), 238-241.

Yamamoto, Y., Kurachi, M., Yamaguchi, K., & Oda, T. (2007b). Stimulation of multiple cytokine production in mice by alginate oligosaccharides following intraperitoneal administration.

Carbohydrate Research, *342*(8), 1133-1137.

Yamasaki, Y., Yokose, T., Nishikawa, T., Kim, D., Jiang, Z., Yamaguchi, K., & Oda, T. (2012). Effects of alginate oligosaccharide mixtures on the growth and fatty acid composition of the green alga Chlamydomonas reinhardtii. *Journal of bioscience and bioengineering*, *113*(1), 112-116.

Yamin, G., Ono, K., Inayathullah, M., & Teplow, D. B. (2008). Amyloid β-protein assembly as a therapeutic target of Alzheimer's disease. *Current Pharmaceutical Design*, *14*(30), 3231-3246.

Yan, G., Guo, Y., Yuan, J., Liu, D., & Zhang, B. (2011). Sodium alginate oligosaccharides from brown algae inhibit Salmonella Enteritidis colonization in broiler chickens. *Poultry science*, *90*(7), 1441-1448.

Yan, J., Liang, X., Ma, C., McClements, D. J., Liu, X., & Liu, F. (2021). Design and characterization of double-cross-linked emulsion gels using mixed biopolymers: Zein and sodium alginate. *Food Hydrocolloids*, *113*, 106473.

Yang, D., & Jones, K. S. (2009). Effect of alginate on innate immune activation of macrophages. *Journal of Biomedical Materials Research Part A*, *90*(2), 411-418.

Yang, J., Xie, Y., & He, W. (2011). Research progress on chemical modification of alginate: A review. *Carbohydrate Polymers*, *84*(1), 33-39.

Yang, M., Yu, Y., Yang, S., Shi, X., Mou, H., & Li, L. (2018). Expression and characterization of a new polyG-specific alginate lyase from marine bacterium Microbulbifer sp. Q7. *Frontiers in microbiology*, *9*, 2894.

Yang, Y., Ma, Z., Yang, G., Wan, J., Li, G., Du, L., & Lu, P. (2017). Alginate oligosaccharide indirectly affects toll-like receptor signaling via the inhibition of microRNA-29b in aneurysm patients after endovascular aortic repair. *Drug design, development and therapy*, *11*, 2565.

Yang, Z., Li, J., & Guan, H. (2004). Preparation and characterization of oligomannuronates from alginate

degraded by hydrogen peroxide. *Carbohydrate Polymers*, *58*(2), 115-121.

Yao, L., Yang, P., Lin, Y., Bi, D., Yu, B., Lin, Z., . . . Xu, X. (2021). The regulatory effect of alginate on ovalbumin-induced gut microbiota disorders. *Journal of Functional Foods*, *86*, 104727.

Yoshida, T., Hirano, A., Wada, H., Takahashi, K., & Hattori, M. (2004). Alginic acid oligosaccharide suppresses Th2 development and IgE production by inducing IL-12 production. *International archives of allergy and immunology*, *133*(3), 239-247.

You, L., Gong, Y., Li, L., Hu, X., Brennan, C., & Kulikouskaya, V. (2020). Beneficial effects of three brown seaweed polysaccharides on gut microbiota and their structural characteristics: An overview. *International Journal of Food Science & Technology*, *55*(3), 1199-1206.

Yu, B., Bi, D., Yao, L., Li, T., Gu, L., Xu, H., . . . Xu, X. (2020). The inhibitory activity of alginate against allergic reactions in an ovalbumin-induced mouse model. *Food & Function*, *11*(3), 2704-2713.

Zhang, C., Li, M., Rauf, A., Khalil, A. A., Shan, Z., Chen, C., . . . Wan, C. (2021). Process and applications of alginate oligosaccharides with emphasis on health beneficial perspectives. *Critical reviews in food science and nutrition*, 1-27.

Zhang, C., Xiong, B., Chen, L., Ge, W., Yin, S., Feng, Y., . . . Shen, W. (2021). Rescue of male fertility following faecal microbiota transplantation from alginate oligosaccharide-dosed mice. *Gut*, *70*(11), 2213-2215.

Zhang, M., Wu, Q., Yao, X., Zhao, J., Zhong, W., Liu, Q., & Xiao, S. (2019). Xanthohumol inhibits tau protein aggregation and protects cells against tau aggregates. *Food & Function*, *10*(12), 7865-7874.

Zhang, P., Feng, Y., Li, L., Ge, W., Yu, S., Hao, Y., . . . Yin, S. (2021). Improvement in sperm quality and spermatogenesis following faecal microbiota transplantation from alginate oligosaccharide

dosed mice. *Gut*, *70*(1), 222-225.

Zhang, P., Liu, J., Xiong, B., Zhang, C., Kang, B., Gao, Y., . . . Hao, Y. (2020). Microbiota from alginate oligosaccharide-dosed mice successfully mitigated small intestinal mucositis. *Microbiome*, *8*(1), 1-15.

Zhang, S., Wei, F., & Han, X. (2018). An edible film of sodium alginate/pullulan incorporated with capsaicin. *New journal of chemistry*, *42*(21), 17756-17761.

Zhang, Z., Wu, Q., Zheng, R., Chen, C., Chen, Y., Liu, Q., . . . Song, G. (2017). Selenomethionine mitigates cognitive decline by targeting both tau hyperphosphorylation and autophagic clearance in an Alzheimer's disease mouse model. *Journal of Neuroscience*, *37*(9), 2449-2462.

Zhang, Z., Yu, G., Guan, H., Zhao, X., Du, Y., & Jiang, X. (2004). Preparation and structure elucidation of alginate oligosaccharides degraded by alginate lyase from Vibro sp. 510. *Carbohydrate Research*, *339*(8), 1475-1481.

Zhang, Z., Yu, G., Zhao, X., Liu, H., Guan, H., Lawson, A. M., & Chai, W. (2006). Sequence analysis of alginate-derived oligosaccharides by negative-ion electrospray tandem mass spectrometry. *Journal of the American Society for Mass Spectrometry*, *17*(4), 621-630.

Zhang, Z.-X., Li, Y.-B., & Zhao, R.-P. (2017). Epigallocatechin Gallate attenuates β-Amyloid generation and oxidative stress involvement of PPARγ in N2a/APP695 cells. *Neurochemical Research*, *42*(2), 468-480.

Zhao, J., Han, Y., Wang, Z., Zhang, R., Wang, G., & Mao, Y. (2020). Alginate oligosaccharide protects endothelial cells against oxidative stress injury via integrin-α/FAK/PI3K signaling. *Biotechnology letters*, *42*(12), 2749-2758.

Zheng, W., Duan, M., Jia, J., Song, S., & Ai, C. (2021). Low-molecular alginate improved diet-induced

obesity and metabolic syndrome through modulating the gut microbiota in BALB/c mice. *International Journal of Biological Macromolecules*, *187*, 811-820.

Zhou, R., Shi, X., Bi, D., Fang, W., Wei, G., & Xu, X. (2015). Alginate-derived oligosaccharide inhibits neuroinflammation and promotes microglial phagocytosis of β-amyloid. *Marine Drugs*, *13*(9), 5828-5846.

Zhou, R., Shi, X., Gao, Y., Cai, N., Jiang, Z., & Xu, X. (2015). Anti-inflammatory activity of guluronate oligosaccharides obtained by oxidative degradation from alginate in lipopolysaccharide-activated murine macrophage RAW 264.7 cells. *Journal of Agricultural and Food Chemistry*, *63*(1), 160-168.

Zhu, B., Li, K., Wang, W., Ning, L., Tan, H., Zhao, X., & Yin, H. (2019). Preparation of trisaccharides from alginate by a novel alginate lyase Alg7A from marine bacterium Vibrio sp. W13. *International Journal of Biological Macromolecules*, *139*, 879-885.

Zhu, B., Ni, F., Sun, Y., Ning, L., & Yao, Z. (2019). Elucidation of degrading pattern and substrate recognition of a novel bifunctional alginate lyase from Flammeovirga sp. NJ-04 and its use for preparation alginate oligosaccharides. *Biotechnology for biofuels*, *12*(1), 1-13.

Zhu, B., Ni, F., Sun, Y., & Yao, Z. (2017). Expression and characterization of a new heat-stable endo-type alginate lyase from deep-sea bacterium Flammeovirga sp. NJ-04. *Extremophiles*, *21*(6), 1027-1036.

Zhu, B., & Yin, H. (2015). Alginate lyase: Review of major sources and classification, properties, structure-function analysis and applications. *Bioengineered*, *6*(3), 125-131.

Zhu, D., Guo, R., Li, W., Song, J., & Cheng, F. (2019). Improved postharvest preservation effects of Pholiota nameko mushroom by sodium alginate–based edible composite coating. *Food and*

Bioprocess Technology, *12*(4), 587-598.

Zhu, Y., Wu, L., Chen, Y., Ni, H., Xiao, A., & Cai, H. (2016). Characterization of an extracellular biofunctional alginate lyase from marine Microbulbifer sp. ALW1 and antioxidant activity of enzymatic hydrolysates. *Microbiological research*, *182*, 49-58.

Zimoch-Korzycka, A., Kulig, D., Król-Kilińska, Ż., Żarowska, B., Bobak, Ł., & Jarmoluk, A. (2021). Biophysico-chemical properties of alginate oligomers obtained by acid and oxidation depolymerization. *Polymers*, *13*(14), 2258.